UNIVERSITY OF SOUTHAMPTON

The Mathematical Modelling of Rock Blasting

by

Andrew Steven Paine

submitted for the degree of

Doctor of Philosophy

Faculty of Mathematical Studies

December 1991

UNIVERSITY OF SOUTHAMPTON

ABSTRACT

FACULTY OF MATHEMATICS

Doctor of Philosophy

THE MATHEMATICAL MODELLING OF ROCK BLASTING

by Andrew Steven Paine

This thesis presents a mathematical model for the motion of high pressure turbulent gas in the radial cracks generated around a borehole during rock blasting. The model equations are solved analytically for certain special cases of the blast parameters and the general solution is obtained numerically. The model solutions show that the initial mechanism for containing the high pressure gas is the clamping force from the natural in-situ stress in the rock. After a sufficient time, however, the borehole gas pressure will substantially decrease as gas is lost to the cracks. The gas will then flow much more slowly than at the start of the rock blast or than in other calculations, Erhie 88, where a constant borehole pressure throughout the blast was assumed. The gas front is in general distinct from the crack tip. As the gas pressure along the cracks decreases then the gas front will catch up with the crack tip. This agrees with the observation that low pressure magma flow in rock tends to have only a small gap between the magma front and the crack tip.

Contents

Acknowledgements

I would like to thank my supervisor Dr Colin Please for his guidance and encouragement throughout the course of my study and to Dr Bob Craine for his help in checking the draft copies of this thesis.

My thanks also go to Dr Peter Lynch my Industrial Supervisor from ICI Nobel Explosives LTD, and to the SERC for financial support during my three years of study.

Finally I would like thank Annie, Emma, Jeremy, Matthew, Chloe, Katherine, my parents and grandparents for their patience and support, without which, this thesis could never have been completed.

Notation List

Section 2:

$\underline{u}=(u_1,u_2,u_3)$	linear elastic diplacement
τ_{ij}	stress tensor
λ, μ	Lamé constants for an isotropic linear elastic material
ν, E	Poissons Ratio and Young's Modulus as alternative forms for the two linear elastic constants, where $E=\frac{\mu(3\lambda+2\mu)}{\lambda+\mu}$, $\nu=\frac{\lambda}{2(\lambda+\mu)}$
E_{ij}	strain tensor
$\underline{v}$	velocity vector
ρ	rock density
g	gravity
χ	Airy Stress Function
a	length of crack
ε	borehole radius
p	gas pressure along cracks
p_b	gas pressure in borehole
s	shear stress along cracks
K	Stress Intensity Factor
n	number of cracks running from the borehole
σ	homogeneous in-situ stress in rock

Section 3:

ρ	gas density
$\underline{v}=(u,v,w)$ $=(u_x,u_y,u_z)$	gas velocity
μ	gas viscosity
μ_{turb}	empirical turbulent viscosity term

$\mathbf{T}$	gas temperatue
$\mathbf{c_p}$, $\mathbf{c_v}$	specific heats of gas at constant pressure and volume
$\mathbf{k}$	thermal conductivity of gas
$\mathbf{k_{rock}}$	thermal conductivity of rock
σ_{ij}	components of the Reynolds Stress
$\mathbf{h_e}$	enthalpy of gas
$\mathbf{c=b-\varepsilon}$	position of gas front
$\mathbf{m}$	mass per metre loading of explosive into the borehole
γ	compressibility index in the adiabatic gas law $\rho=\mathbf{K_g p^{1/\gamma}}$

Appendix B:

If $\mathbf{F(z)=U(z)+iV(z)}$ then the following notation is used in this thesis:-

$$\overline{F(z)} = \overline{F}(z) = U(z) - iV(z)$$

$$\overline{F}(\overline{z}) = U(\overline{z}) - iV(\overline{z})$$

1. INTRODUCTION

1.0 Background to Rock Blasting

The main aim of rock blasting research is to minimise the costs of the complete mining operation. One of the chief costs originates from difficulties in handling the rock debris after the blast. The rock pieces are often too large to move efficiently so require further blasting, or are too small and create other managing difficulties. The rock debris distribution size that arises after blasting is called the **fragmentation**. It is also very important to be able to predict where the rock debris will fall, for obvious reasons! The final rock debris position is called the **muckpile**. There are many other costing factors to be taken into account in rock blasting such as the shape of the new rock face after blasting which affects future blasts, the amount of explosive used, the degree of damage away from the blasting area etc. [6,7,8,10,19,31].

Although blasting techniques have been used in mining and the extraction of ore for over 100 years, only in the last 30 years has a scientific approach been used to describe the physics behind rock blasting. It is hoped that if the overall process is properly understood, then efficiency can be maximised to reduce the overall costs.

Most of the earlier research into rock blasting was based on the effect of the stress wave produced on detonation. A highly compressive stress wave runs through the rock from the borehole to the rock face, and then reflects back as a strong tensile wave. Rock is weak in tension so the tensile wave will break the rock as it propagates back towards the borehole [see 1,10]. This type of theory is quite good for many blasting situations. A major prediction from this theory is that the time taken for initial **burden** movement (the burden is the mass of rock between the borehole and rock-face) must be the same as the time taken for the blast stress wave to travel from the borehole to the rock face ie.

$$t_b = \frac{L}{C}$$

L=distance from borehole to rock-face

C=pressure wave speed of rock

In many rock blasting situations, however, the burden movement time is much greater than (typically 10 times) that predicted by this equation. This can only mean that the initial stress wave cannot be the sole cause of the burden movement.

After the blast stress-wave stage is over, high pressure gas in the borehole must

force a path through cracks and gaps in the rock. This will increase the damage and internal stresses within the rock, until finally the burden will start to move. The relative importance of the stress-wave and the gas pressure stages in rock-blasting is not fully understood. An experiment by Brinkman, however, suggested that the gas pressure stage is the dominant mechanism in most rock blasts [6]. A metal liner was inserted into the borehole to prevent the gas flowing into the cracks but the initial shock wave of the blast was efficiently transmitted through the rock. The damage caused to the rock during this experiment only caused cracking of the rock near to the borehole and left the rock intact elsewhere. Further experimentation of rock blasting is rather limited in view of the difficulties in manufacturing non-destructable monitoring equipment in such high pressure blasts, the speed at which the entire process is completed and not least, the cost to the mining company in performing blasts for solely experimental purposes. Some experimental results are available for small scale bench blasts [21,22,23] which can be used to guide the development of a rock blasting model.

In summary a typical rock blasting process is believed to proceed as follows:

Stage 1

The explosive is detonated and in a couple of milliseconds the borehole pressure will attain near to its maximum value. The stress wave produced at detonation will travel from the borehole to the rock-face and back. Some cracking will occur near the borehole, but elsewhere the rock will remain almost intact. The stress wave will cause crushing of the rock very near to the borehole but this can be minimised by **decoupling** the explosives from the borehole wall ie. the explosive charge radius is made smaller than the borehole radius [1,6,10,19,20,31].

Stage 2

The borehole pressure has reached its maximum value. The rock is in a state of high internal stress but able to contain the high pressure gas and resist the throwing of the burden. The gas forces a path along the cracks, opening and extending them, until a combination of the increased total stress acting on the rock and rock damage causes the rock to fail. The burden starts to move [1,2,6,8,10,14,21,22,23,30,].

Stage 3

The rock is briefly accelerated by the gas and falls to the ground forming the muckpile. Some fragmentation will occur due to collisions of the rock, but this is minimal compared to the fragmentation process occurring during stage 2 [1,7,8,19,31].

A more comprehensive introduction to rock-blasting can be found elsewhere [6,7,10,19,20,31]. Henceforth, we shall only be considering the processes that occur during the relatively unstudied stage 2 phase of rock-blasting.

1.1 The Stage 2 Gas Expansion phase

A Study Case

The Gas Expansion Stage has received little attention in the past, mainly because of the original belief that the stage 1 phase dominated the rock blasting process. A number of blast parameters and conditions have been observed to affect the stage 2 phase and therefore the final fragmentation and muckpile position [6,8,14,19,20,31]. These include:-

i) The geometric layout and firing order of a multi-borehole blast.

ii) The delay time between adjacent blasts. Bench testing experiments show that the best rock fragmentation is obtained with delay times from 0.5 times to 0.75 times the Stage 2 timescale [31] ie. the blasting process and the stress field around the borehole will be semi-developed before a nearby blast (usually the borehole separation is similar to the distance between the borehole and the rockface) is detonated.

iii) The rock face geometry.

iv) Isotropy and pre-existing cracks in the rock.

v) Rock porosity.

A full analysis of all these factors would be an immense task. The aim of this thesis is to study a simple case with blast parameters and conditions that will leave the resulting problem mathematically tractable. Once the basic ideas of the blasting process

are understood, an extension of the model to more complicated cases can be attempted. We shall choose the following :-

i) A single borehole that is very long compared to the crack and gas penetration length around it. This will allow us to ignore any borehole interaction effects and to consider only a 2-D rock blasting model. The 2-D model will not provide a good model of the end regions of the borehole where 3-D effects will occur.

ii) We shall assume that the **stemming** (the packing at the top of the borehole) is sufficient to prevent any unwanted gas losses

iii) The borehole is drilled in an infinite extent of rock or very far away from any rock-face.

iv) The rock is isotropic and hasn't any pre-existing cracks.

v) The rock is non porous.

It has been observed that the planes of each crack in the rock during the stage 2 phase of rock blasting are always along the axis of the borehole [1,8,10,21] (see fig.(1.1;1)).

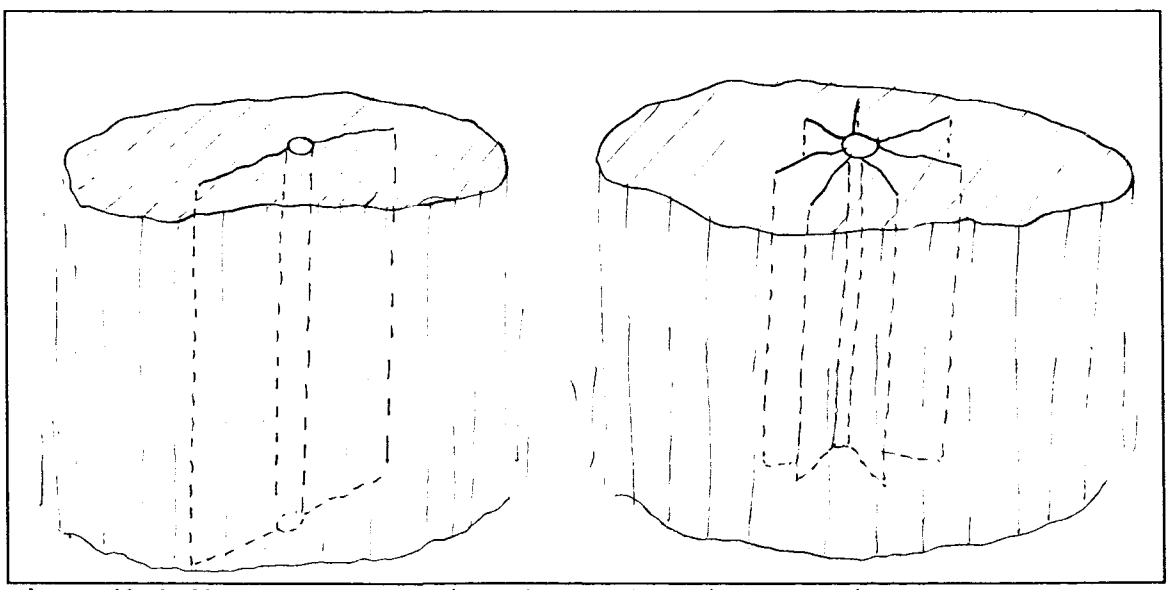

Figure(1.1;1) Crack geometries observed during blasting

The cracks would not in general be perfectly straight lines perpendicular to the borehole but must be so for the study case blast that we have chosen. The number of radial cracks from the borehole depends on the power of the explosive used [1,8,21]. The stress wave of stage 1 initiates the cracking and, as a rule, the higher the borehole pressure at the

beginning of stage 2 the greater the number of radial cracks there will be. Typically only 2 cracks occur for hydro-fracturing, magma flow and low pressure blasts [1,2,21,22,23,30], while 7 or 8 cracks occur during most rock blasts [1,8,21]. The stability of n radial cracks running from the borehole is not well understood. We might expect preferential crack growth in the longer cracks and closing of the lesser cracks. The analysis of the stability will not be covered in this thesis although experimental rock blasting evidence does suggest fairly stable crack growth [8,21].

The simple blast that we shall study here will reveal little information about the fragmentation process in a more complicated blast. The only mechanism that is available to us for rock fracturing is the extension of radial cracks from the borehole due to high tensile forces fracturing the rock at the crack tips. For more realistic blasts the effect of a multi-blast stress field in the presence of a free rock-face in an anisotropic rock with pre-existing cracks creates an extremely complicated stress field and cracking pattern in the rock. The cracks that are generated during this stage of the rock blasting process are the chief factors that determine fragmentation.

We are now going to construct a mathematical model to describe the study case of stage 2 of the rock blasting process set out earlier in this section. In sections 2 and 3 we shall formulate models that describe the crack opening behaviour of rock and the gas flow in cracks respectively. Both of these aspects are brought together in sections 4 and 5 where we obtain the mathematical solutions for gas flowing down cracks in rock and, therefore, solutions to the stage 2 gas expansion phase of rock blasting.

2. THE BEHAVIOUR OF ROCK SUBJECTED TO AN ARBITRARY PRESSURE

2.0 Introduction

The physical behaviour of rock up to quite high stresses is very well approximated by a linear elastic material [17]. Some high powered explosives do however cause some nonlinear effects such as melting, crushing, plastic deformation etc. but these will not be considered here. We shall take the rock to be isotropic. This assumption is valid for many rocks although it should be noted that when anisotropic features of rock exist, the rock blasting process is significantly affected. Using the theory of linear elasticity, the stress-strain distribution of rock is determined for two frequently occuring cracking patterns around the borehole, for an arbitary pressure along the cracks and in the borehole. We can predict when the cracks will propagate by comparing the intensity of the stresses in the rock near the crack tip and the physical strength of the rock. Later on in this thesis we shall see that the heat transfer from the gas to the rock is sufficiently small that thermoelastic effects in the rock are unimportant. We shall only consider the effect of the gas pressure on the stress-strain distribution within the rock since shear stress effects of the gas on the rock will be shown to be negligible.

2.1 The Theory of linear Elasticity

A linear elastic material is one for which the displacement gradients are very small,

$$\left|\frac{\partial u_i}{\partial x_j}\right| \ll 1 \qquad \text{-(2.1;1)}$$

where $\mathbf{x_i}=\mathbf{X_i}+\mathbf{u_i}$

$\mathbf{x_i}$ are the current coordinates

$\mathbf{X_i}$ are the material coordinates

$\mathbf{u_i}$ are the elastic displacement components.

In the classical theory of linear elasticity, there is a linear relationship between the stress τ_{ij} and the strain $\mathbf{E_{ij}}$ through

$$\tau_{ij}=\lambda J_1\delta_{ij}+2\mu E_{ij}$$
$$E_{ij}=\frac{1}{2}\left(\frac{\partial u_i}{\partial x_j}+\frac{\partial u_j}{\partial x_i}\right) \qquad \text{-(2.1;2)}$$

where $J_1=E_{ii}=\text{div } \underline{u}$

λ,μ Lame constants for an isotropic elastic material.

The equation of motion balancing the inertial forces against the body forces and the stress gradients is

$$\rho\frac{Dv_i}{Dt}=\rho b_i+\frac{\partial\tau_{ij}}{\partial x_j} \qquad \text{-(2.1;3)}$$

where $\underline{v}$ is the velocity vector of a particle in the body,

ρ is the rock density (constant to a first approximation),

τ_{ij} is the stress tensor.

$\underline{b}$ is the body force

Combining equations (2.1;2) and (2.1;3) yields the **Navier Equations**

$$\rho\left.\frac{\partial^2\underline{u}}{\partial t^2}\right|_{x_j}=\rho\left.\frac{D^2\underline{u}}{Dt^2}\right|_{x_j}=(\lambda+\mu)\nabla(\nabla.\underline{u})+\mu\nabla^2\underline{u}+\rho\underline{b} \qquad \text{-(2.1;4)}$$

where
$$\left.\frac{\partial}{\partial t}\right|_{\underline{x}}=\left.\frac{D}{Dt}\right|_{\underline{x}}=\left.\frac{\partial}{\partial t}\right|_{\underline{x}}+\underline{v}.\nabla \qquad \text{-(2.1;5)}$$

The Navier Equations are linear. Hence we can find any solution of (2.1;4) with linear boundary conditions as the sum of a complementary function (the equation with $\underline{b}$=0) and a Particular Integral.

2.2 The Quasi-Steady Assumption

If we non-dimensionalise the Navier Equations, we obtain

$$\frac{\rho x_0^2}{\mu t_0^2}\frac{\partial^2\bar{\underline{u}}}{\partial\bar{t}^2}=\left(\frac{\lambda+\mu}{\mu}\right)\bar{\nabla}(\bar{\nabla}.\bar{\underline{u}})+\bar{\nabla}^2\bar{\underline{u}}+\text{CONST}\,\overline{\rho\underline{b}} \qquad \text{-(2.2;1)}$$

where x_0 and t_0 are typical scales for length and time [10,21], and overbarred variables are dimensionless and order unity. The inertial effects will be small if the dimensionless number on the left hand side of (2.2;1) is small, hence

$$(\lambda+\mu)\nabla(\nabla.\underline{u})+\mu\nabla^2\underline{u}+\rho\underline{b}\sim 0$$

$$\text{when } \frac{\rho x_0^2}{\mu t_0^2}\ll 1 \qquad \text{-(2.2;2)}$$

The equation of steady state (2.2;2i) is a good approximation to the time dependent problem (2.1;4) whenever particle velocities within the rock are much smaller than the elastic wave velocity (2.2;2ii). This will be achieved during stage 2 of the rock blasting process apart from the initial transition period from stage 1. Our governing equations can therefore be taken as (2.2;2i).

2.3 The Effects of Pre-Existing Stresses in the Rock

(Solution for the Particular Integral)

The only body force acting on rock is gravity so the body force vector $\underline{b}$ can be written $\underline{b}=(0,0,-g)$. The governing equations of motion (substitute (2.1;2) into (2.2;2)) can be written

$$\frac{\partial\tau_{jx}}{\partial x_j}=\frac{\partial\tau_{jy}}{\partial x_j}=\frac{\partial\tau_{jz}}{\partial x_j}-\rho g=0 \qquad \text{-(2.3;1)}$$

A simple solution can be found by taking the stresses to be independent of **x** and **y**. This solution is that appropriate to a semi infinite extent of unflawed rock. Later it will be seen that this is the most convenient choice for the particular integral. Taking the plane **z=0** to be the stress free upper surface we obtain the stress solutions of (2.3;1) as

$$\tau_{zz}=\rho gz, \qquad \tau_{xz}=\tau_{yz}=0$$

For any given value of the arbitrary stresses $\tau_{xx}(z)$ and $\tau_{yy}(z)$ we can calculate the displacements in the body from (2.1;2). It is found experimentally [25] that the stress distribution in the earth is

$$\tau_{xx}=\beta_1 z-\sigma_1 \quad , \ \sigma_i\sim 5-15\text{MPa}$$

$$\tau_{yy}=\beta_2 z-\sigma_2 \quad , \ \beta_i\sim 2-20\text{MPa/km} \qquad \text{-(2.3;2)}$$

The stress-strain solutions are calculated for the special case $\beta=\beta_1=\beta_2$ and $\sigma=\sigma_1=\sigma_2$ in Appendix A.

From (A2) it is clear that the solution corresponding to the symmetry condition of zero in-plane displacement ($u_r=0$) is

$$\tau_{xx}=\tau_{yy}=\rho g z\left(\frac{\nu}{1-\nu}\right) \Rightarrow \begin{matrix}\beta=7.5\text{MPa/km}\\ \sigma=0\end{matrix} \qquad \text{-(2.3;3)}$$

This solution gives a poor estimate for σ. The large actual observed value for σ arises from the tectonic forces that cause the earth's crust to maintain a state of compression.

As a first approximation of the actual stress distribution given in (2.3;2) we shall take [21]

$$\begin{matrix}\beta=0\\ \sigma=10\ \text{MPa}\end{matrix} \qquad \text{-(2.3;4)}$$

where we have assumed that $\beta z<<\sigma$ for the borehole depth that we are considering. It should be noted that a more complicated model would mean the loss of the symmetry conditions in the following sections 2.4 and 2.9 and hence barely any hope in finding an analytic solution for the stress-strain distribution in rock.

2.4 The Effects of the Gas

(Solution for the complementary function)

In this section we shall look at the stress-strain distribution that is produced by the action of the gas pressure in the borehole and in the cracks, in the absence of gravity and in-situ stress. This effectively gives the complementary function described in section (2.1).

We shall assume that the borehole is very long compared to the crack length around the borehole so that cylindrical symmetry, where the displacements are independent of **z**, can be imposed on the problem. The governing equations of motion (2.1;2) and (2.2;2) with $\underline{b}=0$ will then reduce to both the **antiplane strain** problem for $u_z(x,y)$

$$\nabla^2 u_z=0 \qquad \tau_{xz}=\mu\frac{\partial u_z}{\partial x}\ ,\ \tau_{yz}=\mu\frac{\partial u_z}{\partial y}$$

and the **plane strain** problem for $\mathbf{u_x(x,y)}$ and $\mathbf{u_y(x,y)}$

Cartesian coordinates

$$\nabla^4\chi=\left(\frac{\partial^2}{\partial x^2}+\frac{\partial^2}{\partial y^2}\right)^2\chi=0 \qquad \text{-(2.4;1i)}$$

$$\tau_{xx}=\frac{\partial^2\chi}{\partial y^2}\quad \tau_{xy}=-\frac{\partial^2\chi}{\partial x\partial y}\quad \tau_{yy}=\frac{\partial^2\chi}{\partial x^2} \qquad \text{-(2.4;1ii)}$$

$$\frac{\partial u_x}{\partial x}=\frac{1}{E}(\tau_{xx}-\nu\tau_{yy})\quad \frac{\partial u_y}{\partial y}=\frac{1}{E}(\tau_{yy}-\nu\tau_{xx})$$

Polar coordinates

$$\nabla^4\chi=\left(\frac{1}{r}\frac{\partial}{\partial r}\left(r\frac{\partial}{\partial r}\right)+\frac{1}{r^2}\frac{\partial^2}{\partial\theta^2}\right)^2\chi=0 \qquad \text{-(2.4;2i)}$$

$$\tau_{rr}=\frac{1}{r}\frac{\partial\chi}{\partial r}+\frac{1}{r^2}\frac{\partial^2\chi}{\partial\theta^2}\quad \tau_{\theta\theta}=\frac{\partial^2\chi}{\partial r^2}\quad \tau_{r\theta}=\frac{1}{r^2}\frac{\partial\chi}{\partial\theta}-\frac{1}{r}\frac{\partial^2\chi}{\partial r\partial\theta} \qquad \text{-(2.4;2ii)}$$

$$\frac{\partial u_r}{\partial r}=\frac{1}{E}(\tau_{rr}-\nu\tau_{\theta\theta})\quad \frac{1}{r}\frac{\partial u_r}{\partial\theta}+r\frac{\partial}{\partial r}\left(\frac{u_\theta}{r}\right)=\frac{2(1+\nu)}{E}\tau_{r\theta}$$

where χ is the **Airy Stress Function** and ν and **E** are the usual **Poisson's Ratio** and **Young's Modulus** respectively.

If we assume that the shear stresses τ_{xz} and τ_{yz} are zero at infinity then the solution to the antiplane strain problem is just $\mathbf{u_z}$=0 everywhere.

Next we shall consider the plane strain problem for two different crack geometries around the borehole.

2.5 The Two-Crack problem

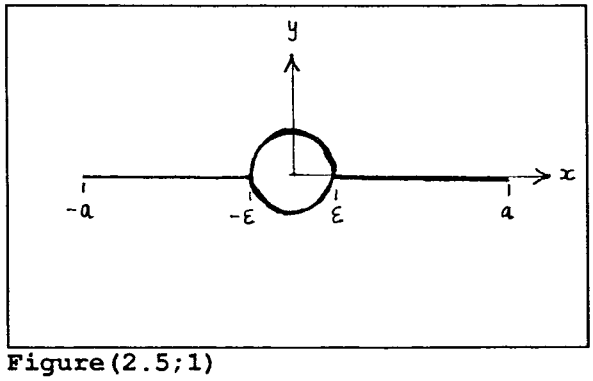

Figure(2.5;1)

$\tau_{rr}=-p(\varepsilon,t)$, $\tau_{r\theta}=0$	on $r=\varepsilon$
$\tau_{xy}=0$	on $x>a$, $y=0$
$\tau_{yy}=-p(x,t)$, $\tau_{xy}=\pm s(x,t)$	on $\varepsilon<x<a$ and $y=\pm 0$
$u_y=0$	on $x>a$ $y=0$
$p(x,t)=p(-x,t)$ and $s(x,t)=-s(-x,t)$	
$\tau_{ij}\to 0$	as $x,y\to\infty$

Both of the cracks from the borehole are assumed to be of the same length and contain

the same gas distribution at all times. For continuity, the borehole pressure $\mathbf{p_b(t)}$ equals the gas pressure at the entrance to the cracks, $\mathbf{p(\varepsilon,t)}$. If the crack length **a** is much longer than the borehole radius $\boldsymbol{\varepsilon}$ (see fig(2.5;1)) then this two crack problem can be asymptotically approximated by an inner solution near the borehole and an outer solution along the rest of the crack. Since the local strains around the borehole are small compared to the global strains caused by the outer region, a first approximation for the large crack length problem is to ignore the borehole geometry and consider a single straight crack. (NB. This does not necessarily mean that we can neglect other borehole quantities such as total force or gas volume eg. $\int_0^{\varepsilon} \mathbf{p}\ dy=\boldsymbol{\varepsilon}\mathbf{p_b}$)

The problem defined with $\boldsymbol{\varepsilon}=0$ was the first crack problem to be addressed and is often referred to as the **Griffith Crack** problem. The solutions for $\mathbf{u_y}$ when $\mathbf{s(x)}=0$ and the crack pressure is $\mathbf{p(x)}$ are [29]

$$u_y|_{y=0}=\frac{16(1-\nu)a}{\pi E}\int_{\frac{x}{a}}^{1}\frac{t}{\sqrt{t^2-\left(\frac{x}{a}\right)^2}}\int_0^t\frac{p(u)\ du}{\sqrt{t^2-u^2}}\ dt \quad |x|<a$$

$$\text{where} \int_{-\varepsilon}^{\varepsilon} p\ dy=2\varepsilon p_b \qquad \text{-(2.5;1)}$$

$$K=\lim_{\substack{x\to a_+\\ y=0}}((2(x-a))^{\frac{1}{2}}\tau_{yy})=\frac{2(2a)^{\frac{1}{2}}}{\pi}\int_0^a\frac{p(u)\ du}{\sqrt{a^2-u^2}} \qquad \text{-(2.5;2)}$$

where **K** is known as the **Stress Intensity Factor** (see section 2.7).

In Appendix B the Griffith Crack problem is solved with both pressure and shear stresses acting [9], and the solution is written as

$$p(x,t)=-\frac{\mu}{2\pi(1-\nu)}\int_{-a}^{a}\left(\frac{\partial u_y}{\partial\zeta}+\frac{1-2\nu}{\mu}s(\zeta)\right)\frac{d\zeta}{\zeta-x} \qquad \text{-(2.5;3)}$$

This solution with the shear stress along the crack $\mathbf{s(x)}=0$ is the inverted form of (2.5;1) that has been used in calculating the flow of magma in rocks [30].

LIBRARY

2.6 The Multi-Radial Crack Problem

2.6.1 Introduction

The cracks from the borehole are assumed to be of the same length, equally separated by an angle 2α and contain the same gas distribution at all times. For continuity, the borehole pressure $\mathbf{p_b(t)}$ equals the gas pressure at the entrance to the cracks, $\mathbf{p(\varepsilon,t)}$. The symmetry of this problem means that we only need to consider a single pie-shaped segment of the rock (see fig(2.6.1;1))

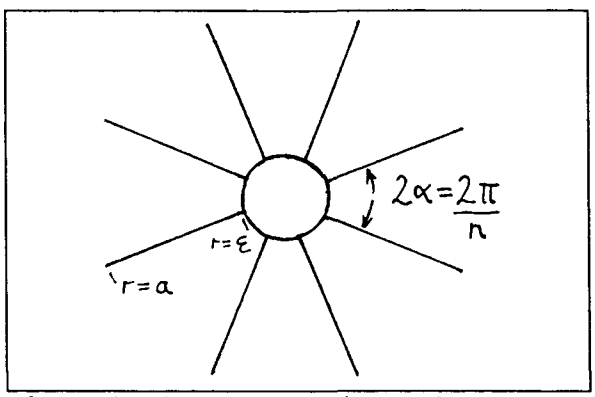

Figure(2.6.1;1) multi-crack geometry

$\tau_{rr}=-p(\varepsilon,t)$, $\tau_{r\theta}=0$ on $r=\varepsilon$

$\tau_{\theta\theta}=-p(r,t)$ on $\varepsilon<r<a, \theta=\pm\pi k/n$

$\tau_{r\theta}=0$ on $r>\varepsilon$, $\theta=\pm\pi k/n$

$u_\theta=0$ on $r>a$, $\theta=\pm\pi k/n$

$\tau_{ij}\rightarrow 0$ as $r\rightarrow\infty$

where $k=1,3,5...$

n number of cracks

A special case of this problem with $\varepsilon=0$, known as the **starcrack** problem, has received some attention in the past [35,36]. Solutions were sought via the Wiener-Hopf technique after taking Mellin transforms of the plane strain equations (2.4;2). Explicit analytical expressions for the crack height in terms of pressure were unobtainable. For the case of constant crack pressure p_0 however an asymptotic expression for the Stress Intensity Factor for large n was hypothesised [35] and proved [36] to be

$$K\sim 2p_0\sqrt{\frac{a}{n}} \qquad n>1 \qquad \text{-(2.6.1;1)}$$

An asymptotic expression of the Stress Intensity Factor when there is a central splitting force F (a force acting at the point (0,0) pushing each pie shaped segment radially outwards) and zero crack pressure has also been obtained for a starcrack [24] as

$$K\sim\frac{F}{2}\left(\frac{n}{\pi a}\right)^{\frac{1}{2}} \qquad n>1 \qquad \text{-(2.6.1;2)}$$

During rock blasting, six to eight radial cracks are usually observed to emanate

from the borehole. To render the multi-radial crack problem tractable we shall look for the asymptotic solution for large **n**. The errors arising from this approach will arguably be no more than those incurred by assuming that the radial cracking during rock blasting is perfectly symmetric.

To date there have been two attempts to calculate this asymptotic model, but both are fundamentally incorrect.

i) H.Erhie [10] "The radial component of displacement is assumed to be zero." This assumption is incorrect and results in the model only having a local crack opening behaviour

$$\underline{u}=\left(0,\frac{-p(r)(1-\nu^2)}{E}y\right) \qquad \begin{aligned}\tau_{yy}&=-p(r)\\ \tau_{xx}&=-\nu p(r)\\ \tau_{xy}&=0\end{aligned} \qquad \text{-(2.6.1;3)}$$

and a crack front condition of zero gas pressure.

ii) R.H.Nilson [21] "The crack heights for the starcrack problem are assumed to be equivalent to those for a Griffith Crack multiplied by a constant factor." The stress intensity factor at the crack-tips is similarly derived in terms of the Griffith Crack result. Its average value is chosen by Nilson to lie between the special cases given in equations (2.6.1;1&2) through

$$K_{Nil}=\frac{1}{2}\left[\frac{\frac{F}{2}\left(\frac{n}{\pi a}\right)^{\frac{1}{2}}}{K(F=cent.split.force)}+\frac{2p_0\sqrt{\frac{a}{n}}}{K(const.press.p_0)}\right]K(p(r)) \qquad \text{-(2.6.1;4)}$$

where **K(p(r))** is the stress intensity factor for the Griffith Crack.

This model is fundamentally flawed because the stress-strain distribution of a Griffith Crack bears little resemblance to that of a single arm of the starcrack.

2.6.2 A New Asymptotic Model for the Multi Radial Crack problem

A Physical Representation

The asymptotic analysis for this problem is very lengthy and can be found fully outlined in Appendix C. By performing a small amount of algebraic manipulation on these solutions the dominant physical stress-strain behaviour (ie the first order asymptotic

solutions) can be explained in a very neat manner.

i)The cracked and borehole region

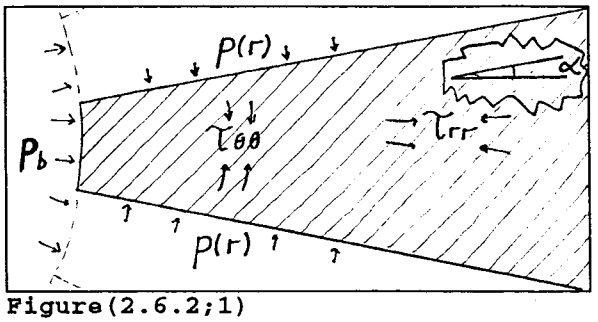

Figure(2.6.2;1)

The wedge is thin so that hoop and shear stresses are uniform through the wedge ie. $\tau_{\theta\theta}$=-**p(r)** and $\tau_{r\theta}$=**0**. The radial stress is the sum of all the radial forces averaged over the length 2rα at radius **r** (C17),

$$\tau_{rr} \propto \frac{1}{2r\alpha}\left[-2\varepsilon\alpha p_b - 2\sin\alpha\int_{\varepsilon}^{r} p(r)dr\right]$$

$$= \frac{1}{2r\alpha}\left[\begin{pmatrix}\text{radial}\\ \text{forces}\\ \text{from}\\ \text{borehole}\end{pmatrix}+\begin{pmatrix}\text{radial}\\ \text{forces}\\ \text{from}\\ \text{crack}\end{pmatrix}\right]$$

$$\propto -\frac{1}{r}\left[\varepsilon p_b + \int_{\varepsilon}^{r} p(x)dx\right]$$

The hoop component of displacement (C17), which equals half the crack height along $\theta=\pm\pi/\mathbf{n}$, is

$$u_\theta = \frac{\theta r}{E}(\tau_{\theta\theta} - \nu\tau_{rr}) - \theta u_r$$

$$= \begin{Bmatrix}\textit{local}\\ \textit{strain}\end{Bmatrix} + \begin{Bmatrix}\textit{wedge}\\ \textit{divergence}\end{Bmatrix}$$

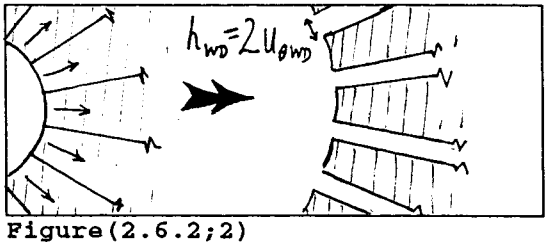

Figure(2.6.2;2)

where the local displacement is approximately equal to the displacement in a piece of rock with parallel sides, and the divergence part is the gap created between the wedge pieces as they are all pushed radially outwards (Figure(2.6.2;2)).

ii) The crack tip region

The geometry of the crack tip region approaches that of an infinite row of parallel semi-infinite cracks.

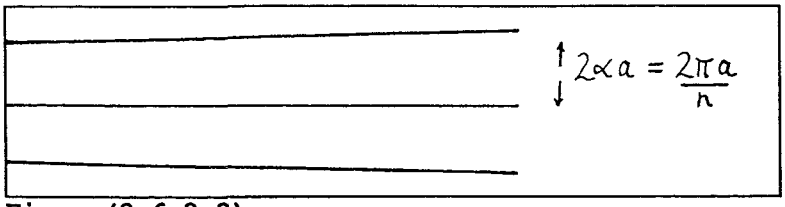

Figure(2.6.2;3)

In this case the Stress Intensity Factor for a constant crack pressure is $K=p(a)\sqrt{(a/n)}$ [28]. The Stress Intensity Factor for the multi radial crack problem (C18) is

$$K = \sqrt{\frac{a}{n}}\left[p(a)+\frac{1}{a}\left(\varepsilon p_b+\int_{\varepsilon}^{a} p(y)dy\right)\right]$$

$$= \left\{\begin{matrix}\text{from}\\ \text{pressure}\\ \text{at tip}\end{matrix}\right\}+\left\{\begin{matrix}\text{from}\\ \text{divergence}\\ \text{at tip}\end{matrix}\right\}$$

iii) The outer region

Stresses decay as $1/r^2$ and radial displacement as $1/r$ which is the same as the case of the stress-strain distribution around a uniformly loaded hole of radius **a**.

2.7 Crack Propagation and the Stress Intensity Factor

As the gas from the borehole penetrates the cracks, stresses at the crack tips will eventually exceed the strength of the rock and cause the cracks to propagate. The rock blasting model that we consider will only allow the cracks to propagate in straight lines, which means that by symmetry shear forces at the crack tips are zero. The crack tip condition therefore is that the tensile stresses at the crack tip must be less than or equal to the material strength of the rock [2,33].

The crack tip stresses that we have derived for our crack geometries have square root singularities. This is a general feature for any given crack geometry [33] when using the theory of linear elasticity. An infinite stress at the crack tip cannot exist and, in reality, around the crack tip the small strain rate assumption (2.1;1) is violated and a zone

of non-linear rock behaviour occurs. Our model is reasonable however, since it has been argued that [2]:-

i) The non-linear zone is usually small compared to the crack geometry length scale.

ii) The linear elastic solution is still the valid solution outside the non-linear zone.

iii) A local analysis of the non-linear zone shows that the amplitude of the stress intensity, the **Stress Intensity Factor K**, cannot exceed the **Physical Stress Intensity Factor K_{phys}** of a given material.

$$K=\lim_{\substack{r\to a \\ \theta=\pm\frac{\pi k}{n}}} \left\{(2(r-a))^{\frac{1}{2}}\ \tau_{\theta\theta}\right\} \qquad \text{-(2.7;1)}$$

$$K \le K_{phys}$$

The values of K_{phys}'s are given in [1] for various types of rock and range from about 0.1 to 5 MPa $m^{0.5}$.(NB. some authors use a factor 2π in place of the **2** in the above expression for **K**.)

Illustrative example: In granite a Griffith Crack of length 4 m is slowly filled with fluid. At what fluid pressure will the crack tip propagate ?

Answer: From (2.5;2) $K=p_0\sqrt{c}$ for a fluid of constant pressure in a Griffith Crack of length c. The K_{phys} for granite is 2 MPa $m^{0.5}$ [1] so the crack will start to propagate when $2p_0=2$ ie. $p_0=1$ MPa.

As the crack tip marches forward through the uncracked rock, the crack volume will increase thus reducing the fluid pressure. In fact, once the crack tip is in a state of forward propagation through un-cracked rock then **K** is maintained at K_{phys}

$$K=K_{phys} \qquad \text{-(2.7;2)}$$

In real crack propagation K_{phys} may increase slightly with fracture velocity [1], although this effect will not be of major significance and is ignored in this thesis. If a pre-existing crack is being opened then **K**=0 as the crack tip advances.

2.8 The Effects on the Crack Height of Shear Stress along the cracks.

In section 3 we shall see that the Mach number during rock blasting is small so that the equations of motion for the gas reduce to the pressure gradient balancing the

effective shear stress on the crack wall.

$$s(x)=\frac{h}{2}\frac{\partial p}{\partial x} \qquad \text{-(2.8;1)}$$

If in the Griffith Crack problem, with solution (2.5;3), a pressure **p** yields a crack height **h** when **s(x)=0**, then including a shear stress **s(x)** and maintaining the same crack height would require a pressure **P**, where

$$p=P+\frac{1-2\nu}{2\pi(1-\nu)}\int_{-a}^{a} h\frac{\partial P}{\partial x}\frac{d\zeta}{\zeta-x} \sim P+O\left(\frac{y_0}{x_0}\right) \qquad \text{-(2.8;2)}$$

In the lubrication approximation, y_0/x_0 tends to zero (see page 33), so we have **P≈p**, showing that shear stress effects are negligible. Similarly, for the **n** crack problem, shear stresses would only affect crack height if **s(x)~O(πp/n)** (Appendix C), ie. since shear stresses **s** are **O(py$_0$/x$_0$n)** then they can be neglected because $\pi >> y_0/x_0$.

2.9 The In-Situ Stress Dominant Crack Model

If we add the particular integral and complementary function solutions together we obtain the linear elastic solution for the crack problems under discussion. The correct boundary conditions are maintained because the particular integral obeys the conditions of zero shear stress and zero perpendicular displacement along the lines of the cracks. The main difference between the complementary function and the full solution is that the pressure **p** is replaced by **p-σ**. The crack-length equations ((2.5;2) and (C18)) for the two-crack and **n**-crack problems can now be written

$$K=\sqrt{\frac{a}{n}}\left[p(a)+\frac{1}{a}\left(\varepsilon p_b+\int_{\varepsilon}^{a} p\,dy\right)-2\sigma\right] \qquad \text{n crack}$$

$$K=2\frac{(2a)^{\frac{1}{2}}}{\pi}\int_{0}^{a}\frac{p(u)-\sigma}{\sqrt{a^2-u^2}}du \qquad \text{2 crack} \qquad \text{-(2.9;1)}$$

$$\text{where} \quad \int_{0}^{\varepsilon} p\,dy=\varepsilon p_b$$

The crack length is a function of **K** and σ. The Stress Intensity factor **K** is the resistance

to crack propagation arising from the rock strength, whereas the in-situ stress σ is an all round clamping stress which pushes the cracks back together. For many rock blasting situations the action of the in-situ stress on crack length is, at least initially, the most significant effect. An expansion of (2.9;1i) for large σ gives

$$a \sim \frac{\left(\varepsilon p_b + \int_{\varepsilon}^{a} p dy\right)}{2\sigma - p(a)} \qquad \text{-(2.9;2)}$$

$$\text{provided} \quad \frac{nK^2}{(2\sigma - p(a))(\varepsilon p_b + \int_{\varepsilon}^{a} p dy)} < 1$$

an inequality which is valid for a large portion of many blasts. Equation (2.9;2) will be used frequently in section 5.

3. THE BEHAVIOUR OF GAS PASSING THROUGH ROCK

3.0 Introduction

We shall now consider how gas flows through cracks within rock. This requires us to consider a compressible gas flowing down a narrow channel at high pressures. A number of typical parameters for both rock and gas will be needed in order to determine what type of gas flow we must consider. The parameters we shall use are [10,21]:-

	[21]	[10]
Peak Borehole Pressure $\mathbf{p_b(0)}$	90×10^6 Pa	10^9
Peak Borehole Density $\rho_b(0)$	500 kg/m^3	same as [21]
In-situ Stress σ	10×10^6 Pa	"
Initial Gas Temperature $\mathbf{T(0)}$	3000 K	1000
Specific Heat at constant volume $\mathbf{c_v}$	1000 J/(kg K)	same as [21]
Specific Heat at constant pressure $\mathbf{c_p}$	1400 J/(kg K)	2500
Number of Cracks $\mathbf{n}$	7	same as [21]
Young's Modulus $\mathbf{E}$	5.5×10^{10} Pa	"
Poissons Ratio ν	0.3	"
Borehole Radius ε	0.1 m	"
Gas Viscosity μ	5×10^{-5} Pa s	"
Gas Thermal Conductivity $\mathbf{k}$	7×10^{-2} kg m/(s^3 K)	"
Rock Thermal Conductivity $\mathbf{k_{rock}}$	2 kg m/(s^3 K)	"
Stress Intensity Factor $\mathbf{K}$	1×10^6 Pa m$^{0.5}$	"

where the parameters in [21] are from a bench blasting experiment and those given in [10] are more typical for a full scale field blast.

The experiments in [10,21] involve cracks that run out to 10 and 2.5m. By using these values for $\mathbf{a}$, the above values for $\mathbf{p_b(0)}$, $\mathbf{K}$ and σ and the crack opening equations (2.9;1), we can find the appropriate typical length scales for crack height and gas penetration length.

	[21]	[10]
Typical crack height y_0	$1x10^{-3}$ m	$1x10^{-2}$
Typical gas penetration length x_0	1 m	0.3

3.1 The General Governing Equations

The gas flow is governed by the usual conservation equations [11]

3.1.1 The Conservation of Mass

$$\underset{(i)}{\frac{\partial \rho}{\partial t}} + \underset{(ii)}{div \rho \underline{v}} \equiv \frac{D\rho}{Dt} + \rho div \underline{v} = 0 \qquad \text{-(3.1.1;1)}$$

The rate of change of mass in any fixed volume (i) balances the flux of mass through the surface of that volume(ii).

3.1.2 The Conservation of Momentum

$$\underset{(i)}{\rho \frac{D\underline{v}}{Dt}} = \underset{(ii)}{\rho \underline{b}} \underset{(iii)}{- \nabla p} + \underset{(iv)}{\mu \nabla^2 \underline{v}} \qquad \text{-(3.1.2;1)}$$

The rate of change of momentum (i) balances the total forces acting, which are the body force (ii), the pressure gradients (iii) and shear stress gradients (iv).

In deriving this equation we had to assume that:

i) The fluid viscosity μ is constant.

ii) The molecular forces acting in addition to the pressure forces (the **Bulk Viscosity**) are small and can be neglected. The gas pressure then becomes independent of fluid velocity [11] and can be expressed as $\mathbf{p=p(\rho,T)}$. This relation is called the equation of state.

The Equation of State

For an ideal gas, the theory of thermodynamics gives $\mathbf{p=\rho RT}$, but a more realistic equation in rock blasting is $\mathbf{p=\rho^2 ST}$ (**R** and **S** are gas constants). An incompressible fluid (such as water with pressures $<<3x10^8$Pa) has ρ=**CONST**. In summary, the equation of state can be written as

$$p = \rho^{\alpha} R_{\alpha} T \qquad \text{-(3.1.2;2)}$$

where α=1 $\Rightarrow$Ideal, $2<\alpha<2.5$ $\Rightarrow$Rock Blasting [10], $\alpha>>1$ $\Rightarrow$Incompressible

3.1.3 The Conservation of Energy

$$\underset{(i)}{\rho\frac{D}{Dt}\left(c_v T+\frac{|\underline{v}|^2}{2}\right)}\underset{(ii)}{+p\nabla.\underline{v}}\ =\ \underset{(iii)}{k\nabla^2 T}\ +\ \underset{(iv)}{\Phi} \qquad \text{-(3.1.3;1)}$$

where

$$\Phi=\mu\left[2\left[\left(\frac{\partial u}{\partial x}\right)^2+\left(\frac{\partial v}{\partial y}\right)^2+\left(\frac{\partial w}{\partial z}\right)^2\right]+\left(\frac{\partial v}{\partial x}+\frac{\partial u}{\partial y}\right)^2+\left(\frac{\partial w}{\partial y}+\frac{\partial v}{\partial z}\right)^2+\left(\frac{\partial u}{\partial z}+\frac{\partial w}{\partial x}\right)^2-\frac{2}{3}(\nabla.\underline{v})^2\right]$$

The rate of change of the total energy (i), which is the sum of the internal energy and the kinetic energy, must balance the work done by the pressure (ii), the flux of heat by conduction (iii) and the viscous heating (iv) (potential energy is ignored as $c_v T>>gz_0$).

3.2 Analysis to obtain the resulting Turbulent Gas Flow Equations

3.2.1 Introduction to turbulence

The appropriate Reynolds number for gas flow in a crack for our problem is

$$\mathrm{Re}=\frac{\rho_0 u_0 y_o}{\mu}\quad =O(10^5 u_0) \qquad \text{-(3.2.1;1)}$$

which indicates that the flow will be **turbulent**. Unfortunately turbulent flow is not well understood. As a rule a large Reynolds number flow is unstable to small perturbations so that energy from the mean flow is quickly transferred to small vortex regions, called **eddies**, within the fluid. The flow, which may have been a very simple 2-dimensional flow at low Reynolds numbers, becomes a highly intricate 3-dimensional flow at high Reynolds numbers. In principle this behaviour can still be modelled by the flow equations in section (3.1) because the small eddy length scale is still large compared to the length scale over which the continuum hypothesis fails. In practice this approach cannot be adopted. Even the most powerful computers today cannot process the amount of data that would be generated by a 3-dimensional flow whilst retaining the intricate eddy behaviour.

To proceed with the analysis of turbulence in an analytical manner we must make some quite sweeping simplifications. These are based on empirical observations of the general behaviour of turbulent flow [3,4,5,13,27], namely

i)When experiments are repeated for a particular turbulent flow, it is observed that each experiment has the same average flow behaviour, with a superimposed small

apparently random fluctuation about this average flow value. Thus, for example, the turbulent velocity can be expressed

$$u_i=\bar{u}_i+u_i' \quad \bar{u}_i'=0 \qquad \text{-(3.2.1;2)}$$

where $\overline{}$ denotes the average over many experiments and $'$ the fluctuating part of the fluid velocity for one experiment.

ii)The density fluctuations ρ' can usually be neglected in the turbulent flow equations, provided the Mach number of the flow is less than about 5, and across the flow the temperature varies from its mean by less than about 500%. In many situations, therefore, we can assume that

$$\rho=\bar{\rho}+\rho'\simeq\bar{\rho} \qquad \text{-(3.2.1;3)}$$

iii)Turbulent fluctuations are three dimensional even when the mean flow is only one or two dimensional and the components of a fluctuating vector quantity are the same order of magnitude.

iv)We assume that the fluctuating terms for pressure and velocity are much smaller than their mean values. ie. the turbulent intensity is quite small.

If we substitute equations (3.2.1;2) and (3.2.1;3) into the mass equation (3.1.1;1), and then average the equation over many experiments, we find that

$$\frac{\partial\bar{\rho}}{\partial t}+div(\bar{\rho}\,\bar{\underline{v}})=0 \qquad \text{-(3.2.1;4)}$$

and

$$div(\overline{\rho\underline{v}})=0 \qquad \text{-(3.2.1;5)}$$

The mass conservation law for mean flow variables (3.2.1;4) is unchanged in form from (3.1.1;1). Equation (3.2.1;5) says that the turbulent mass flux at any point is zero, which is consistent with the zero density fluctuation assumption (3.2.1;3). In a similar way we can use the assumptions (i) to (iv) to derive the momentum equation for averaged flow variables (ignoring the body forces from gravity as $\mathbf{p_o}>>\rho g\mathbf{x_0}$)

$$\bar{\rho}\frac{\overline{D\underline{v}}}{Dt}=-\nabla\bar{p}-\frac{\partial}{\partial x_j}\left(\overline{\rho u_j'\underline{v}'}\right)+\mu\nabla^2\bar{\underline{v}} \qquad \text{-(3.2.1;6)}$$

This equation is similar to (3.1.2;1), but we have an additional term on the right hand side which has originated from the fluctuating inertial terms. This extra term

$$\sigma_{ij}=\overline{\rho u_i'u_j'} \qquad \text{-(3.2.1;7)}$$

acts like a stress and is often referred to as the **Reynolds Stress**. Similarly the heat equation (3.1.3;1), ignoring the kinetic energy terms ($v^2_0 << 2c_v T_0$), becomes

$$\bar{\rho}\frac{\bar{D}}{Dt}(c_v\bar{T})+\bar{p}\nabla.\underline{\bar{v}}=k\nabla^2\bar{T}-\frac{\partial}{\partial x_i}(c_v\overline{\rho u_i'T'})+\bar{\Phi} \qquad \text{-(3.2.1;8)}$$

This equation is similar to (3.1.3;1) except for a term which originates from the fluctuating inertial energy transport which behaves as an additional conducting term on the right hand side. This effective turbulent conductivity usually swamps the effect of the real heat conduction and the viscous dissipation terms.

Equations (3.2.1;4,6 and 8)) can now be expressed in an approximate form by introducing the lubrication approximation, $y_0/x_0 \to 0$, and the small Mach number approximation, $\rho u_0^2/p_0 \to 0$. The resulting system is

$$\frac{\partial\bar{\rho}}{\partial t}+div(\overline{\rho\underline{v}})=0$$

$$\frac{\partial\bar{p}}{\partial x}+\frac{\partial}{\partial y}(\overline{\rho u'v'})=0 \qquad \text{-(3.2.1;9)}$$

$$\text{(i)}$$

$$\text{(ii)}$$

$$\frac{\partial\bar{p}}{\partial y}=0 \quad \rightarrow \bar{p}=\bar{p}(x,t) \qquad \text{(iii)}$$

$$\text{(iv)}$$

$$\bar{p}=\bar{\rho}^{\alpha}R_{\alpha}\bar{T} \qquad \text{(v)}$$

$$\bar{\rho}\frac{\bar{D}(c_v\bar{T})}{Dt}+\bar{p}\nabla.\underline{\bar{v}}=k\frac{\partial^2\bar{T}}{\partial y^2}-\frac{\partial}{\partial y}(c_v\overline{\rho v'T'})+\bar{\Phi}$$

To complete the above system it is necessary to add equations for the averaged fluctuating products. These can be expressed in terms of higher order products which are then expressed empirically, but this makes the resulting equations far more complicated. We shall look at the simplest Zeroth Order model of turbulence where the fluctuating cross products in (3.2.1;9) are determined empirically.

3.2.2 The Eddy Viscosity and Eddy Conductivity Concept

Standard representations for the averaged fluctuating products are the eddy viscosity and eddy conductivity equations [3,4,5,15,27]

$$\rho\overline{u'v'}=-\rho\varepsilon_m\frac{\partial\bar{u}}{\partial y}\ ,\ \rho\overline{vT}=\rho\varepsilon_h\frac{\partial T}{\partial y} \qquad \text{-(3.2.2.;1)}$$

where ε_m and ε_h are quantities that can be determined empirically. Values for ε_m and ε_h have been given for many types of turbulent flow [3,4,5,13,27]. A useful parameter in turbulent flow is the Prandtl Number, defined through $\mathbf{Pr}=\varepsilon_m/\varepsilon_h$. A common assumption in turbulent flow is that $\mathbf{Pr}=1$ which is called the **Reynolds analogy**. This indicates that the same mechanism drives the turbulent viscosity and the turbulent conductivity [15]. Although this assumption is not exactly satisfied for many flow situations the Prandtl Number will always be of order unity. From equations (3.2.1;9) and (3.2.2;1) we can determine a size for the product $\overline{v'T'}$ as

$$\overline{vT} \sim O\left(\frac{p_0 y_0 T_0}{\rho x_0 u_0}\right) \qquad \text{-(3.2.2;2)}$$

Non-dimensionalisation of the energy equation (3.2.1;9v) shows that the viscous heating terms are very small ($\mu << \rho c_v T_0 y_0^2/x_0 u_0$ and $\mu << \rho y_0 u_0$) so we shall neglect this henceforth. Also the turbulent conductivity term is much larger than any other energy transfer term (as $p_0 >> \rho u_0^2$). Therefore a first approximation to the energy equation with the aid of (3.2.2;1), (3.2.1;9iii and iv) and assuming ε_h is constant across the crack is

$$\frac{\partial}{\partial y}(c_v \rho \overline{v'T'}) = 0 \quad \Rightarrow \overline{T} = \overline{T}(x,t) \qquad \text{-(3.2.2;3)}$$

This equation shows that a temperature gradient cannot exist across the crack. In view of the fact that p and ρ are also constant across the crack width (3.2.1;9), the integration of the gas flow equations (3.2.1;9) over the crack width can then easily be performed. This is a wise manoeuvre because we would obtain a simpler set of equations without losing information about any of the quantities we need in future analysis. Pressure as a function of crack height is preserved, whereas fluid velocity along the crack, which we do not really need to know about specifically , is now averaged across the crack.

After integration, the system of equations (3.2.1;9) become (dropping the average bar notation)

$$\frac{\partial(\rho h)}{\partial t} + \frac{\partial(\rho u h)}{\partial x} = 0 \qquad \text{-(3.2.2;4)}$$

$$h\frac{\partial p}{\partial x} + \rho(\overline{u'v'})\Big|_{-\frac{h}{2}}^{\frac{h}{2}} = 0 \qquad \text{(i)}$$

$$p = \rho^{\alpha} R_{\alpha} T \qquad \text{(ii)}$$

$$\text{(iii)}$$

$$\frac{\partial(\rho h c_v T)}{\partial t}+\frac{\partial(\rho u h c_v T)}{\partial x}+p\left(\frac{\partial h}{\partial t}+\frac{\partial(uh)}{\partial x}\right)=k\frac{\partial T}{\partial y}\Big|_{-\frac{h}{2}}^{\frac{h}{2}}-(\rho c_v\overline{v'T'})\Big|_{-\frac{h}{2}}^{\frac{h}{2}} \qquad \text{(iv)}$$

$$\text{where}\quad u(x,t)=\frac{1}{h}\int_{-\frac{h}{2}}^{\frac{h}{2}}\bar{u}(x,y,t)\,dy \qquad \text{(v)}$$

$$h=h(x,t)=\{\text{crackheight}\}$$

The turbulent conduction terms are not nescessarily zero at the crack walls because a boundary layer very near the crack walls may allow heat exchange from the gas to the rock even though from (3.2.2;3) the gas temperature is fairly constant across the crack.

3.2.3 The Heating of the Rock by the Gas

The terms on the right hand side of the heat equation (3.2.2;4iv) represent the heat that flows from the gas into the rock by conduction so can also be written

$$k\frac{\partial T}{\partial y}-\rho(c_v\overline{v'T'})\Big|_{-\frac{h}{2}}^{\frac{h}{2}}=2k_{rock}\frac{\partial T}{\partial y}\Big|_{y=\frac{h}{2}} \qquad \text{-(3.2.3;1)}$$

A full treatment of the heat equation (3.2.2;4iv) would require the solution of the heat equation in the rock so that the heat flux from the gas into the rock could be determined at any time. This would add another partial differential equation into the system of equations in (3.2.2;4). As a first approximation to this complicated problem, let us assume the heat flow into the rock is small compared to the other terms in the energy equation. In this case (3.2.2;4iv) reduces to

$$\frac{\partial(\rho h c_v T)}{\partial t}+\frac{\partial(\rho u h c_v T)}{\partial x}+p\left(\frac{\partial h}{\partial t}+\frac{\partial(uh)}{\partial x}\right)\approx 0 \qquad \text{-(3.2.3;2)}$$

$$\text{provided}\quad u_0>\frac{k_{rock}x_0}{\rho y_0^2 c_v}$$

This is the **Adiabatic Approximation** which is quite a good approximation for the blast parameters stated in (3.0).

Equation (3.2.3;2) can be solved analytically by using the mass continuity and state equations (3.2.2;4i and iii) to express it in an integrable form with respect to the

total derivative D/Dt, to give

$$p \propto \rho^{\alpha} \exp\left(\frac{\rho^{\alpha-1} R_{\alpha}}{c_v(\alpha-1)}\right) \quad \alpha \neq 1$$

$$p \propto \rho^{\gamma} \qquad \alpha = 1 \qquad \text{-(3.2.3;3)}$$

$$\text{where} \quad \gamma = 1 + \frac{R_1}{c_v}$$

and α is the index of ρ in the equation of state (3.2.2;4iii).

When the work done by the pressure is small compared to the inertial transport of energy $p_0 << \rho_0 c_v T_0$ there is no remaining mechanism left to change the fluid temperature, so we have **Isothermal flow.**

To complete the fluid equations we need an empirical relation for the Reynolds stress. This reduces to choosing from the relevant literature suitable $\bar{u}$ and ε_h for the eddy viscosity model (3.2.2;1) . A simple empirical model by Hirs [13] based on the **Mixing Length** hypothesis [15,27] is

$$\rho \left.\overline{u'v'}\right|_{-\frac{h}{2}}^{\frac{h}{2}} = l\rho u^2 \qquad \text{-(3.2.3;4)}$$

$$\text{where } l \simeq 0.1$$

and a less accurate, but often adopted, model based on a simple choice of $\bar{u}$ and ε_m in the **Eddy Viscosity** concept [10,15,27] gives

$$\rho \left.\overline{u'v'}\right|_{-\frac{h}{2}}^{\frac{h}{2}} = 12\frac{\mu_{turb} u}{h} \qquad \text{-(3.2.3;5)}$$

where the Reynolds stress acts like the viscous stresses in laminar flow, but typically $\mu_{turb} >> \mu$.

3.2.4 Summary

In our model we shall consider either isothermal gas flow or adiabatic gas flow for an ideal gas. The turbulent friction term in the momentum equation is modelled by either an empirically based model (3.2.3;4) or an increased viscosity model (3.2.3.;5). The former model will probably be more accurate although we shall still keep the latter model

for ease of analysis. Substituting the momentum equation into the mass equation (3.2.2;4) the final form of the gas flow equations is

$$\frac{\partial(\rho h)}{\partial t} = \frac{1}{12\mu_{turb}} \frac{\partial}{\partial x}\left(\rho h^3 \frac{\partial p}{\partial x}\right) \quad \text{Eddy-Viscosity Model}$$

$$\frac{\partial(\rho h)}{\partial t} = -\frac{\partial}{\partial x}\left[\left(-\frac{h^3 \rho}{l}\frac{\partial p}{\partial x}\right)^{\frac{1}{2}}\right] \quad \text{Mixing Length Model} \qquad \text{-(3.2.4;1)}$$

$$\text{where} \quad \rho = K_g\, p^{\frac{1}{\gamma}} \qquad 1<\gamma<2.5$$

$$l \approx 0.1$$

assuming that all the assumptions for the model given through this section hold. The dimensionless parameters that were assumed to be small are summarised in section 4.

3.3 The Boundary and Initial Conditions of the Gas Flow

The gas flow equations that we have just derived are **parabolic** because of the omission of the inertial terms from (3.2.1;8) for low Mach numbers. If the inertial terms were included, the flow would of course be hyperbolic [32].

To ensure that a parabolic equation of this type is well posed, we need the initial condition of the gas distribution and a boundary condition at each end of the gas for all time [32].

i)The Initial Condition

At zero time we assume that the stage 1 process, described in section 1.0, is complete and gas commences to flow into the cracks. A transitional period between stages 1 and 2 will occur in practice but, as a first approximation, we can assume that stage 2 commences with all the gas from the explosion still contained in the borehole. We shall also assume that the gases are fully burnt at the beginning of stage 2, ie.

$$p(x,t)\big|_{t=0} = 0 \quad x>\varepsilon$$

$$\{\text{Initial borehole pressure}\} = p(\varepsilon,t)\big|_{t=0} = p_b(0) \qquad \text{-(3.3;1)}$$

ii)The Boundary Condition at the Gas Front

From the crack-length equations (2.9;1) we can see that the position of the crack

tip is independent of the gas front position so that in general a separate gas and crack front will exist. The condition to be imposed at the gas front at **x=b** has in the past lead to a great deal of confusion. Some authors have let the gas density go to zero at the crack tip [10,21,22,23], while others assume that because fluid such as magma can sustain a negative pressure it must always fill the crack [30]. Both of these assumptions are incorrect, although magma flow in cracks does in practice come very close to the crack tip [2].

In general a fluid travelling down a narrow channel has a front.

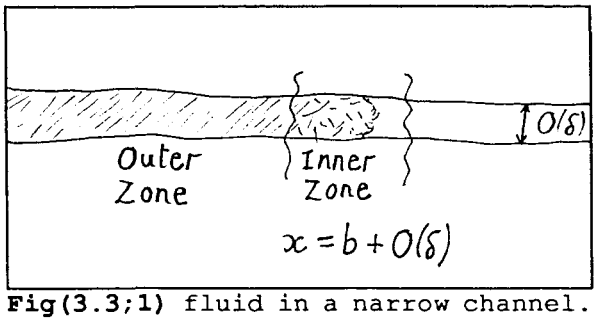

Fig(3.3;1) fluid in a narrow channel.

The mass conservation law for the inner zone reduces to **div(v)=0** which when integrated over y gives **∂u/∂x=0** where **u** is the averaged component of horizontal velocity over the crackwidth (3.2.2;4v). The value for **u** is conserved through the inner region so that matching to the outer zone gives

$$\lim_{x \to b} u(x,t) = \dot{b} \qquad \text{-(3.3;2)}$$

$\dot{b}$ is the velocity of the inner zone region.

We must also consider what the gas pressure will be near the gas front. For continuity of pressure at the front, the pressure must be zero. The gas pressure in the inner zone will therefore be $O(y_0\, \partial p/\partial x)$ so matching to the inner zone gives the first approximation as

$$p(b(t),t) = 0 \qquad \text{-(3.3;3)}$$

These equations will be valid unless the gas front catches up with the crack front. In this case we could not insist on zero pressure at the front but would replace this condition with

$$a = b \qquad \text{-(3.3;4)}$$

Before proceeding, let us consider briefly the situation for liquids:-

Liquids possess properties that gases do not:-

i)Ability to withstand negative pressures

ii)Ability to stick to the crack wall. The stickiness is defined as the maximum tensile stress that can be supported at the crack-fluid interface. If the stickiness is exceeded, then the fluid will separate from the crack wall.

If a 'sticky' fluid completely filled a crack at time zero, then it would continue to fill the crack provided the tensile forces of the crack upon the fluid (the maximum of which is at the crack tip) do not exceed the stickiness of the fluid. If the stickiness is exceeded the liquid would separate from the crack wall causing an instantaneous small region of zero pressure. The liquid would then settle down and obey the separate gas-crack front condition described for a gas.

The success in assuming that magma fills a crack in the study of magma flow in rocks could be because magma is a very sticky fluid and the slow magma flow only generates quite small tensile pressures along the crack. A more likely explanation though is that the magma pressure is only just greater than the surrounding in-situ stress so that the crack opening equations (2.9;1) will only locate the crack front just ahead of the gas front.

Let us now return to our problem.

iii)The Boundary Condition at the Borehole

The borehole is sufficiently large to prevent any resistance to gas flowing from regions of high to low pressures, so to a first approximation the borehole pressure is spatially uniform. We therefore require a boundary condition giving us the borehole pressure as a function of time and this comes from considering the mass of gas. If we assume that the total mass of gas **m** in the borehole and cracks is always constant, that is we incur no mass loss through gas venting or porous seepage into the rock, then

$$m=\begin{pmatrix}\text{mass of gas}\\ \text{in borehole}\end{pmatrix} + \begin{pmatrix}\text{mass of gas}\\ \text{in cracks}\end{pmatrix}$$

$$m=\rho_b(t)\pi(\varepsilon+u_r|_\varepsilon)^2+n\int_\varepsilon^b \rho(x,t)h(x,t)dx \qquad \text{-(3.3;5)}$$

h is the crackheight of the **n** radial cracks

ρ_b is the borehole density

m is the total mass of gas

This equation may also be written in differental form, describing the change of borehole mass in terms of the flux of mass through the n cracks, simply by differentiating with respect to time and substituting the momentum equation (3.2.2;4ii).

4. SUMMARY OF THE NON-DIMENSIONAL MODEL OF ROCK BLASTING

All the ingredients of the rock blasting model have now been developed. Henceforth we shall primarily be interested in the **n** radial crack model given in Appendix C. This model is more closely related to rock blasting than the two crack model and has not recieved much attention in previous research. In this section the governing equations describing rock blasting are collected together and non-dimensionalised. Solutions to the rock blasting problem in later sections will usually refer directly to the equations written down below.

The following non-dimensionalisation will be used:-

$$\zeta=\frac{r}{\varepsilon} \quad A=\frac{a}{\varepsilon} \quad B=\frac{b}{\varepsilon}$$

$$f=\frac{p}{2\sigma}$$

$$H=\frac{hEn}{4\pi\sigma\varepsilon}$$

$$U_r=\frac{u_r E}{2\sigma\varepsilon}$$

$$\kappa=\frac{K}{2\sigma\varepsilon^{\frac{1}{2}}} \qquad \text{-(4;1)}$$

$$M=\left(\frac{E}{4\sigma}\right)^2\left(\frac{m}{K_g(2\sigma)^{\frac{1}{\gamma}}\varepsilon^2\pi}\right)$$

$$\tau_{EV}=\frac{8\pi^2\sigma^3 t}{3\mu_{turb}E^2n^2} \qquad \tau_{ML}=\frac{2\sigma}{\varepsilon}\left(\frac{2\pi}{lK_gEn(2\sigma)^{\frac{1}{\gamma}}}\right)^{\frac{1}{2}}t$$

the dimensionless equations governing the rock blasting process can now be written

Gas flow in crack *(3.2.4;1);*

$$\frac{\partial}{\partial\tau}(f^{\frac{1}{\gamma}}H)=-\frac{\partial}{\partial\zeta}\left(-f^{\frac{1}{\gamma}}H^3\frac{\partial f}{\partial\zeta}\right)^q \qquad q=\begin{cases}1 & \text{EV model}\\ \frac{1}{2} & \text{ML model}\end{cases} \qquad \text{-(4;2)}$$

Gas in borehole *(3.3;5);*

$$\frac{d}{d\tau}\left[f_1(\tau)^{\frac{1}{\gamma}}\left(\frac{E}{4\sigma}+\frac{U_r}{2}\right)^2\right]+\frac{E}{4\sigma}\left(-f^{\frac{1}{\gamma}}H^3\frac{\partial f}{\partial\zeta}\right)^q\Big|_{\zeta=1}=0 \qquad \text{-(4;3)}$$

$$\text{or } f_1^{\frac{1}{\gamma}}\left[\frac{E}{4\sigma}+\frac{U_r}{2}\right]^2+\frac{E}{4\sigma}\int_1^B f^{\frac{1}{\gamma}}H(\zeta,\tau)d\zeta=M$$

Radial borehole expansion *(C17);*

$$U_r(1,\tau)=U_r(\tau)=H(1,\tau)+(\nu-1)f_1(\tau) \qquad \text{-(4;4)}$$

Crack height and crack length;

full model (C17):

$$H=\zeta f+\ln\left(\frac{A(\tau)}{\zeta}\right).\left[f_1(\tau)+\int_1^B f(y,\tau)dy\right]+\int_\zeta^B f\ln\left(\frac{\zeta}{x}\right)dx+\left(f_1+\int_1^B f dy\right)-A$$

$$\kappa=\sqrt{\frac{A}{n}}\left[f(A,\tau)+\frac{1}{A}\left(f_1+\int_1^B f dy\right)-1\right] \qquad \text{-(4;5)}$$

in-situ stress dominant model ((C17) and (2.9;2)):

$$H=\zeta f+\log_e\left(\frac{A}{\zeta}\right).\left[f_1+\int_1^B f\,dx\right]+\int_\zeta^B f\,\log_e\left(\frac{\zeta}{x}\right)dx-Af(A,\tau)$$

$$A=\frac{\left[f_1+\int_1^B f\,dx\right]}{1-f(A,\tau)} \qquad \text{-(4;6)}$$

$$\text{when } \frac{n\kappa^2}{4(1-f(A))\left(f_1+\int_1^B f\,dy\right)}<1$$

Boundary and initial conditions (section 3.3);

$$f_1(\tau)\big|_{\tau=0}=\frac{p_b(0)}{2\sigma}$$

$$f(\zeta,\tau)\big|_{\substack{\zeta>1\\ \tau=0}}=0$$

$$\dot{B}(\tau)=\left(-f^{\frac{1}{\gamma}}H^3\frac{\partial f}{\partial\zeta}\right)^q\frac{1}{Hf^{\frac{1}{\gamma}}}\Bigg|_{\zeta=B} \qquad \text{-(4;7)}$$

where $f(\xi,\tau)=0$ when $B\le\xi<A$

The rock blasting model is valid when the following dimensionless numbers are either small or large (the conditions for the validity of the rock blasting model to references [10] and [21] are given to the right)

	[21]	[10]
Mach number;		
$\frac{\rho_0 u_0^2}{p_0}\ll 1$	u_0<<450 m/s	u_0<<1500 m/s
Borehole depth;		
$\frac{\beta z}{\sigma}\ll 1,\ \frac{z}{a}\gg 1$	z<<1000 m z>>2.5 m	z<<1000 m z>>10 m
Lubrication number;		
$\frac{y_0}{x_0}\ll 1$	10^{-3}	10^{-2}
Number of cracks;		
$n\gg 1$	7	7
Small kinetic energy;		
$\frac{u_0^2}{2c_v T}\ll 1$	u_0<<2500 m/s	u_0<<1500 m/s

Small viscous heating;

$$\frac{\mu x_0 u_0}{\rho c_v T\, y_0^2} \ll 1, \quad \frac{\mu}{\rho y_0 u_0} \ll 1$$

$10^{-6} \ll u_0 \ll 10^{7}$ $\qquad$ $10^{-5} \ll u_0 \ll 10^{9}$

Adiabatic aproximation number;

$$\frac{u_0 \rho y_0^2 c_v}{k_{rock} x_0} \gg 1$$

$u_0 \gg 4$ m/s $\qquad$ $u_0 \gg .01$ m/s

and whenever the semi-empirical turbulent gas model is valid for rock blasting.

5. SOLUTIONS TO THE ROCK BLASTING PROBLEM

5.0 Introduction

The full rock blasting problem defined in section 4 is very complicated and cannot be solved analytically. In this section we shall find some approximate solutions corresponding to extreme choices of blasting parameters often approached in real blasting. These solutions will also provide us with some results with which to test the numerical schemes for the full problem presented at the end of this section.

5.1 Large Borehole Pressure Problems

In many rock blasting situations the gas pressure in the borehole will remain many times larger than the surrounding in-situ stress field for quite a long period of time. It would be useful to see how the rock blasting problem behaves for $\mathbf{p_b>>\sigma}$, that is in dimensionless variables, $\mathbf{f(1,\tau)>>1}$. We shall also use the in-situ stress dominant model (2.9;2) for crack opening. The conditions for this model to be valid can be shown to be satisfied for the blast parameters in section 3.0 since during the initial stages of rock blasting it is the in-situ stress field that holds the crack tip together and not the material strength of the rock.

The first order in-situ stress dominant equation for the crack height (4;6) can be written

$$H=f_1(\tau)\log_e f_1(\tau)\left[1+\frac{1}{f_1(\tau)}\int_1^B f(y,\tau)\,dy\right]+ \qquad \text{-(5.1;1)}$$

$$f_1(\tau)\left[\log_e\left(\frac{1+\frac{1}{f_1(\tau)}\int_1^B f\,dy}{\zeta}\right)\left[1+\frac{1}{f_1(\tau)}\int_1^B f\,dy\right]+\frac{\zeta f}{f_1}+\int_\zeta^B \frac{f}{f_1}\log_e\left(\frac{\zeta}{x}\right)dx\right]$$

where $\mathbf{f_1(\tau)=f(1,\tau)}$. This equation can be taken as a formal asymptotic expansion for large $\mathbf{f_1(\tau)}$. The first approximation for **H** and $\mathbf{U_r}$ are

$$H \sim U_r \sim f_1 \log f_1 \left[1 + \frac{1}{f_1} \int_1^B f \, dy \right] = A \log f_1 \qquad \text{-(5.1;2)}$$

This equation will only be valid if the second bracketed term in (5.1;1) remains ~**O(1)**. It is difficult to see exactly when this condition will hold without prior knowledge of the gas distribution in the crack. A condition such as **B~O(1)** would be sufficient. As the rock blasting solutions are developed we shall see that the conditions on **B** are less restrictive than this so that (5.1;2) will be valid not just for gas penetration on the borehole length scale but on longer scales also. Equation (5.1;2) corresponds to the case when almost all of the crack opening is due to the divergence of the pie shaped rock segments by the gross action of the borehole pressure and the gas pressure on the cracks.

5.1.1 The Small Time Solution

For a short time after the blast initiation, the gas penetration into the crack is small ie. **B-1<<1**, and the crack opening equations become

$$H = U_r = f_1(\tau) \log f_1(\tau) + O(B-1) + O\left(\frac{1}{\log f_1(\tau)} \right) \qquad \text{-(5.1.1;1)}$$

The total mass conservation equation (4;3) will approximately lead to a constant borehole pressure ($\mathbf{f_1}$=constant) if the losses of gas into the cracks and the borehole expansion are small compared to the compressibility effects of the gas. The condition for this is

$$\gamma < O\left(\frac{E}{4\sigma(B-1)A} \right) \quad \text{where} \quad \frac{E}{2\sigma} > (B-1)U_r \qquad \text{-(5.1.1;2)}$$

where γ is the compressibility index given in (3.2.4;iii).

The equations from section 5 describing the gas motion now reduce to

$$\frac{\partial F^{\frac{1}{\gamma}}}{\partial t} = -\frac{\partial}{\partial \zeta} \left(-F^{\frac{1}{\gamma}} \frac{\partial F}{\partial \zeta} \right)^q$$

$$\dot{B}(t) = \left(-F^{\frac{1}{\gamma}} \frac{\partial F}{\partial \zeta} \right)^q \frac{1}{F^{\frac{1}{\gamma}}} \Bigg|_{\zeta = B} \qquad \text{-(5.1.1;3)}$$

where $F(1,\tau)=1,\ F(B(t),t)=0$

and the dimensionless time and the pressure have been re-scaled to

$$t=f_1^{q\left(1+\frac{1}{\gamma}\right)-\frac{1}{\gamma}}(f_1\log_e f_1)^{3q-1}\ \tau,\ f=f_1F \qquad \text{-(5.1.1;4)}$$

The resulting equations can be written in terms of the similarity variable

$$z=\frac{\xi}{((q+1)t)^{\frac{1}{q+1}}} \qquad \xi=\zeta-1 \qquad \text{-(5.1.1;5)}$$

$$\text{where}\quad B(t)-1=C_0((q+1)t)^{\frac{1}{q+1}}$$

This equation can be solved numerically for all γ, and asymptotically for large and small γ (Appendix E) to yield solutions of gas flow down a crack of constant height. It should be noted, however, that $\gamma<1$ does not arise in practice and also that more than one term of the large gamma solution is not justified in predicting gas flow occuring in rock blasting in view of the fact that the errors in the crackheight approximation ($1/\log_e f_1$) are just as big as those incurred through assuming an incompressible flow ($1/\gamma$). Within the errors of the model then it is the first order large gamma asymptotic solution ($\gamma=\infty$) which has the most practical significance. On using (4;1), (5.1.1;4) and (5.1.1;5) this asymptotic solution (E3) can be expressed in terms of dimensional quantities as

$$b\sim\varepsilon\left(1+\frac{\pi P_b}{En}\log_e\left(\frac{P_b}{2\sigma}\right)\left(\frac{2P_b t}{3\mu_{turb}}\right)^{\frac{1}{2}}\right) \qquad \text{EV model}$$

$$b\sim\varepsilon\left(1+\left(3P_b^{\,1-\frac{1}{2\gamma}}\left[\frac{\pi}{2EnlK_g}\log_e\left(\frac{p_b}{2\sigma}\right)\right]^{\frac{1}{2}}\frac{t}{\varepsilon}\right)^{\frac{2}{3}}\right) \qquad \text{ML model} \qquad \text{-(5.1.1;6)}$$

These early time solutions show that the initial gas velocities will be very large, but fall quickly as the gas pressure gradient falls.

After a short time, however, the assumptions made in order for the short time model to be valid will be violated and an intermediate time model will have to be

considered.

5.1.2 The Intermediate time Solution

Once again we shall assume that the gas in the cracks can be approximated as incompressible. The errors incurred will be no more than those we have introduced through using our crack-height approximation (5.1;2) (as indicated in (5.1.1;1)).

In practice, as the gas streams down the cracks the borehole pressure will decrease. In the following analysis we shall consider two extreme cases of the intermediate time model. The first where the borehole pressure remains constant, and the second where any fluid flow into the cracks must be compensated by the borehole cavity shrinking in order to preserve the fluid volume. These cases correspond to when the compressibility of the gas in the borehole is very large (5.1.1;2), and small ((5.1.1;2) with the inequality reversed) respectively.

i)The EV model (q=1) with constant borehole pressure.

If the gas is sufficiently compressible for the borehole pressure to remain constant ($\mathbf{f}_1(\tau)$=constant), but sufficiently incompressible to allow the behaviour of the gas along the crack to be nearly incompressible then γ obeys

$$1<\gamma<<\frac{E}{4\sigma BA}, \quad \text{and} \quad \frac{E}{2\sigma}>U_r \qquad \text{-(5.1.2;1)}$$

The equations for rock blasting in section 4 along with (5.1;2) become

$$\int_1^B \frac{\partial f}{\partial t}\,dy=\left(1+\frac{1}{f_1}\int_1^B f\,dy\right)^3\frac{\partial^2 f}{\partial \zeta^2}$$

$$\dot{B}=-\frac{1}{f_1}\left[1+\frac{1}{f_1}\int_1^B f\,dy\right]^2\left.\frac{\partial f}{\partial \zeta}\right|_{\zeta=B} \qquad \text{-(5.1.2;2)}$$

$$f(B,t)=0 \qquad f_1=\text{constant}$$

where the time has been re-scaled to

$$t=f_1^3(\log f_1)^2\,\tau \qquad \text{-(5.1.2;3)}$$

Equation (5.1.2;2) shows that **f** must be a quadratic function of ζ. Including the conditions (5.1.2;2iii), **f** may therefore be written

$$f(\zeta,t)=f_1\left[(F(t)-1)\left(\frac{\zeta-1}{C(t)}\right)^2-F(t)\left(\frac{\zeta-1}{C(t)}\right)+1\right] \qquad \text{-(5.1.2;4)}$$

where **C=B-1** and **F** are functions to be determined from substituting (5.1.2;4) into the flow equations (5.1.2;2) giving

$$\frac{dC}{dt}=\left(1+C\left(\frac{2}{3}-\frac{F}{6}\right)\right)^2\left(\frac{2-F}{C}\right)$$

$$\frac{2(F-1)}{C^2}=\frac{\left\{-\frac{1}{6}\frac{d(FC)}{dt}+\frac{2}{3}\frac{dC}{dt}\right\}}{\left(1+C\left(\frac{2}{3}-\frac{F}{6}\right)\right)^3} \qquad \text{-(5.1.2;5)}$$

$$F(0)=1 \qquad C(0)=0$$

Time **t** can be eliminated from (5.1.2;5) to give the first order ODE in **F** and **C**

$$\frac{dF}{dC}=\frac{-3CF^2+(F-1)(12+16C)}{C^2(F-2)} \qquad \text{-(5.1.2;6)}$$

$$F(0)=1$$

We find solutions to (5.1.2;6) and then solve (5.1.2;5i) to give **F** and **C** as functions of **t** (Appendix F). Numerical solutions for **C(t)** are given in figs(5.1.2;1,2 and 3), and **F(C)** in Appendix F. Asymptotic solutions for small and large **t** (Appendix F) are given as

small time

$$C(t)\sim\sqrt{2t}+\frac{t}{2}+\ldots$$

$$F(t)\sim 1+\frac{1}{2}\sqrt{\frac{t}{2}}+\ldots \qquad \text{-(5.1.2;7)}$$

large time

$$C(t)\sim\exp\frac{32}{243}(t-t_0)-\frac{63}{11}+\ldots$$

$$F(t)\sim\frac{4}{3}-\frac{6}{11\ \exp\frac{32}{243}(t-t_0)}+\ldots \qquad \text{-(5.1.2;8)}$$

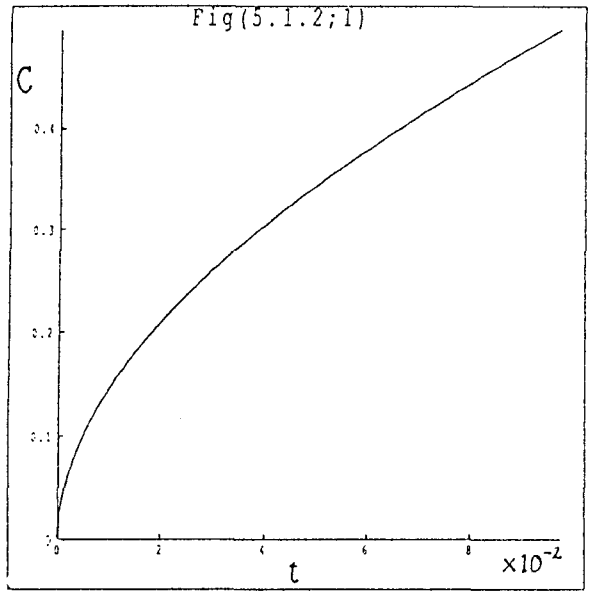

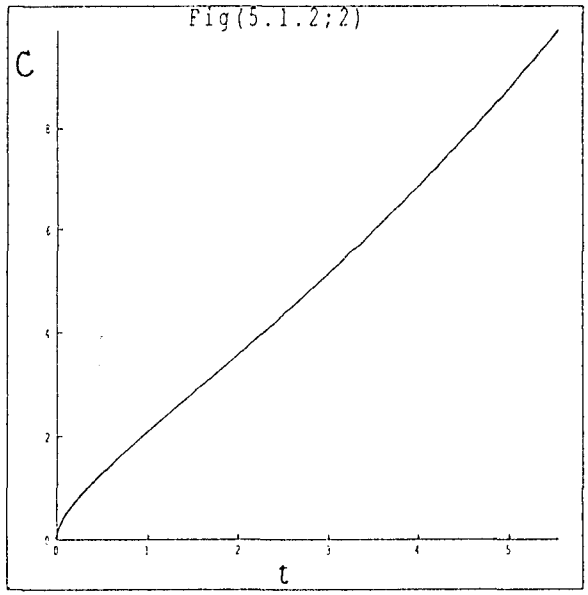

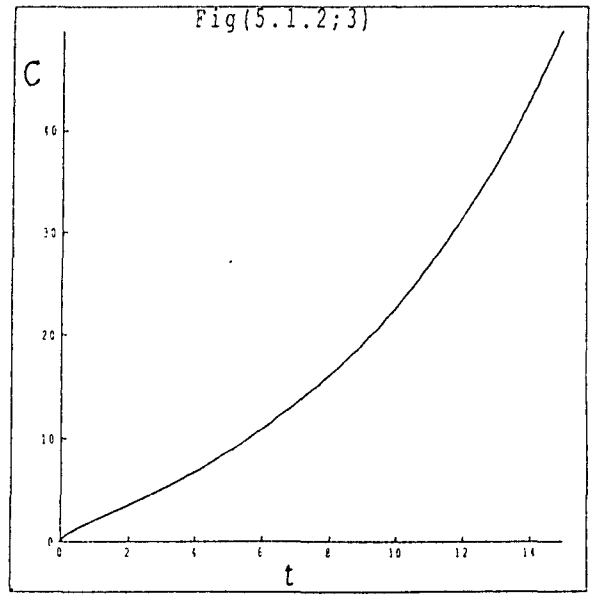

These figures show the numerical solutions for the gas front position corresponding to the case of large constant borehole pressure with $\gamma=\infty$. The small and large time solutions, figures 1 and 3, show good agreement with the asymptotic solutions given in (5.1.2;7 and 8).

where $\mathbf{t_0}$ is a reference time undefined in this analysis.

The small time solution shows how the gas flow behaviour departs from the very small time problem considered previously (5.1;1). The long time solution can only be of any use if (5.1.2;1) remains satisfied and we can verify that the crack height approximation is still valid for large **B**. Substituting (5.1.2;4) into the full crack height expression (5.1.2) shows that for large **B**

$$H=f_1\log_e f_1\left(1+\frac{C}{6}(4-F)\right)+O(f_1C)$$

$$H_{approx}=f_1\log_e f_1\left(1+\frac{C}{6}(4-F)\right) \qquad \text{-(5.1.2;9)}$$

which verifies the validity of the crack height approximation (5.1.2) for large **B** in this case. A simple approximation of the pressure distribution along the cracks can be obtained from the long time asymptotic model

$$f=f_1\left[\left\{\frac{1}{3}\left(\frac{\zeta-1}{C}\right)^2-\frac{4}{3}\left(\frac{\zeta-1}{C}\right)+1\right\}+\frac{1}{C}\left\{\frac{6}{11}\left(\left(\frac{\zeta-1}{C}\right)-\left(\frac{\zeta-1}{C}\right)^2\right)\right\}+\ldots\right]$$

$$A=f_1\left[\frac{4C}{9}+\frac{12}{11}+\ldots\right] \qquad \text{-(5.1.2;10)}$$

$$C\ \alpha\ \exp\frac{32}{243}t$$

From the two sets of blast parameters in section 3.0, we can calculate that near the end of the blast **A**=25,100 **C**=12.5,5 and **t**=7,3. From these values and using (5.1.2;1), however, we must have that $1<<\gamma<<4.5$, $1<<\gamma<<2.3$ for the borehole pressure to remain constant. In practice then, for realistic γ, we would expect the borehole depressurisation to be a significant feature of rock blasting.

ii) The EV Model for a nearly Incompressible Fluid

We shall assume that the fluid obeys

$$\gamma\geq O\left(\frac{E}{4\sigma BA}\right),\ \gamma>1 \qquad \text{-(5.1.2;11)}$$

This condition could be satisfied if the gas or fluid is very incompressible and/or the crack length **a** is large.

We shall assume that the large borehole pressure approximation for crack height (5.1;2) is still valid which means that the following solutions will only be valid during a time scale of moderate borehole decompression.

$$f_1(\tau)=f_1 g(t)$$

$$\text{where } g(0)=1 \qquad \text{-(5.1.2;12)}$$

$$\text{and } \frac{1}{g}\sim O(1)\ \forall\ t$$

The time has been re-scaled according to (5.1.2;3). The analysis in this section is similar to the previous example but instead of constant borehole pressure, we must impose the borehole mass conservation equation (4;3) with $\gamma=\infty$. The dimensionless gas pressure in this case can be written

$$f=f_1\left[(F-g)\left(\frac{\zeta-1}{C}\right)^2-F\left(\frac{\zeta-1}{C}\right)+g\right] \qquad \text{-(5.1.2;13)}$$

and the governing equations from section 4 are

$$\frac{dC}{dt}=\left(1+C\left(\frac{2}{3}-\frac{F}{6g}\right)\right)^2\left(\frac{2g-F}{C}\right)g^2$$

$$\frac{2(F-g)}{C^2}=\frac{\left\{-\frac{1}{6}\frac{d(FC)}{dt}+\frac{d}{dt}\left(g\left(1+\frac{2C}{3}\right)\right)\right\}}{g^3\left(1+C\left(\frac{2}{3}-\frac{F}{6g}\right)\right)^3} \qquad \text{-(5.1.2;14)}$$

$$F(0)=1 \qquad C(0)=0 \qquad g(0)=1$$

Using (5.1.2;13) and approximating to the same order as (5.1;2), the borehole mass equation (4;3) becomes

$$g\left[1+C\left(\frac{2}{3}-\frac{F}{6g}\right)\right](C+1)=1 \qquad \text{-(5.1.2;15)}$$

The solution to this problem may be found by substituting (5.1.2;15) into (5.1.2;14) and

solving a simple first order separable ODE in C to give

$$t=\frac{C^6}{18}+\frac{C^5}{3}+\frac{5C^4}{6}+C^3+\frac{C^2}{2}$$

$$g=\frac{3(C+2)}{(C+1)(2C^2+6C+6)} \qquad \text{-(5.1.2;16)}$$

$$F=\frac{2g}{C+2}$$

In this example A can be written

$$A=\frac{f_1}{C+1} \qquad \text{-(5.1.2;17)}$$

which shows that as the fluid front moves forward, the crack tip moves backwards!

Explicit representations of C in terms of t can be found by inverting (5.1.2;16i) to give

$$C(t)=(3\sqrt{2t}+1)^{\frac{1}{3}}-1 \qquad \text{-(5.1.2;18)}$$

Although the solutions for this problem are only valid whilst $\mathbf{f}_1(\tau)$ remains large, we can see how dramatic an effect borehole decompression will have during fluid flow in rock whenever (5.1.2;11) is satisfied (see figure (5.1.2;4)). In practice we need to start considering borehole decompression when

$$\gamma \sim O\left(\frac{E}{4\sigma(B-1)A}\right)$$

$$\Rightarrow B \sim O\left(\sqrt{\frac{E}{P_b\gamma}}\right) \qquad \text{-(5.1.2;19)}$$

This condition will lie within the limits of most rock blasting situations, so that borehole decompression will be a significant feature during most rock blasts.

iii) The ML model

A similar argument as used above with the EV model would show that the dimensionless pressure **f** would be cubic in ζ. The analysis of this case would be similar to that for the EV model. The algebra in this calculation however, is far more

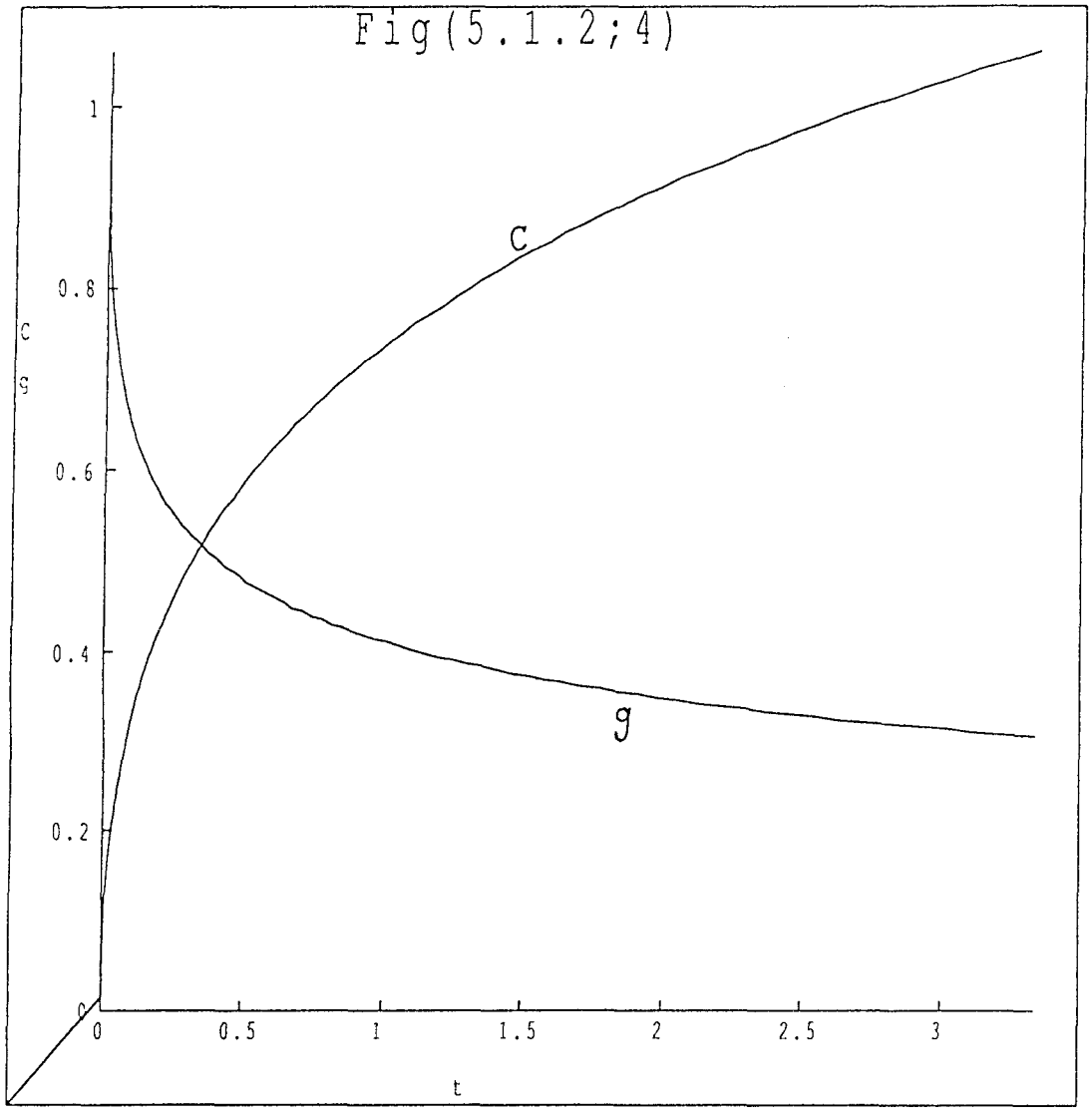

The gas front position **C=B-1** and the borehole depressurisation **g** are plotted against time **t** for the intermediate time EV model where

$$t=f_1^3(\log f_1)^2 \qquad f_1(\tau)=f_1(0)g$$

compressibility effects are significant

$$\gamma > \frac{E}{4\sigma(B-1)A}$$

and the borehole pressure is large.

complicated and is omitted from this thesis.

Solutions for the intermediate time model however can still be found for small and large times, analogous to the results (5.1.2;7 & 8). The first order small time solution has already been found in section 5.11 and the large time solution will be found as one of the solutions of the long time rock blasting model considered in the following section.

5.2 Long Time Solutions

5.2.1 Introduction

We define a long time solution as one in which the gas penetration length along the cracks is much greater than the borehole radius. ie. **B>>1**.

Equations (4;6) for the crack height and crack length become

$$H=\zeta f+\int_{\zeta}^{A}\frac{1}{y}\int_{o}^{y} f\,dxdy-Af(A,\tau)\ +O\left(\frac{1}{B}\right)$$

$$\kappa=\sqrt{\frac{A}{n}\left[f(A,\tau)+\frac{1}{A}\int_{0}^{B} f\,dy-1\right]}\ +O\left(\frac{1}{B}\right) \qquad \text{-(5.2.1;1)}$$

These equations show that the effect of the borehole pressure on the crack height and crack length becomes less and less significant as the gas penetrates deeper into the cracks. The borehole mass equation (4;3) may still initially be approximated by a constant borehole pressure provided

$$\gamma<\frac{E}{4\sigma BA}$$

although eventually as **B** increases, borehole decompression must occur. We shall consider two cases for analysis. The first for constant borehole pressure and the other for the very long time problem where the borehole has decompressed to just above the in-situ stress. The former case will be solved approximately for large borehole pressure, and the results shown to be consistent with section (5.1.2). The latter case corresponds to the gas behaviour just before the gas stops. Although this example may not be of direct relevance to blasting, it may be of some use when the containment of explosives underground is at issue. Both of these solutions will be useful for validating numerical solutions of the rock blasting process (although a full numerical scheme for the long time model is not

pursued in this thesis).

5.2.2 The Constant Borehole Pressure Case

Assuming that the in-situ stress effect is the dominant crack opening mechanism ((5.2.1;1) and (4;6)), the solution to the rock blasting problem can be written as a similarity solution. Analysis of all the equations and conditions shows that the resulting problem is

i) EV model

$$D\xi^2\frac{d}{d\xi}\left(\frac{f^{\frac{1}{\gamma}}G}{\xi}\right)=-\frac{d}{d\xi}\left(f^{\frac{1}{\gamma}}G^3\frac{df}{d\xi}\right)$$

$$D\mu=-G^2\frac{df}{d\xi}\bigg|_{\xi=\mu},\ \int_0^{\mu} f\,dz=\lambda,\ f(0)=\frac{p_b}{2\sigma} \qquad \text{-(5.2.2;1)}$$

where $\xi=\dfrac{\zeta}{\exp D\tau}$, $A=\lambda\exp D\tau$, $B=\mu\exp D\tau$, $H=\exp D\tau\ G$

where **D** is a constant that will be determined when the boundary conditions for the problem are satisfied.

ii) ML model

$$\xi^2\frac{d}{d\xi}\left(\frac{f^{\frac{1}{\gamma}}G}{\xi}\right)=\frac{d}{d\xi}\left(-f^{\frac{1}{\gamma}}G^3\frac{df}{d\xi}\right)^{\frac{1}{2}}$$

$$\mu=\left(-f^{\frac{1}{\gamma}}G^3\frac{df}{d\xi}\right)^{\frac{1}{2}}\frac{1}{Gf^{\frac{1}{\gamma}}}\bigg|_{\xi=\mu},\ \int_0^{\mu} f\,dz=\lambda,\ f(0)=\frac{p_b}{2\sigma} \qquad \text{-(5.2.2;2)}$$

where $\xi=\dfrac{\zeta}{\tau}$, $A=\lambda\tau$, $B=\mu\tau$, $H=\tau G$

In both cases **G** is given by

$$G=\xi f+\lambda\log_e\left(\frac{\lambda}{\xi}\right)+\int_{\xi}^{\mu} f\log_e\left(\frac{\xi}{z}\right)dz$$

$$=\xi f+\int_{\xi}^{\lambda}\frac{1}{z}\int_{0}^{z} f\,dydz \qquad \text{-(5.2.2;3)}$$

The similarity analyses above have shown that the EV and ML models lead to exponential and linear gas front velocities respectively. The difference between these two results indicates, in this example, the failure of at least one of the models in predicting the long time turbulent flow behaviour.

The above equations are very complicated and would need to be solved numerically. We shall not proceed down that avenue in this thesis but we shall examine the approximate solutions for large borehole pressure, and large γ. We shall then compare these results to those in section (5.1.2).

Approximate solutions

Assuming that the distance from the borehole to the crack front is much greater than the distance from the borehole to the gas front (ie. $\lambda>>\mu$ from $\mathbf{A}=\lambda\tau$ and $\mathbf{B}=\mu\tau$) then (5.2.2;3) can be approximated

$$G\simeq\lambda\log_e\lambda+O(\lambda\log_e\mu) \qquad \text{-(5.2.2;4)}$$

Substituting (5.2.2;4) into (5.2.2;1 and 2) and taking $\gamma=\infty$ gives the following analytical results for **f**

i) EV model

$$f\simeq\frac{f_1}{3\mu^2}((\xi-2\mu)^2-\mu^2)$$

$$D=\frac{32}{243}f_1^3(\log_e f_1)^2,\ f_1=\frac{9\lambda}{4\mu} \qquad \text{-(5.2.2;5)}$$

This is identical to the results we obtained in (5.1.2;10).

ii) ML model

$$f \propto \frac{f_1}{7\mu^3}[(2\mu-\xi)^3-\mu^3]$$

$$f_1 = \frac{28\lambda}{11\left(\frac{12}{11}\lambda^2\log_e\lambda\right)^{\frac{1}{4}}} \qquad \text{-(5.2.2;6)}$$

This model is cubic in ξ as suggested in section (5.1.2;iii).

A note on stability (5.2.2;5) is clearly the stable long time solution of the constant borehole pressure EV model case as can be seen from the solution curves in the phase plane analysis in Appendix F. Similarly (5.2.2;6) is probably the stable long time solution for the corresponding ML model, although to prove this statement, further analysis of the phase plane for the intermediate time ML model would be necessary.

5.2.3 The Very Long Time Solution

As the blast continues the gas pressures will decrease. If the rock had no strength whatsoever (K_{phys}=0) the blast would continue indefinitely. For the gas to stop, a time must come when the gas pressure is so low that the rock strength is sufficient to prevent continued crack growth. This means that the in-situ stress dominance holding the crack tip together is gradually replaced by a model incorporating both in-situ stress and the effect of the rock strength. The analysis of this transition would be complicated so we shall examine two simple cases.

i) The first order large time solution (ie. when the gas flow has stopped)

ii) The first order large time model assuming the rock strength is very small. In practice this model will only be valid when the in-situ stress model for crack propagation remains valid at large times.

i) The final gas state

The gas has stopped flowing so the gas pressure must be uniform throughout the borehole and cracks. From the conservation of mass (4;3ii), the crack height*(4;5) and borehole expansion equations (4;4) we have

$$f_1^{\frac{1}{\gamma}}\left\{\left[\frac{E}{4\sigma}+\frac{1}{2}\left(\frac{n\kappa^2}{2f_1-1}+f_1(\nu-1)\right)\right]^2+\frac{E}{4\sigma}\left(\frac{n\kappa^2}{(2f_1-1)^2}-1\right)\left(\frac{n\kappa^2}{2f_1-1}\right)\right\}=M \qquad \text{-(5.2.3;1)}$$

(* we assume that **K** is maintained at the maximum value just before the gas stops)

where $A=\dfrac{n\kappa^2}{(2f_1-1)^2}$

We shall assume that enough explosive was used so that the final crack length is much longer than the borehole radius (A>>1). The first order equations for large **A** are therefore

$$\left(\frac{1}{2}\right)^{\frac{1}{\gamma}}\left[\left(\frac{E}{4\sigma}\right)^2+\left(\frac{E}{4\sigma}\right)\left[\frac{n^2\kappa^4}{(2\delta f_{11})^3}\right]\right]=M \qquad \text{-(5.2.3;2)}$$

$$\text{where } f_1=\frac{1}{2}+\delta f_{11}+\ldots,\ A=\frac{n\kappa^2}{(2\delta f_{11})^2}+\ldots$$

which yield the solutions

$$\delta f_{11}=\frac{1}{2}\left(\frac{n^2\kappa^4}{\dfrac{4\sigma M\ 2^{\frac{1}{\gamma}}}{E}-\dfrac{E}{4\sigma}}\right)^{\frac{1}{3}},\quad A=\left\{\frac{1}{n^{\frac{1}{2}}\kappa}\left(\frac{4\sigma M\ 2^{\frac{1}{\gamma}}}{E}-\frac{E}{4\sigma}\right)\right\}^{\frac{2}{3}} \qquad \text{-(5.2.3;3)}$$

$$\text{provided } \left(\frac{n^2\kappa^4}{\dfrac{4\sigma M\ 2^{\frac{1}{\gamma}}}{E}-\dfrac{E}{4\sigma}}\right)^{\frac{1}{3}}<1$$

For the first set of parameters in section 3.0, the above equation gives **a**≈15.4m and **p**≈1.03σ although in practice gas venting would occur before the cracks could extend to anything like this length.

ii) The long time behaviour for cases when the in-situ stress crack opening model holds

A similarity solution for this example is not possible because we also have to satisfy the equation for the conservation of total gas mass (4;3ii). The long time gas pressure will be just above the in-situ stress so that a long time first approximation of

equation (4;3ii) is

$$\int_0^A H\,dx=\frac{4\sigma\,2^{\frac{1}{\gamma}}M}{E}-\frac{E}{4\sigma} \qquad \text{-(5.2.3;4)}$$

We note that at this stage of the gas flow, the gas and crack fronts must coincide (A=B) and the front pressure is not necessarily zero (3.3.;4).

Assuming the long time expansions

$$f(\zeta,\tau)=\frac{1}{2}+\delta\left(\frac{1}{\tau}\right)F_1+\ldots$$
$$A(\tau)=\delta_{-n}\left(\frac{1}{\tau}\right)A_{-n}+\delta_{-n+1}\left(\frac{1}{\tau}\right)A_{-n+1}+\ldots \qquad \text{-(5.2.3;5)}$$

then in Appendix G it is shown that

i) EV model

$$A\sim 1.39\left(\frac{4\sigma 2^{\frac{1}{\gamma}}M}{E}-\frac{E}{4\sigma}\right)^{\frac{1}{2}}\tau^{\frac{1}{6}}+\ldots \qquad \text{-(5.2.3;6)}$$
$$f=\frac{1}{2}+\ldots$$

ii) ML model

$$A\sim 1.64\;2^{\frac{1}{6\gamma}}\left(\frac{4\sigma\;2^{\frac{1}{\gamma}}M}{E}-\frac{E}{4\sigma}\right)^{\frac{1}{3}}\tau^{\frac{1}{3}}+\ldots \qquad \text{-(5.2.3;7)}$$
$$f=\frac{1}{2}+\ldots$$

where the numerical quantities **1.39** and **1.64** have been obtained from the numerical scheme outlined in Appendix G.

We observe from (4;5) that the above long time solutions will only be valid if κ is sufficiently small (5.2.3;8) or for gas flow in pre-existing cracks where the resistance to crack opening is zero (K=0) ie. this occurs if κ obeys,

$$\kappa \ll \tau^{-\frac{1}{4q}} \qquad q = \begin{cases} 1 & \text{EV model} \\ \frac{1}{2} & \text{ML model} \end{cases} \qquad \text{-(5.2.3;8)}$$

5.3 Numerical Solutions

The analytical solutions that we have obtained above have revealed some important features of the rock blasting process. These will be summarised fully in section 6. To conclude this study of rock blasting, we shall now formulate a numerical scheme to solve the general problem given in section 4 for any given rock blasting parameter values.

5.3.1 The EV model

From (4;2),(4;5) and (4;7) we can see that when the gas front catches up with the crack tip the mathematical problem has to be reformulated. We shall not consider this reformulation in this thesis and will only run the program for situations when the gas front is behind the crack tip. We can consider the solution for the dimensionless pressure on a range of 0 to 1 by defining the variable

$$\xi = \frac{\zeta - 1}{B - 1}$$

(4;2) can now be expanded and discretised into n+1 points from 0 to n. Using a simple trapezoidal rule for the integrals in the expansions of (4;2), a system of **n**-1 equations for **n**+1 values of$(\partial \mathbf{f}/\partial\tau)_i$ is obtained. The remaining pair of equations in **n**+1 values of $(\partial \mathbf{f}/\partial\tau)_i$ are obtained from the borehole mass equation (4;3i) and the gas tip condition (4;7). An **nxn** matrix is then inverted to solve for $(\partial \mathbf{f}/\partial\tau)_i$, **f** is updated and the process continued. Forward differencing must be used for the borehole equation because the flow of gas from the borehole will depend on the pressure gradient of the gas just inside the cracks. The same differencing technique was used along the cracks and although a backward difference technique may appear more natural near the gas front (as the gas equations "run out" at the gas front), the errors in continuing a forward difference scheme (and estimating a point past the gas front for numerical reasons) is small because the gas behaviour near the front has little effect on the overall behaviour of the gas in the cracks and borehole.

The numerical scheme cannot be expected to cope with the singular behaviour of the solution near **t**=0, so we choose the initial data for **f** corresponding to a small gas penetration into the cracks (a linear pressure distribution from the borehole to **C**=**B**-1=0.45). A simple way of checking the validity of the numerical solutions is to check that the total mass of gas is conserved (4;3i).

Figures (5.3.1;i-iv,vi-ix) are presented for a variety of γ's and initial values for **f(1,0)** of 4.5 and 45.0 corresponding to the initial borehole pressure case given in 3.0. The other blast parameters are as given in section 3.0.

5.3.2 The ML model

This model can be developed in exactly the same way as in section (5.3.1) after we have made the change in variable used in appendix E, namely

$$g=f^{1-\frac{1}{\gamma}}$$

which avoids the numerical difficulty in the calculation of the quantity $f'/f^{1/\gamma}$ as $f,f'\to 0$. The numerical solutions for this case however are not included in this thesis.

5.3.3 Numerical results

To demonstrate the agreement between the numerical and analytic results that we have obtained, the analytic solutions derived in section 5.1.2 are included in Figures (5.3.1;v and x).

The solution in section 5.1.2i, where the borehole pressure is assumed to remain constant, is valid provided the conditions in (5.1.2;1), (4;6iii) and $f_1 \gg 1$ are satisfied. For the blast parameters in section 3 this reduces to

[21]

$$\gamma>1,\quad B<\sqrt{\frac{300}{\gamma}},\quad \kappa\sim 0.16<1.6,\quad f_1=4.5>1$$

[10]

$$\gamma>1,\quad B<\sqrt{\frac{20}{\gamma}},\quad \kappa\sim 0.16<5.1,\quad f_1=45 \text{ to } 70 >1$$

The region of validity for either of these parameter sets is very limited. The restriction on [21] is slightly less, so the analytic solution is given for this case only. It should be noted that the analytic solution is only valid for quite small **B** so the agreement with the numerical results is only brief.

The solution in section 5.1.2ii, where the borehole pressure decreases rapidly, is valid provided the conditions in (5.1.2;11),(4;6iii) and $\mathbf{f_1}$>>1 are satisfied. For the blast parameters in section 3 this reduces to

[21]

$$\gamma>1,\ B\geq O\left(\sqrt{\frac{300}{\gamma}}\right),\ \kappa\sim 0.16<\frac{1.6}{\sqrt{C+1}},\ f_1=4.5>1$$

[10]

$$\gamma>1,\ B\geq O\left(\sqrt{\frac{20}{\gamma}}\right),\ \kappa\sim 0.16<\frac{6.3}{\sqrt{C+1}},\ f_1=45 \text{ to } 70>1$$

The region of validity for the parameter set in [21] is limited in that even for γ as large as 50 we still require **B**~3. For the parameter set in [10] however the region of validity is much broader and this is reflected in agreement between the analytic solution for $\gamma\rightarrow\infty$ and the numerical solutions for large γ (the analytic solution is compared to the numerical solution by choosing an $\mathbf{f_1(0)}$ in (5.1.2;17) that lets the dimensionless borehole pressure $\mathbf{f_1}(\tau)$ equal 45 when **C**=0.45)

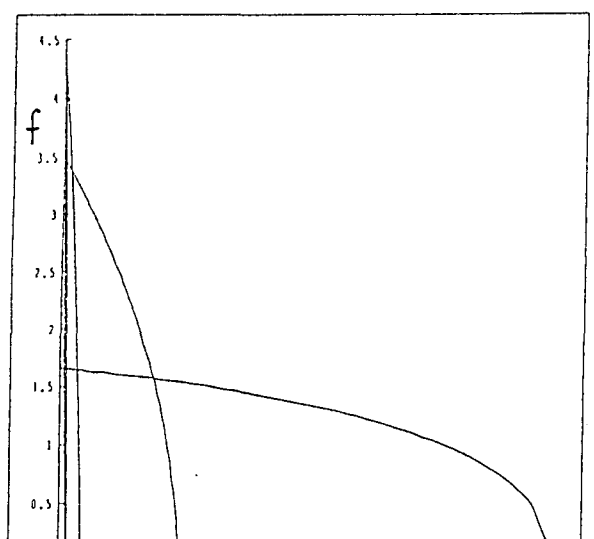

Pressure profiles **f** for τ=0, 10^{-4},10^{-3}, 10^{-2}, 10^{-1} where

$$p = 2\sigma f, \quad x = \varepsilon\zeta$$

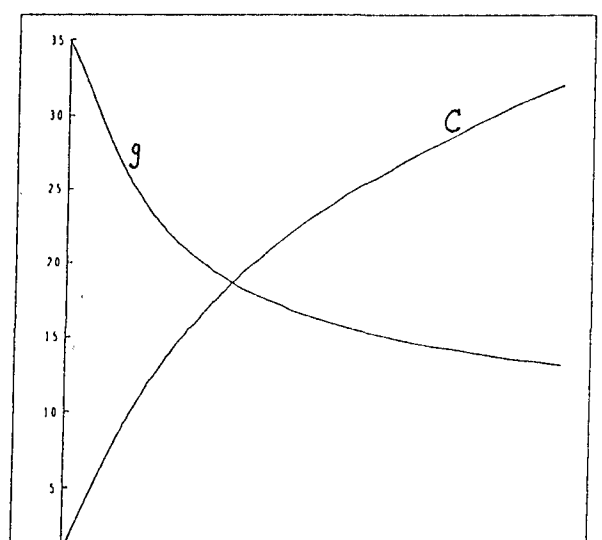

The gas penetration into the cracks **c**=ε**C** and the borehole decompression ratio **g** are plotted against time. **g** is scaled to fit on the graph and **g**(0)=1.

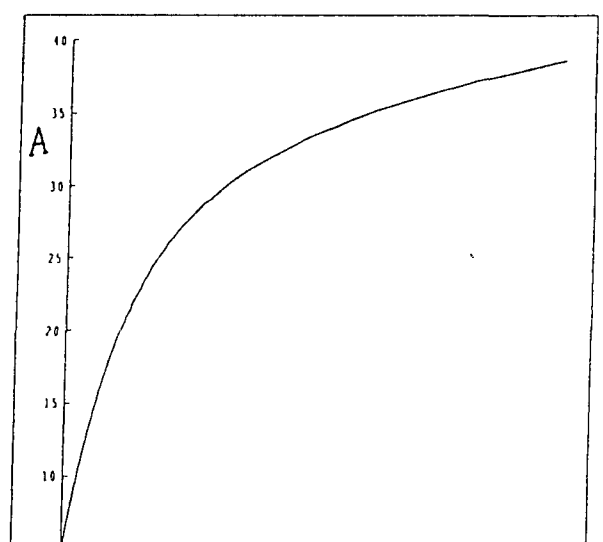

The crack tip **a**=ε**A** is plotted against time.

Figure 1

γ=1.4: In this case, the initial **f** value is 4.5, which is approximately the same value as when there is no gas in the cracks. Checking the numerics via the conservation of total gas mass (4;3ii) the errors are always less than 1% for the τ given in figure(i). The parameters chosen for this case are as on page 17, section 3.0.

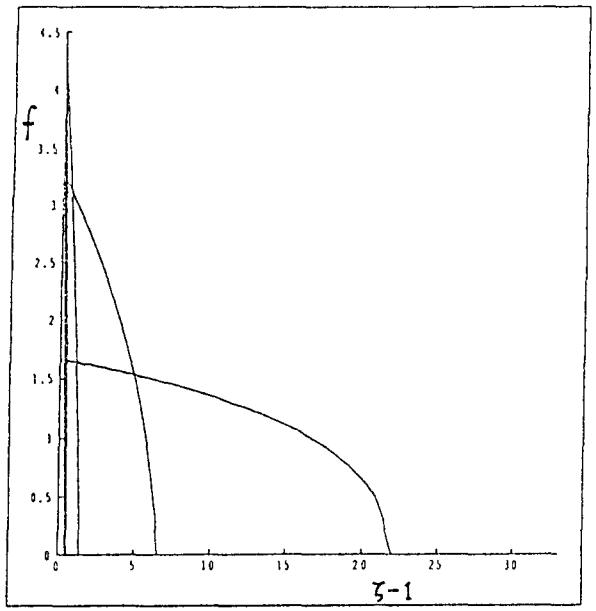

Pressure profiles **f** for τ=0, 10^{-4},10^{-3}, 10^{-2}, 10^{-1} where

$$p = 2\sigma f, \quad x = \varepsilon\zeta$$

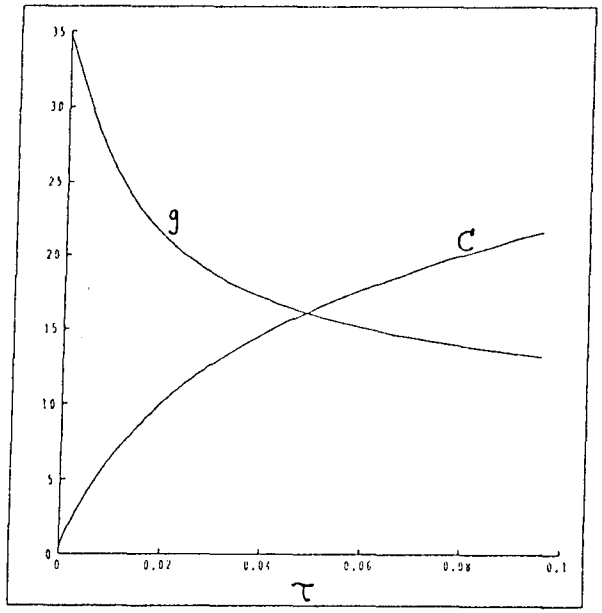

The gas penetration into the cracks $\mathbf{c}=\varepsilon\mathbf{C}$ and the borehole decompression ratio **g** are plotted against time. **g** is scaled to fit on the graph and **g(0)=1.**

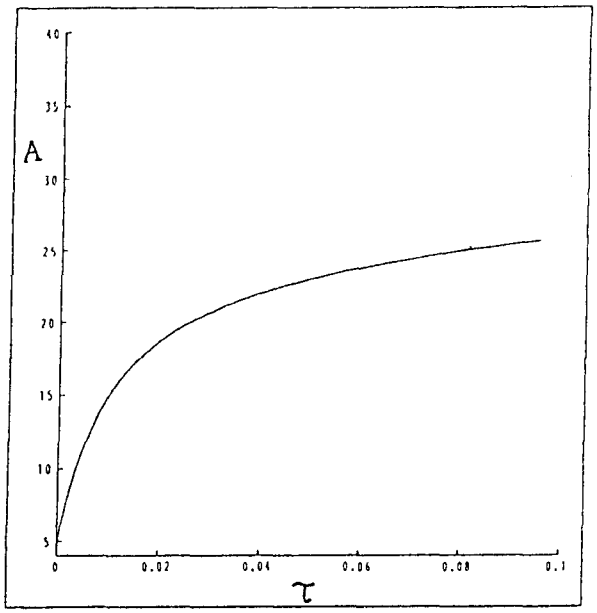

The crack tip $\mathbf{a}=\varepsilon\mathbf{A}$ is plotted against time.

Figure ii

<u>γ=2.5</u>: In this case the initial **f** value is 4.5, which is approximately the same value as when there is no gas in the cracks. Checking the numerics via the conservation of total gas mass (4;3ii) the errors are always less than 1% for the τ given in figure(i). The parameters chosen for this case are as on page 17, section 3.0.

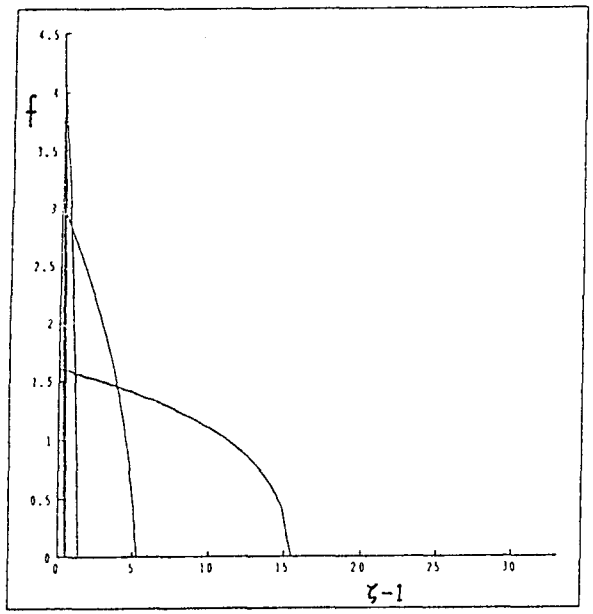

Pressure profiles **f** for τ=0, 10^{-4},10^{-3}, 10^{-2}, 10^{-1} where

$$p = 2\sigma f, \quad x = \varepsilon\zeta$$

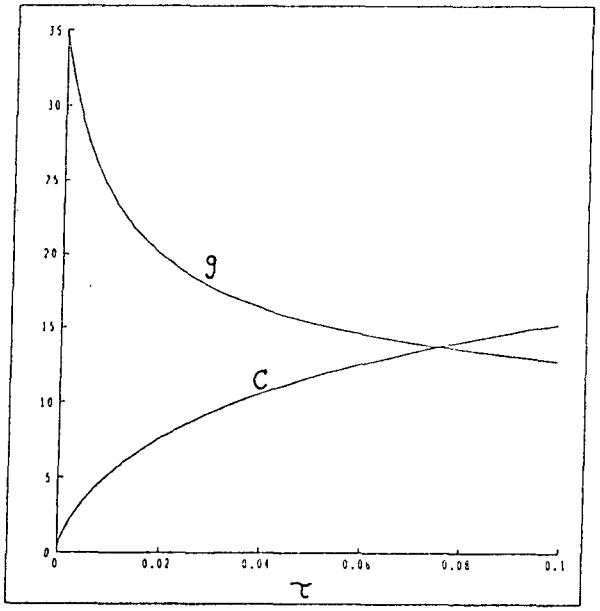

The gas penetration into the cracks $\mathbf{c}=\varepsilon\mathbf{C}$ and the borehole decompression ratio **g** are plotted against time. **g** is scaled to fit on the graph and **g(0)**=1.

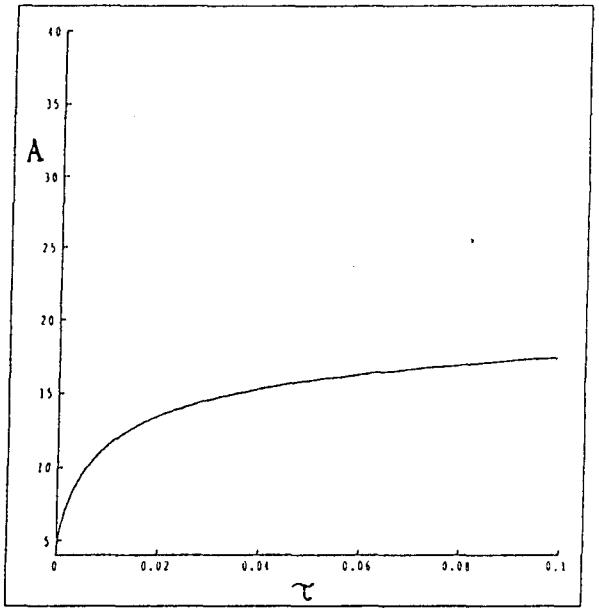

The crack tip $\mathbf{a}=\varepsilon\mathbf{A}$ is plotted against time.

Figure iii

γ=5: In this case, for an initial **f** value of 4.5, an original estimate of **f** when there is no gas in the cracks is **f**=4.7 (using ((4;3ii) and (4;7)). Checking the numerics via the conservation of total gas mass (4;3ii) the errors are always less than 1,1,1,2% for the τ given in figure(i). The parameters chosen for this case are as on page 17, section 3.0 except for $\mathbf{p_b}$=94x10^6 Pa and γ=5.

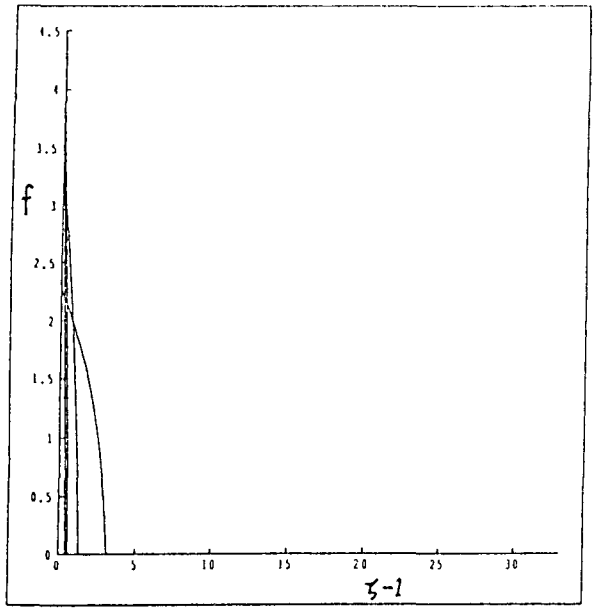

Pressure profiles **f** for τ=0, 10^{-4},10^{-3}, 10^{-2} where

$$p = 2\sigma f, \quad x = \varepsilon\zeta$$

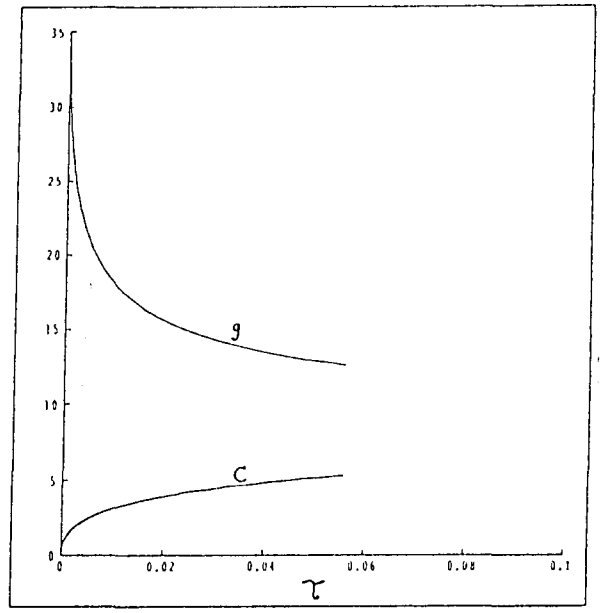

The gas penetration into the cracks **c=εC** and the borehole decompression ratio **g** are plotted against time. **g** is scaled to fit on the graph and **g(0)=1.**

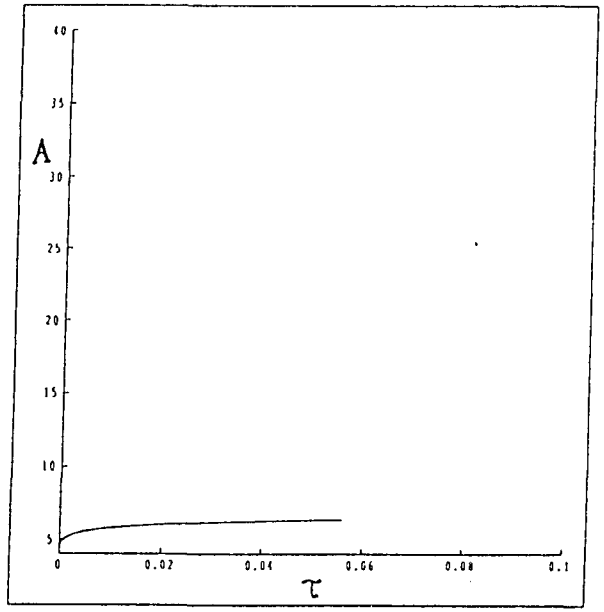

The crack tip **a=εA** is plotted against time.

Figure iv

<u>γ=50</u>: In this case, for an initial **f** value of 4.5, an original estimate of **f** when there is no gas in the cracks is **f**=6.0 (using ((4;3ii) and (4;7)). Checking the numerics via the conservation of total gas mass (4;3ii) the errors are always less than 1% * for the τ given in figure(i). The parameters chosen for this case are as on page 17, section 3.0 except for p_b=120x10^6 Pa and γ=50.

* A solution for τ=0.1 is not given.

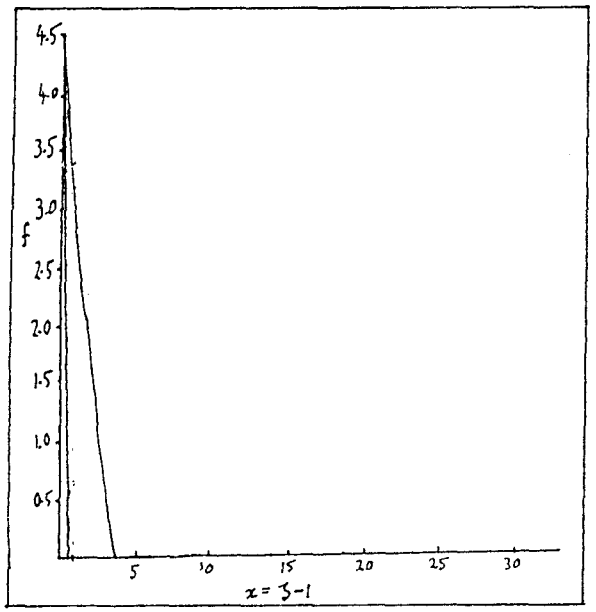

Pressure profiles **f** for $\tau=0,\ 10^{-2}$, where

$p=2\sigma f,\quad x=\varepsilon\zeta$

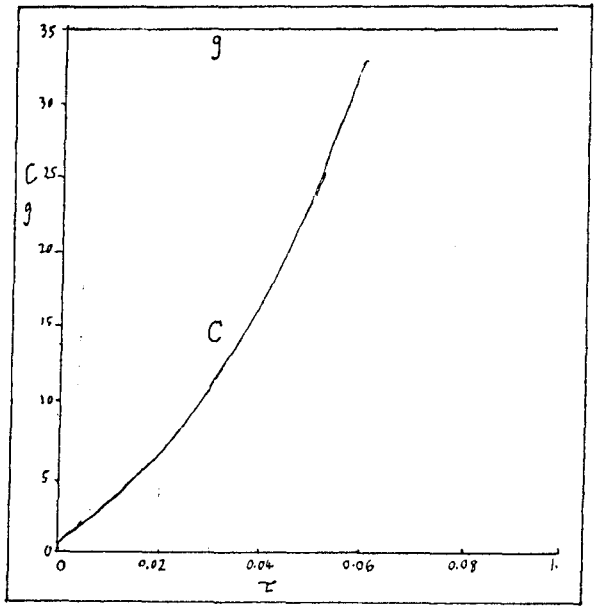

The gas penetration into the cracks $\mathbf{c}=\varepsilon\mathbf{C}$ and the borehole decompression ratio $\mathbf{g}\ (\mathbf{g}(\tau)=1)$

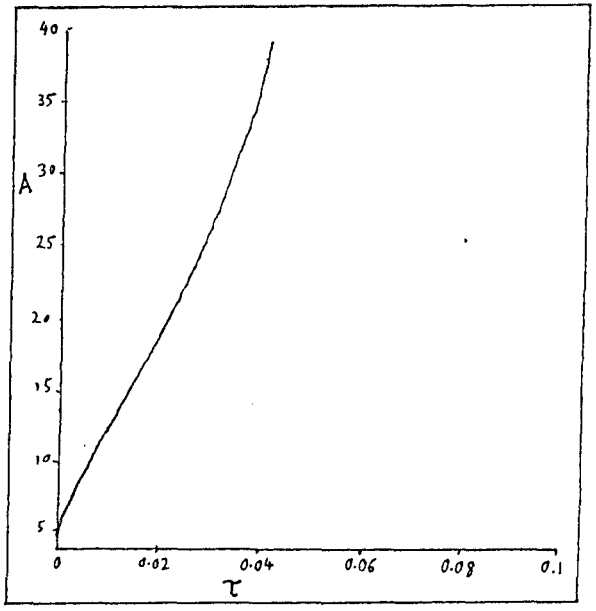

The crack tip $\mathbf{a}=\varepsilon\mathbf{A}$ is plotted against time.

Figure v

These figures are derived from the analytic solution given in (5.1.2i) representing the limiting solution for large $\mathbf{f}_1$, large γ, small κ and small borehole decompression.

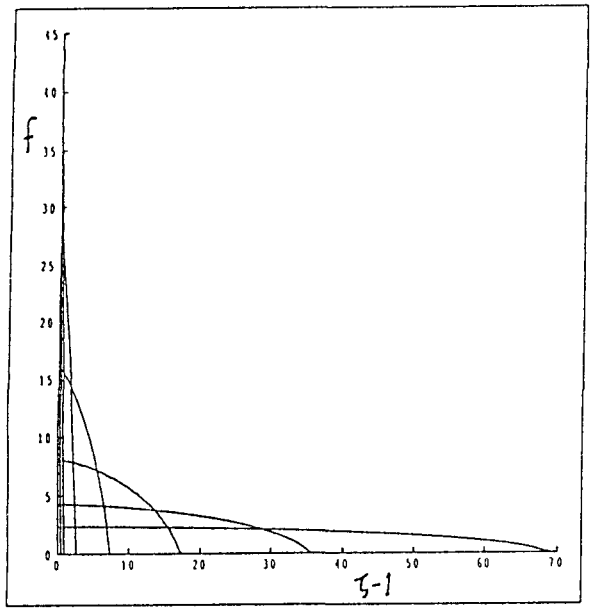

Pressure profiles **f** for τ=0, 10^{-7},10^{-6}, 10^{-5}, 10^{-4}, 10^{-3}, 10^{-2}, where

$$p = 2\sigma f, \quad x = \varepsilon\zeta$$

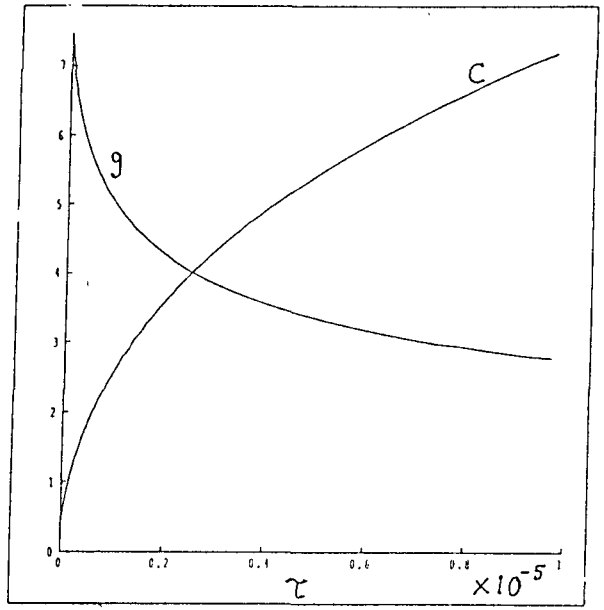

The gas penetration into the cracks $\mathbf{c}=\varepsilon\mathbf{C}$ and the borehole decompression ratio **g** are plotted against time. **g** is scaled to fit on the graph and g(0)=1.

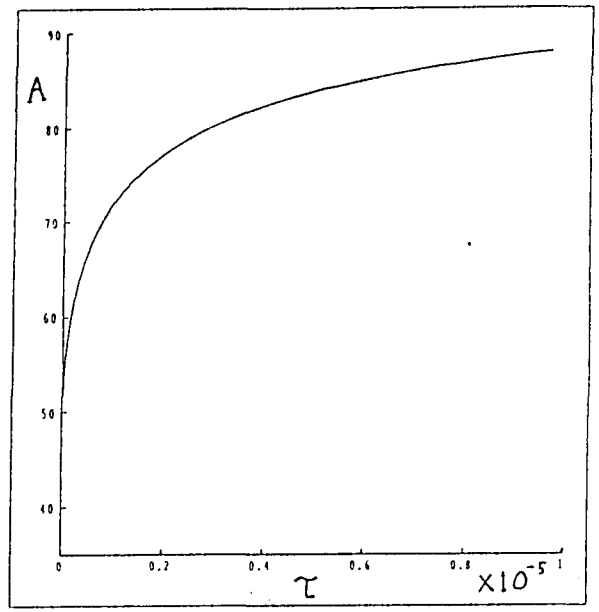

The crack tip $\mathbf{a}=\varepsilon\mathbf{A}$ is plotted against time.

Figure vi

<u>γ=1.4</u>: In this case, for an initial **f** value of 45.0, an original estimate of **f** when there is no gas in the cracks is at **f**=51.0 (using ((4;3ii) and (4;7)). Checking the numerics via the conservation of total gas mass (4;3ii) the errors are always less than 1,1,1,2,3,4% for the τ given in figure(i). The parameters chosen for this case are as on page 17, section 3.0 except for p_b=2.0x10^9 Pa.

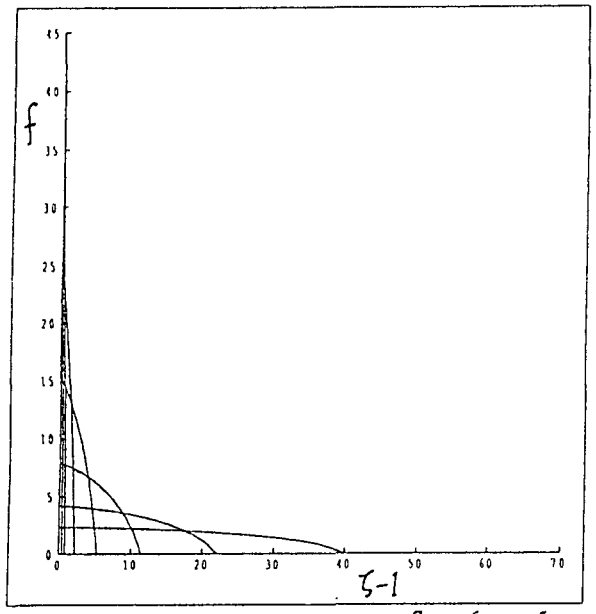

Pressure profiles **f** for τ=0, 10^{-7},10^{-6}, 10^{-5}, 10^{-4}, 10^{-3}, 10^{-2}, where

$$p = 2\sigma f, \quad x = \varepsilon\zeta$$

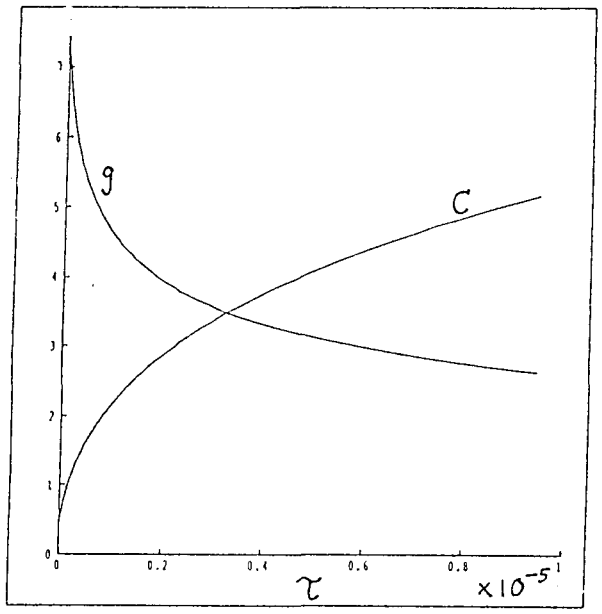

The gas penetration into the cracks $\mathbf{c}=\varepsilon\mathbf{C}$ and the borehole decompression ratio **g** are plotted against time. **g** is scaled to fit on the graph and **g(0)**=1.

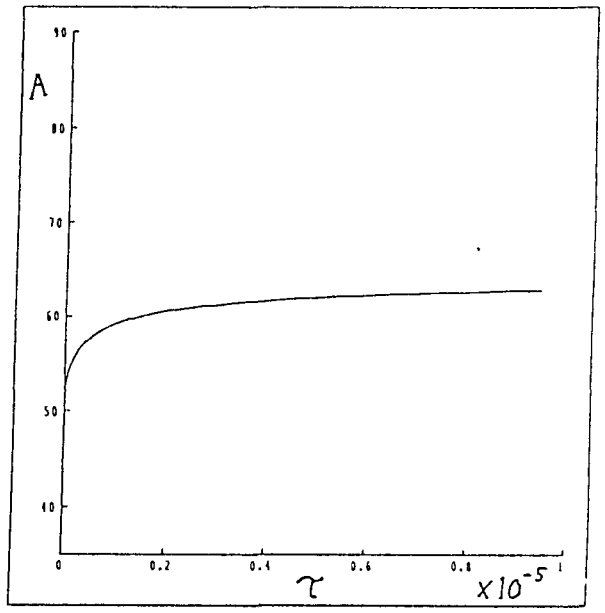

The crack tip $\mathbf{a}=\varepsilon\mathbf{A}$ is plotted against time.

Figure vii

<u>γ=2.5</u>: In this case, for an initial **f** value of 45.0, an original estimate of **f** when there is no gas in the cracks is at **f**=55.0 (using ((4;3ii) and (4;7)). Checking the numerics via the conservation of total gas mass (4;3ii) the errors are always less than 1% for the τ given in figure(i). The parameters chosen for this case are as on page 17, section 3.0 except for $\mathbf{p_b}=1.1\times10^9$ Pa.

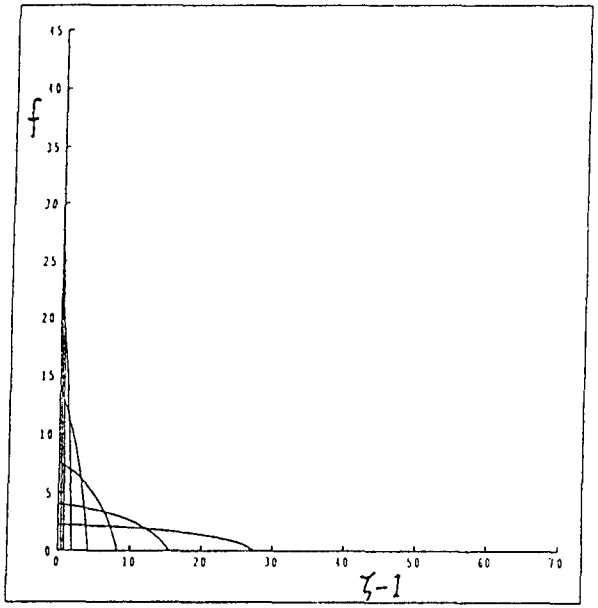

Pressure profiles **f** for τ=0, 10^{-7},10^{-6}, 10^{-5}, 10^{-4}, 10^{-3}, 10^{-2}, where

$$p = 2\sigma f, \quad x = \varepsilon\zeta$$

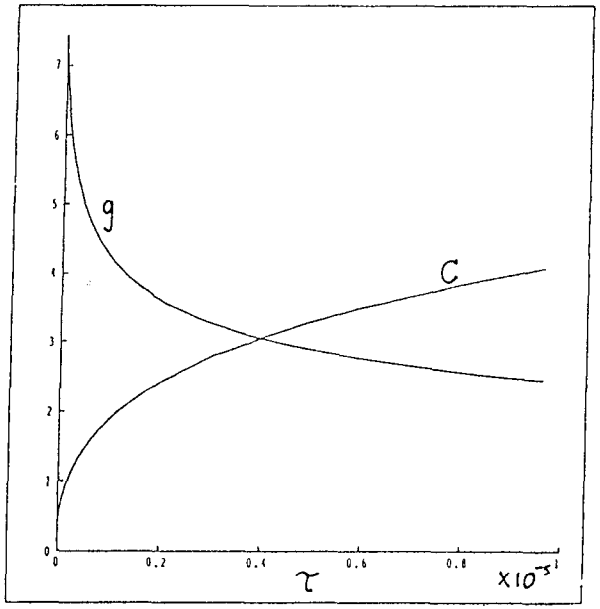

The gas penetration into the cracks $\mathbf{c}=\varepsilon\mathbf{C}$ and the borehole decompression ratio **g** are plotted against time. **g** is scaled to fit on the graph and **g(0)**=1.

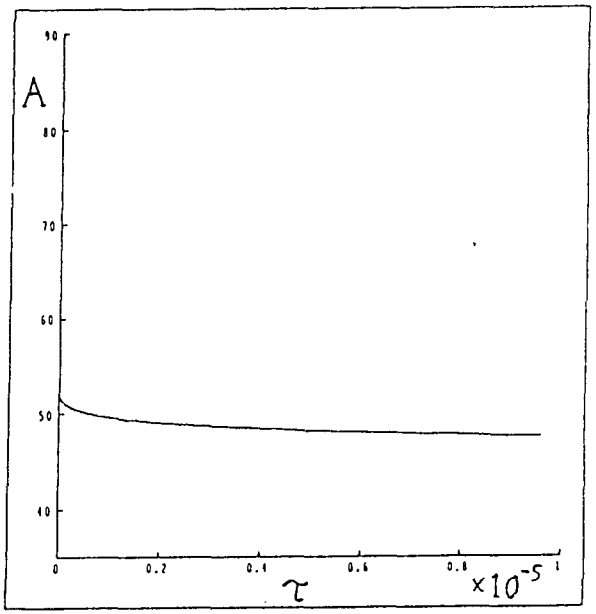

The crack tip $\mathbf{a}=\varepsilon\mathbf{A}$ is plotted against time.

Figure viii

<u>γ=5</u>: In this case, for an initial **f** value of 45.0, an original estimate of **f** when there is no gas in the cracks is at **f**=59.0 (using ((4;3ii) and (4;7)). Checking the numerics via the conservation of total gas mass (4;3ii) the errors are always less than 1,1,2,3,5,7% for the τ given in figure(i). The parameters chosen for this case are as on page 17, section 3.0 except for p_b=1.2x10^9 Pa and γ=5.

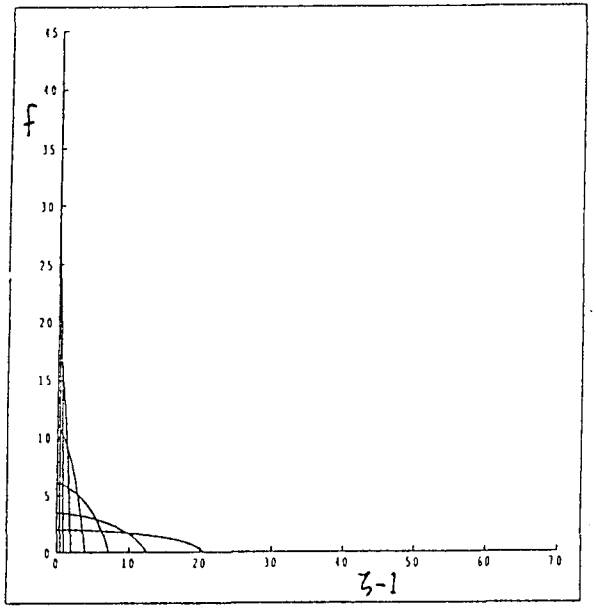

Pressure profiles **f** for τ=0, 10^{-7},10^{-6}, 10^{-5}, 10^{-4}, 10^{-3}, 10^{-2}, where

$$p = 2\sigma f, \quad x = \varepsilon\zeta$$

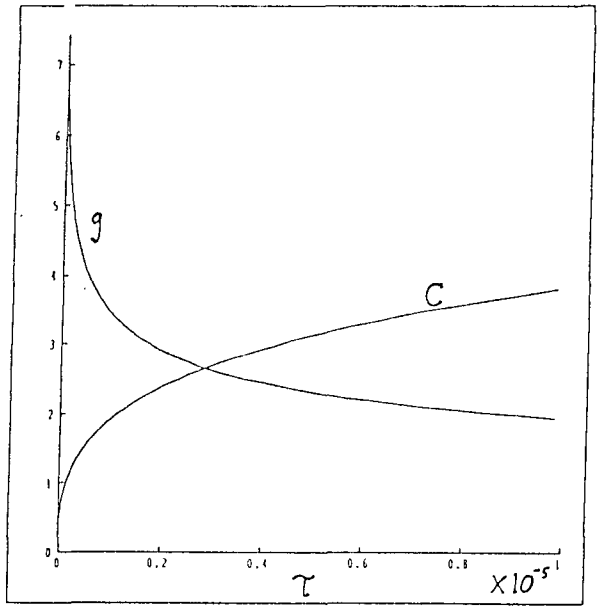

The gas penetration into the cracks $\mathbf{c}=\varepsilon\mathbf{C}$ and the borehole decompression ratio **g** are plotted against time. **g** is scaled to fit on the graph and **g(0)**=1.

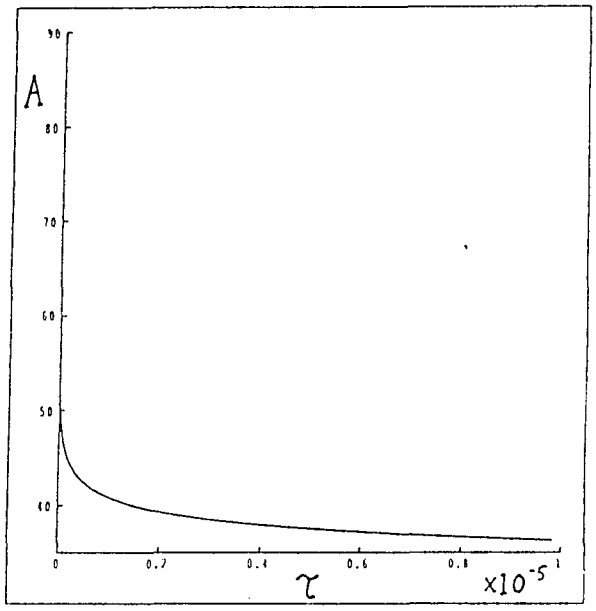

The crack tip $\mathbf{a}=\varepsilon\mathbf{A}$ is plotted against time.

Figure ix

<u>γ=50</u>: In this case, for an initial **f** value of 45.0, an original estimate of **f** when there is no gas in the cracks is **f**=69.0 (using ((4;3ii) and (4;7)). Checking the numerics via the conservation of total gas mass (4;3ii) the errors are always less than 3,6,12,18,25,31% for the τ given in figure(i). The parameters chosen for this case are as on page 17, section 3.0 except for $\mathbf{p_b}=1.4\text{x}10^9$ Pa and γ=50.

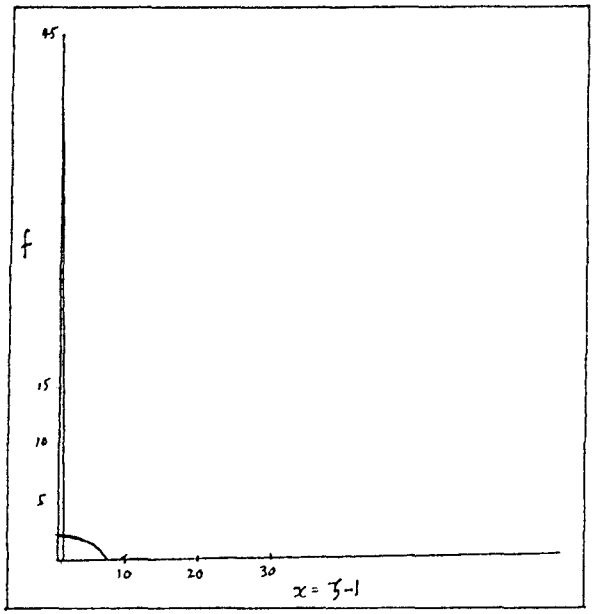

Pressure profiles **f** for $\tau=0,\ 10^{-3}$ where

$$p=2\sigma f,\quad x=\varepsilon\zeta$$

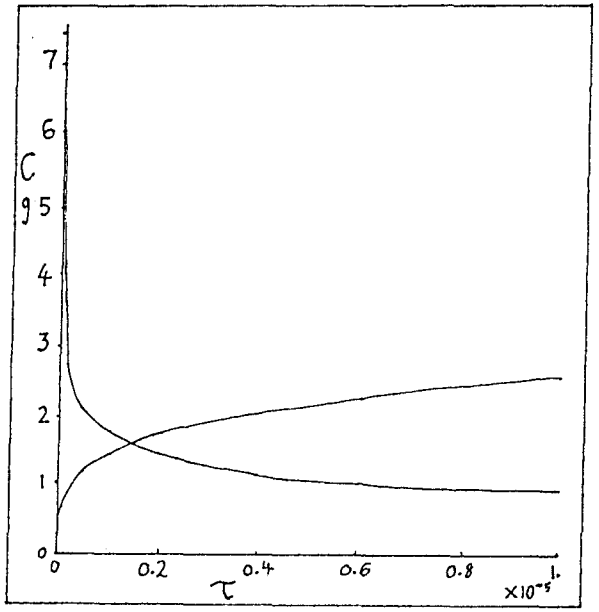

The gas penetration into the cracks $\mathbf{c}=\varepsilon\mathbf{C}$ and the borehole decompression ratio **g** are plotted against time. **g** is scaled to fit on the graph and $\mathbf{g}(0)=1$.

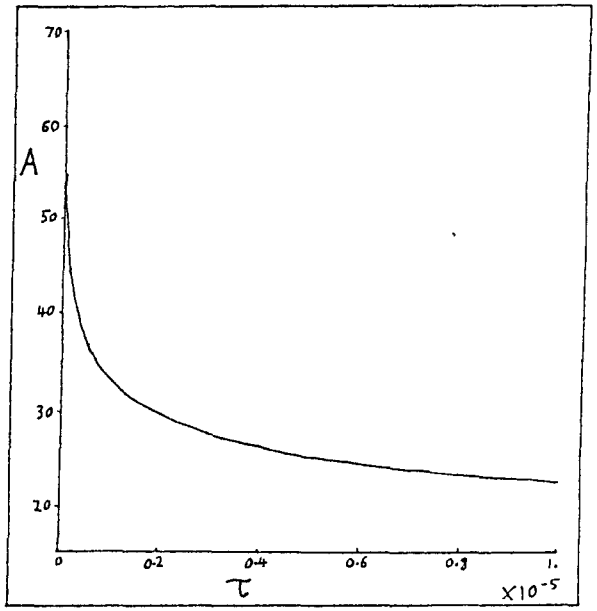

The crack tip $\mathbf{a}=\varepsilon\mathbf{A}$ is plotted against time.

Figure x

These figures are derived from the analytic solution given in (5.1.2ii) representing the limiting solution for large $\mathbf{f}_1$, large γ, small κ and large borehole decompression.

6. SUMMARY AND CONCLUSIONS

A simple example of the stage two gas penetration stage of rock blasting has been described in section 1.1. The physics and mathematics describing this process have been presented thoroughly in sections 2 and 3 and the non-dimensionalised mathematical model of rock blasting is summarised and written down in section 4. Some key points to be noted about these sections are:-

i) A model to determine the stress-strain relationship of rock containing a number of radial cracks emanating from a borehole has been developed (Appendix C). The model revealed that the crack height consists not only of a component due to local pressure [10], but also of a component due to the total force of the gas pressure in the cracks and borehole causing a divergence of the pie shaped pieces of rock (section(2.6.2)). The crack tip position can be determined by considering whether or not the stresses acting at the crack tip are sufficient to overcome the strength of the rock. This is not, in general, the same position as the gas front as would necessarily be the case in the local crack opening model of Erhie [10].

ii) The gas inside the crack will in general have a front distinct from the tip of the crack. From the gas front to the crack tip there will be a vacuum. After the gas and crack fronts meet, the pressure of the gas at the front is not zero, but can be calculated as an integral part of the mathematical model given in section 4.

iii) The Mach number of the gas flow along the cracks is quite small so that the inertial terms in the governing equations of motion are ignored. The resistance to gas flow along the cracks is governed by a simple turbulent viscosity model. Energy considerations for the gas flow lead us to assume an adiabatic gas law which seems quite a reasonable approximation for this study.(All the parameter assumptions for the gas flow model in this thesis are given in section 4.)

iv) The in-situ stress field within the rock can be identified as the main

prohibiting mechanism for crack growth, at least during the earlier stages of rock blasting (section(2.9)).

In section 5 the flow of gas from the borehole into the surrounding cracks was considered via the solution of the mathematical model proposed in section 4. A number of important features of stage 2 of the rock blasting process were then identified. These include:-

v) At early times during the blast the borehole pressure significantly affects the crack height. The gas from the borehole will flow into the open cracks and cause the initial gas velocities to be very large.

vi) Even when good stemming of the explosives is obtained and all gas is retained in the borehole and cracks, we can expect massive borehole decompression as the gas from the borehole moves into the cracks. Typically this decompression will occur on a time scale of

EV model;

$$t_{ev} \sim O\left(\frac{3\mu_{turb} E^2 n^2}{\pi^2 p_b^3 \left[\log_e \left(\frac{p_b}{2\sigma} \right) \right]^2} \right)$$

ML model;

$$t_{ml} \sim O\left(\varepsilon \left(\frac{l K_g E n}{2\pi p_b^{2-\frac{1}{\gamma}} \log_e \left(\frac{p_b}{2\sigma} \right)} \right)^{\frac{1}{2}} \right)$$

and a gas penetration length scale into the crack of

$$b \sim O\left(\varepsilon \sqrt{\frac{E}{p_b \gamma}} \right)$$

vii) After the borehole has suffered the massive decompression described in

(vi), the blasting process will continue on a much larger time-scale typified by *EV model;*

$$t_{ev} \sim O\left(\frac{3\mu_{turb}E^2n^2}{8\pi^2\sigma^3}\right)$$

ML model;

$$t_{ml} \sim O\left(\frac{e}{2\sigma}\left(\frac{lK_gEn(2\sigma)^{\frac{1}{\gamma}}}{2\pi}\right)^{\frac{1}{2}}\right)$$

or more precisely, see figures(5.3.i-x). This change in time-scale may explain previous difficulties that have occured in predicting blast time-scales whenever a constant borehole pressure is assumed [10].

viii) It was noticed that for large γ and large initial borehole pressure the initial direction of motion for the crack tip is backwards, towards the borehole ((5.1.2;17) and full numerical solutions for $\mathbf{p_b}$=45 and γ=5,50) otherwise it is outwards from the borehole (Appendix F, fig(5.1.2;17) and figs(5.3;")). The position of the crack tip is indicative of the stresses that the blast is generating on the surrounding rock (C18 and C19) and therefore at what stage of the blast the burden will typically start to move.

Further Work

There are many additional features of the rock blasting process that could be included into the model presented in this thesis (see section 1). The most important of these are probably:-

i) The inclusion of a free rock face in order to study the throwing of the burden. For a very simple model the effects of fragmentation could be ignored if we assumed that a single pie-shaped piece of rock is thrown. In reality the cracks would curve towards the rock face but, in order to make the model mathematically tractable, a predetermined crack path would have to be

approximated as a straight line (Figure 1).

ii) It still remains an open question as to how long during the rock blast we can expect the growth of more than two radial cracks to remain stable. It is possible that for the model in (i) above there are only two cracks that travel from the borehole to the rock face, and it is these cracks which determine the approximate shape of the burden.

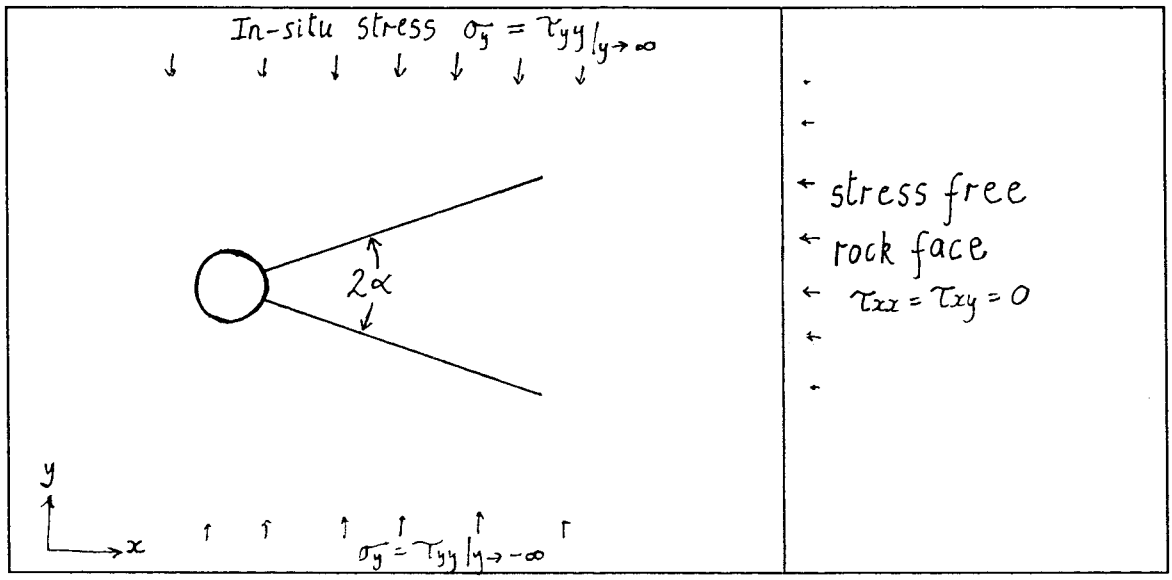

Figure 1 A simple rock blasting geometry that includes the rock face

Appendix A

The rock strains due to gravity and in-situ stress.

Given the internal stresses $\tau_{xx}=\tau_{yy}=\beta z-\sigma$ $\tau_{xz}=\tau_{yz}=0$ $\tau_{zz}=\rho g z$, and taking $\tau_{xy}=0$ as $r\rightarrow\infty$ (implying that $\tau_{xy}=0$ everywhere) then the displacements from equations (2.1;2) can only be of the form

$$u_x=Axz+Bx$$

$$u_y=Ayz+By \qquad \text{-(A1)}$$

$$u_z=C(x^2+y^2)+Dz^2+ez$$

where A,B,C,D,and e are constants. These constants can now be determined from the given stress distribution to give the final solutions

Cartesian coordinates.

$$u_x=\left(\frac{\beta(1-\nu)}{E}-\frac{\rho g\nu}{E}\right)xz-\frac{\sigma(1-\nu)x}{E}$$

$$u_y=\left(\frac{\beta(1-\nu)}{E}-\frac{\rho g\nu}{E}\right)yz-\frac{\sigma(1-\nu)y}{E} \qquad \text{-(A2)}$$

$$u_z=-\frac{1}{2}\left(\frac{\beta(1-\nu)}{E}-\frac{\rho g\nu}{E}\right)(x^2+y^2)+\left(\frac{\rho g}{2E}-\frac{\beta\nu}{E}\right)z^2+\frac{2\nu\sigma z}{E}$$

Polar coordinates.

$$u_r=\left(\left(\frac{\beta(1-\nu)}{E}-\frac{\rho g\nu}{E}\right)z-\frac{\sigma(1-\nu)}{E}\right)r$$

$$u_\theta=0$$

$$u_z=-\frac{1}{2}\left(\frac{\beta(1-\nu)}{E}-\frac{\rho g\nu}{E}\right)r^2+\left(\frac{\rho g}{2E}-\frac{\beta\nu}{E}\right)z^2+\frac{2\nu\sigma z}{E} \qquad \text{-(A3)}$$

where $\tau_{rr}=\tau_{\theta\theta}=\beta z-\sigma$

E and ν are the Young's Modulus and the Poissons Ratio respectively ☺

Appendix B

The Linear Elastic Solution for the Griffith Crack.

We shall use a complex variable method [9], to solve the stress-strain distribution for the Griffith crack problem. The 2-dimensional problem in the x-y plane is transformed into a problem in the complex plane **z=x+iy**.

The steady state equations of linear elasticity ((2.1;2) and (2.2;2) with $\underline{b}$=0) can be written

$$\frac{\partial H}{\partial \bar{z}}=0$$

$$\text{where} \quad H=2(\lambda+\mu)\left(\frac{\partial D}{\partial z}+\frac{\overline{\partial D}}{\partial z}\right)+4\mu\frac{\partial D}{\partial z} \qquad \text{-(B1)}$$

$$D=u_x+iu_y \quad \underline{u}=(u_x,u_y)$$

$$z=x+iy \quad \bar{z}=x-iy$$

where **i** is the imaginary number $\sqrt{-1}$.

D and **H** must be single valued in order that the stress-strain distribution is unique. In the following analysis we shall assume that all the partial derivatives of **u** and **v** with respect to **x** and **y**, to at least second order, exist and are single valued.

We shall refer to the region that is occupied by the linear elastic material as S^+. Hence the equations of elasticity (B1) must be satisfied in S^+. The crack region in which the linear elastic equations do not have to hold is labelled S^-. eg. the crack is a boundary to the elastic region and we can impose whatever conditions we wish upon it.

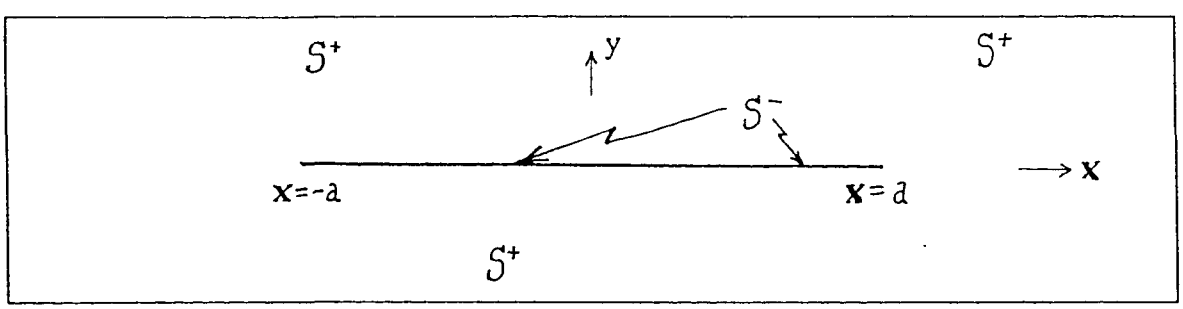

Figure B1 The Griffith Crack

Since **z** and $\bar{z}$ are an independent pair of **x** and **y**, the solution of (B1i) is simply

$$H=\theta'(z) \qquad \text{-(B2)}$$

H is only a function of **z** so that the Cauchy Riemann equations will hold. Since **H** is single valued then it is also an analytic function in S^+. Using Laurents theorem, **H** can be written

$$H=\sum_{-\infty}^{\infty} a_n(z-z_0)^n \quad \forall z \in S^+ \qquad \text{-(B3)}$$

where z_0 is a point contained somewhere within S^-. Integration of equation (B3) will yield another analytic function except for the a_{-1} term which will give multi-valued log terms. From (B2) and (B3) we deduce

$$\theta(z)=a_{-1}\log_e(z-z_0)+\theta^*(z) \qquad \text{-(B4)}$$

We can now express $\partial D/\partial z$ in terms of $\theta'(z)$ by taking real and imaginary parts of (B1ii) and using (B2) to give

$$8\mu(\lambda+2\mu)\frac{\partial D}{\partial z}=(\lambda+3\mu)\theta'(z)-(\lambda+\mu)\overline{\theta'(z)} \qquad \text{-(B5)}$$

$$=\text{function of}(z,\bar{z})$$

Equation (B5) is linear so we seek a solution for **D** in terms of a complementary function and a particular integral D_c and D_p. Noting that for an arbitrary function **s(z)** of **z**, $\bar{s}(z)$ is a function of $\bar{z}$, we obtain

$$8\mu(\lambda+2\mu)D_c=\overline{\phi(z)}$$

$$8\mu(\lambda+2\mu)D_p=(\lambda+3\mu)\theta(z)-(\lambda+\mu)z\ \overline{\theta'(z)} \qquad \text{-(B6)}$$

In order that **D** is single valued, $\phi(z)$ must be of the form

$$\phi(z)=\overline{a_{-1}}K\ (\lambda+\mu)\log_e(z-z_0)+\phi^*(z)$$

$$\text{where}\quad K=\frac{\lambda+3\mu}{\lambda+\mu} \qquad \text{-(B7)}$$

$\phi^*(z)$ is analytic in S^+ and z_0 is a point in S^- . If we now define the functions ω and Ω by

$$\theta(z)=\frac{4(\lambda+2\mu)}{\lambda+\mu}\Omega(z)$$
$$\phi=-4(\lambda+2\mu)\omega(z) \qquad \text{-(B8)}$$

then equations (B4) and (2.1;2) become

$$2\mu D=K\Omega(z)-z\overline{\Omega'(z)}-\overline{\omega(z)}$$
$$\tau_{xx}+\tau_{yy}=2(\Omega'(z)+\overline{\Omega'(z)}) \qquad \text{-(B9)}$$
$$\tau_{xx}-\tau_{yy}+2i\tau_{xy}=-2(z\overline{\Omega''(z)}+\overline{\omega'(z)})$$

In general there may be more than one crack or cavity in the linear elastic material so that the fuctions Ω and ω consist of a sum of log term contributions from each S^- plus an analytic function.

We shall now show how the quantity $\mathbf{a}_{-1}$ can be expressed in terms of the resultant force acting over each crack or cavity. The stress acting along some parameterised curve in the material is

$$\tau_{ij}n_i\underline{e}_j=P\underline{i}+Q\underline{j}$$
$$\text{where } \underline{n}=\left(\frac{dy}{ds},-\frac{dx}{ds}\right) \qquad \text{-(B10)}$$

Using the stress expressions in (B9) we obtain

$$P+iQ=-i\frac{d}{ds}\left[\Omega(z)+z\overline{\Omega'(z)}+\overline{\omega(z)}\right] \qquad \text{-(B11)}$$

Integrating this expression on a closed curve around S^- shows that

$$X+iY=2\pi a_{-1}(K+1) \qquad \text{-(B12)}$$

where (X,Y) is the total force acting on the crack region S^-.

Cracks may individually possess a net resultant force provided that the total force due to all of the cracks in the material is zero leading to the steady state system (B1). It is for this reason that we shall find that the single Griffith Crack, which cannot have a resultant force in a stationary elastic material, has $\mathbf{a}_{-1}=0$ and that Ω and ω are analytic in S^+.

We now need to work through a series of steps to obtain the solution to the crack

problem as described by figure (2.5;1). To avoid confusion between the upper and lower surfaces of the crack we shall attach suffices + and - as appropriate.

i) Ω and ω must be analytic in S^+ because the resultant force around the crack in figure (2.5;1) is zero, which using (B12) means that $\mathbf{a}_{-1}$ is zero.

ii) For convenience define a new analytic function θ in S^+ as

$$\theta(z)=\Omega(z)-z\overline{\Omega'(\bar{z})}-\overline{\omega(\bar{z})} \qquad \text{-(B13)}$$

iii) Substitute (ii) into (B9) to obtain

$$\begin{aligned} 2\mu D&=K\Omega(z)-\Omega(\bar{z})+(\bar{z}-z)\overline{\Omega'(z)}+\theta(\bar{z}) \\ \tau_{yy}-i\tau_{xy}&=\Omega'(z)+\Omega'(\bar{z})+(z-\bar{z})\overline{\Omega''(z)}-\theta'(\bar{z}) \end{aligned} \qquad \text{-(B14)}$$

iv) The known boundary conditions for this example are

$$\begin{aligned} \tau_{xy}&=\pm s(x) && y=0_{\pm},|x|<a \\ &=0 && y=0,|x|>a \\ u_y&=\frac{h(x)}{2}=Im(D) && y=0_{\pm},|x|<a \\ &=0 && y=0,|x|>a \end{aligned} \qquad \text{-(B15)}$$

and the unknown quantities to be calculated are the crack pressure **p** and the x component of displacement, $\mathbf{u}_x$

v) Due to the symmetries of the stresses and displacements in this problem, $\mathbf{D}=\mathbf{u}_x+i\mathbf{u}_y$ can be written as $4\mu i\mathbf{u}_y=2\mu(\mathbf{D}(z,\bar{z})-\mathbf{D}(\bar{z},z))$ and τ_{xy} as $-2i\tau_{xy}(z,\bar{z})=(\tau_{yy}(z,\bar{z})-i\tau_{xy}(z,\bar{z}))-(\tau_{yy}(\bar{z},z)-i\tau_{xy}(\bar{z},z))$ so that near the crack (B14) can be written

$$\begin{aligned} 2\mu ih(x)&=(K\Omega^+(x)-\Omega^-(x)+\theta^-(x))-(K\Omega^-(x)-\Omega^+(x)+\theta^+(x)) \\ -2is(x)&=\theta'^+(x)-\theta'^-(x) \end{aligned} \qquad \text{-(B16)}$$

The solution to (B16ii) is simply the Hilbert transform

$$\theta'(z) = -\frac{1}{\pi}\int_{-a}^{a}\frac{s(x)}{x-z}\,dx \qquad \text{-(B17)}$$

outline of proof

$\theta' \to 0$ as $|z| \to \infty$. The contour integral of $\theta'(z)/z_0 - z$ as $z \to \infty$ is also zero. Contracting this contour around the crack and the region around z_0 gives the required result.

Equations (B16ii,B17) can be integrated to give the solution for $\theta(z)$. If we then substitute θ into (B16i) a similar problem to (B16ii) emerges for $\Omega(z)$, given as

$$2\mu i h(x) - 2i\Sigma(x) = (K+1)[\Omega^{+}(x) - \Omega^{-}(x)]$$
$$\text{where} \quad \Sigma(x) = \int_{-a}^{x} s(\gamma)\,d\gamma \qquad \text{-(B18)}$$

with the solution

$$\Omega(z) = \frac{1}{\pi(K+1)}\int_{-a}^{a}(\mu h(t) - \Sigma(t))\frac{1}{t-z}\,dt$$
$$\Omega'(z) = \frac{1}{\pi(K+1)}\int_{-a}^{a}\left(\mu\frac{\partial h}{\partial t} - s(t)\right)\frac{1}{t-z}\,dt \qquad \text{-(B19)}$$

Using the real parts of (B14), we can write down the solutions for pressure and the x component of displacement (although the x component of displacement will not be of any use in future modelling)☺

$$p(x) = -\frac{E}{4\pi(1-\nu^2)}\int_{-a}^{a}\left(\frac{\partial h}{\partial \zeta} + \frac{2(1+\nu)(1-2\nu)}{E}s(\zeta)\right)\frac{d\zeta}{\zeta - x}$$
$$u_x = \frac{1}{4\pi(1-\nu)}\int_{-a}^{a}\left(2(1-2\nu)h(t) - \frac{2(1+\nu)(3-4\nu)}{E}\Sigma(t)\right)\frac{dt}{t-x} \qquad \text{-(B20)}$$

where:

E Young's Modulus

ν Poisson's Ratio

p pressure along crack

h crack height

s shear along crack

u_x x-component of displacement along crack.

and the relation between E and ν and λ,K and μ is

$$\mu=\frac{E}{2(1+\nu)},\quad \lambda=\frac{\nu E}{(1-2\nu)(1+\nu)},\quad K=\frac{\lambda}{3}\frac{1+\nu}{\nu}$$

Appendix C

The linear elastic solution for the n radial cracks problem

The mathematical problem is defined by equation (2.4.;2) and the boundary conditions are given in fig (2.6.1;1). This problem cannot be tackled analytically so we shall find an asymptotic solution for large n.

If we assume an asymptotic expansion of the form

$$\chi \sim \sum_{j=0}^{N} \chi_j \alpha^j \qquad \text{-(C1)}$$

$$\text{where } \alpha = \frac{\pi}{n} \quad \text{and } \theta = \alpha\phi$$

then (2.4;2) (all including the boundary condition $\tau_{r\theta}=0$ on $\phi=\pm 1$) can be expressed as *the stress function*

$$\chi_0 = B(r)$$

$$\chi_1 = D(r)$$

$$\chi_2 = er\phi^2 + F(r)$$

$$\chi_3 = Gr\phi^2 + H(r)$$

$$\chi_4 = \frac{\zeta(r)\phi^4}{24} + \frac{1}{12}(Nr - \zeta(r))\phi^2 + K(r)$$

$$\chi_5 = \frac{\eta(r)\phi^4}{24} + \frac{1}{12}(Pr - \eta(r))\phi^2 + M(r) \qquad \text{-(C2)}$$

$$\textit{where} \begin{cases} \zeta(r) = -r^4\left[\left\{\frac{1}{r}\frac{d}{dr}\left(r\frac{d}{dr}\right)\right\}^2 B(r) + \frac{4e}{r^3}\right] \\ \quad = -r^4 B^{(iv)} - 2r^3 B''' + r^2 B'' - rB' - 4er \\ \xi(r) = -r^4\left[\left\{\frac{1}{r}\frac{d}{dr}\left(r\frac{d}{dr}\right)\right\}^2 D(r) + \frac{4G}{r^3}\right] \\ \quad = -r^4 D^{(iv)} - 2r^3 D''' + r^2 D'' - rD' - 4Gr \end{cases}$$

the stresses:-

$$\tau_{rr}=\frac{B'(r)+2e}{r}+\alpha\frac{D'(r)+2G}{r}+\frac{\alpha^2}{r}\left(e\phi^2+F'(r)+\frac{N}{6}+\frac{\zeta(r)}{r}\left(\frac{\phi^2}{2}-\frac{1}{6}\right)\right)+$$

$$\frac{\alpha^3}{r}\left(G\phi^2+H'(r)+\frac{P}{6}+\frac{\eta(r)}{r}\left(\frac{\phi^2}{2}-\frac{1}{6}\right)\right)+\ldots$$

$$\tau_{\phi\phi}=B''(r)+\alpha D''(r)+\alpha^2F''(r)+\alpha^3H''(r)+\alpha^4\left(\frac{\zeta''(r)(\phi^2-1)^2}{24}-\right. \qquad \text{-(C3)}$$

$$\left.\frac{\zeta''(r)}{24}+K''(r)\right)+\alpha^5\left(\frac{\eta''(r)(\phi^2-1)^2}{24}-\frac{\eta''(r)}{24}+M''(r)\right)+\ldots$$

$$\tau_{r\phi}=\alpha^3\left(\frac{\phi(\phi^2-1)}{6}\left(\frac{\zeta(r)}{r^2}-\frac{\zeta'(r)}{r}\right)\right)+\alpha^4\left(\frac{\phi(\phi^2-1)}{6}\left(\frac{\eta(r)}{r^2}-\frac{\eta'(r)}{r}\right)\right)+\ldots$$

the strains:-

$$u_r=\frac{1}{E}\int_a^r\left(\frac{B'+2e}{y}-\nu B''\right)dy+A_1+\alpha\left(\frac{1}{E}\int_a^r\left(\frac{D'+2G}{y}-\nu D''\right)dy+A_2\right)+\ldots$$

$$u_\phi=\alpha\left(-\frac{r\phi}{E}\int\frac{1}{r^2}\left\{2e\log_e r+\int\frac{\zeta(r)}{r}dr\right\}dr\right)+$$

$$\alpha^2\left(-\frac{r\phi}{E}\int\frac{1}{r^2}\left\{2G\log_e r+\int\frac{\eta(r)}{r^2}dr\right\}dr\right)+\ldots \qquad \text{-(C4)}$$

or

$$u_\phi=\alpha\left[-\frac{r\phi}{E}\left[-B''(r)+\frac{1}{r}\int_a^r\left(\frac{B'+2e}{y}\right)dy\right]-A_1\phi-\frac{\nu\phi}{E}(B'(a)+2e)\right]+$$

$$\alpha^2\left[-\frac{r\phi}{E}\left[-D''+\frac{1}{r}\int_a^r\left(\frac{D'+2G}{y}\right)dy\right]-A_2\phi-\frac{\nu\phi}{E}(D'(a)+2G)\right]+..$$

We should note that in deriving these equations, the quantities A_i ϕ in (C4) assume a general form $A_i(\phi)$. Only by considering the full linear elasticity equations in polar form

[17] can this simplification be shown.

The conditions in fig (2.6.1;1) can be satisfied by these asymptotic expansions in the following two regions of the elastic material:-

i) From the borehole to the crack tip where the boundary conditions are

$$\tau_{\theta\theta}|_{\phi=\pm 1} = -p(r) \qquad \varepsilon < r < a - O(\alpha|a|)$$
$$\tau_{rr} = -p_b \qquad r = \varepsilon \qquad \text{-(C5)}$$

ii) From the crack tip to infinity where the boundary conditions are

$$u_\phi|_{\phi=\pm 1} = 0 \qquad a + O(\alpha|a|) < r < \infty \qquad \text{-(C6)}$$

(NB. calculations for this region are simpler if the second expression for $\mathbf{u}_\phi$ (C4ii) is used in the calculations.)

The resulting expansions cannot be asymptotically matched because the crack tip region undergoes changes in the stress-strain distribution on a much smaller length scale than the crack length **a**. This means that we need to study the behaviour of the **Boundary Layer** at the crack tip and match the solutions of this region to both of the **outer regions** calculated above.

The Crack tip Region

The intricacies of the stress-strain distribution will only be seen if we look at the crack tip region on a much smaller lengthscale than **a**. It is quite simple to show this length scale to be ~O(αa) by showing that

$$\rho = \frac{r-a}{\alpha} \qquad \text{-(C7)}$$

is the only re-scaling of r which will allow a solution for the required boundary conditions, given as

$$\tau_{\theta\theta}|_{\phi\pm 1} = -p(r) = -p(a) - \rho\alpha p'(a) + \ldots \qquad \rho < 0$$
$$u_\phi|_{\phi=\pm 1} = 0 \qquad \rho > 0 \qquad \text{-(C8)}$$

Substituting (C7) into (C2,C3,C4) yields the boundary layer problem

the stress function:-

$$\chi^i = -\alpha\rho\left(\varepsilon p_b + \int_\varepsilon^a p(y)dy\right) + \alpha^2\chi^i{}_2 + \ldots \qquad \text{-(C9)}$$

$$\text{where} \quad \left\{\frac{\partial^2}{\partial\rho^2} + \frac{1}{a^2}\frac{\partial^2}{\partial\phi^2}\right\}^2 \chi^i{}_2 = 0$$

the stresses:-

$$\tau^i{}_{\rho\rho} = -\frac{1}{a}\left(\varepsilon p_b + \int_\varepsilon^a p(y)dy\right) + \frac{1}{a^2}\frac{\partial^2\chi^i{}_2}{\partial\phi^2} + \ldots$$

$$\tau^i{}_{\phi\phi} = \frac{\partial^2\chi^i{}_2}{\partial\rho^2} + \ldots \qquad \text{-(C10)}$$

$$\tau^i{}_{\rho\phi} = -\frac{1}{a}\frac{\partial^2\chi^i{}_2}{\partial\rho\partial\phi} + \ldots$$

the strains:-

$$u^i{}_\rho = u^i{}_{\rho 0} + \alpha u^i{}_{\rho 1} + \ldots$$

$$u^i{}_\phi = \alpha u^i{}_{\phi 1} + \ldots$$

$$\text{where} \quad \frac{\partial u^i{}_{\rho 1}}{\partial\rho} = \frac{1}{E}((\tau^i{}_{\rho\rho})_0 - \nu(\tau^i{}_{\phi\phi})_0) \qquad \text{-(C11)}$$

$$\text{and} \quad \frac{1}{a}\frac{\partial u^i{}_{\rho 1}}{\partial\phi} + a\frac{\partial u^i{}_{\phi 1}}{\partial\rho} = -\frac{2(1+\nu)}{E}\frac{\partial^2\chi^i{}_2}{\partial\rho\partial\phi}$$

Asymptotic matching has been performed to obtain the first approximation for χ^i, and $\mathbf{u}_\rho$. The quantity $\mathbf{u}_{\rho 0}$ is a constant in the inner region which means that it will be equal to the terms $\mathbf{u}_{r0}$ in both of the outer regions.

The equation for $\mathbf{u}_\phi$ in (C11) can be simplified by a manipulation of equations (C9,C11) to obtain

$$\frac{1}{a}\frac{\partial u^i{}_{\phi 1}}{\partial\phi} = \frac{1}{E}[(\tau^i{}_{\phi\phi})_0 - \nu(\tau^i{}_{\rho\rho})_0] + \rho F_1(\phi) + F_2(\phi) \qquad \text{-(C12)}$$

where $\mathbf{F}_1$ and $\mathbf{F}_2$ are functions of ϕ to be determined. These functions can be found by

asymptotic matching of (C12) to the outer regions to give

$$F_1(\phi)=0$$

$$F_2(\phi)=-\frac{A_1}{a}=-\frac{u^i{}_{\rho 0}}{a} \qquad \text{-(C13)}$$

It is now convenient to express the boundary layer problem as the sum of 2 problems similar to the method of finding a complementary function and a particular integral

the particular integral solution:-

$$\tau_{\rho\rho}=-\frac{1}{a}\left[\varepsilon p_b+\int_{\varepsilon}^{a} p(y)dy\right]$$

$$\tau_{\phi\phi}=-\tau_{\rho\rho}$$

$$\tau_{\rho\phi}=0 \qquad \text{-(C14)}$$

$$u_{\rho 1}=-\frac{\rho(1+\nu)}{Ea}\left[\varepsilon p_b+\int_{\varepsilon}^{a} p(y)dy\right]$$

$$u_{\phi 1}=0$$

the complementary function problem:-

$$\left(\frac{\partial^2}{\partial\rho^2}+\frac{1}{a^2}\frac{\partial^2}{\partial\phi^2}\right)^2\chi^i{}_2=0$$

$$\tau_{\phi\phi}=\frac{\partial^2\chi^i_2}{\partial\rho^2} \quad \tau_{\rho\phi}=-\frac{1}{a}\frac{\partial^2\chi^i_2}{\partial\rho\partial\phi} \quad \tau_{\rho\rho}=\frac{1}{a^2}\frac{\partial^2\chi^i_2}{\partial\phi^2} \qquad \text{-(C15)}$$

$$\frac{\partial u^i{}_{\rho 1}}{\partial\rho}=\frac{1}{E}(\tau_{\rho\rho}-\nu\tau_{\phi\phi}) \quad \frac{1}{a}\frac{\partial u^i{}_{\phi 1}}{\partial\phi}=\frac{1}{E}(\tau_{\phi\phi}-\nu\tau_{\rho\rho})$$

with the boundary conditions:-

$$\tau_{\phi\phi}|_{\phi=\pm 1}=-p(a)-\frac{1}{a}\left[\varepsilon p_b+\int_{\varepsilon}^{a} p(y)dy\right] \quad \rho<0$$

$$u_{\phi 1}|_{\phi=\pm 1}=0 \quad \rho>0 \qquad \text{-(C16)}$$

$$\tau_{\rho\phi}|_{\phi=\pm 1}=0, \quad \lim_{\rho\to-\infty}\tau_{\rho\rho}=0$$

The problem for the complementary function is equivalent to the problem for an infinite row of semi infinite cracks in cartesian coordinates. The solution to this problem is dealt with in Appendix D. The stress-strain distribution cannot be given in an explicit form but this is not of much significance for applications to rock blasting, since we only lose information about the crack height in a small region near the crack tip. Of much more importance however, is the calculation of the Stress Intensity Factor (defined as $\mathbf{K=\lim_{r\to a}}\ (2(r-a))^{0.5}\tau_{\theta\theta}$) which is given analytically in Appendix D.

Finally collecting together all of the solutions for the first order asymptotic solution of the multi-radial crack problem:-

$\varepsilon<r<a-O(\alpha/a/)$

$$\tau_{\theta\theta}=-p(r)+O(\alpha^4)$$

$$\tau_{rr}=-\frac{1}{r}\left[\varepsilon p_b+\int_{\varepsilon}^{r}p(y)dy\right]+O(\alpha^2)$$

$$\tau_{r\theta}=O(\alpha^3)$$

$$u_\theta=-\frac{\alpha\phi}{E}\left[r\left(p(r)+\frac{1}{r}\int_{r}^{a}\frac{1}{\zeta}\left[\varepsilon p_b+\int_{\varepsilon}^{\zeta}p(y)dy\right]d\zeta\right)+\left(\varepsilon p_b+\int_{\varepsilon}^{a}p(y)dy\right)\right]+O(\alpha^3) \qquad \text{-(C17)}$$

$$u_r=\frac{1+\nu}{E}\left[\varepsilon p_b+\int_{\varepsilon}^{a}p(y)dy\right]+\frac{1}{E}\int_{a}^{r}\left[\nu p(\zeta)-\frac{1}{\zeta}\left[\varepsilon p_b+\int_{\varepsilon}^{\zeta}p(y)dy\right]\right]d\zeta+O(\alpha^2)$$

$r-a/-O(\alpha a)$

$$K=\sqrt{\frac{a}{n}}\left(p(a)+\frac{1}{a}\left[\varepsilon p_b+\int_{\varepsilon}^{a}p(y)dy\right]\right)+O\left(\frac{1}{n}\right) \qquad \text{-(C18)}$$

where $K=\lim_{\substack{r\to a\\ \phi=\pm1}}(\sqrt{2(r-a)}\ \tau_{yy})$

$a+O(\alpha|a|)<r<\infty$

$$\tau_{\theta\theta}=\frac{a}{r^2}\left(\varepsilon p_b+\int_{\varepsilon}^{a}p(y)dy\right)+O(\alpha^2)$$

$$\tau_{rr}=-\frac{a}{r^2}\left(\varepsilon p_b+\int_{\varepsilon}^{a}p(y)dy\right)+O(\alpha^2)$$

$$\tau_{r\theta}=O(\alpha^5)$$

$$u_\theta=O(\alpha^3)$$

$$u_r=\frac{(1+\nu)a}{Er}\left[\varepsilon p_b+\int_{\varepsilon}^{a}p(y)dy\right]+O(\alpha^2)$$

-(C19)

Appendix D

The solution for an infinite number of semi-infinite cracks subject to a constant pressure via the Wiener Hopf Technique

Introduction to the Wiener Hopf Technique

The basic principle of the Wiener Hopf Technique is extremely simple. If a complex variable equation can be written in the form

$$f(z)=g(z) \qquad \text{-(D1)}$$

where f is analytic in Im(z)>α

and g is analytic in Im(z)<β

f,g →0 as z →∞

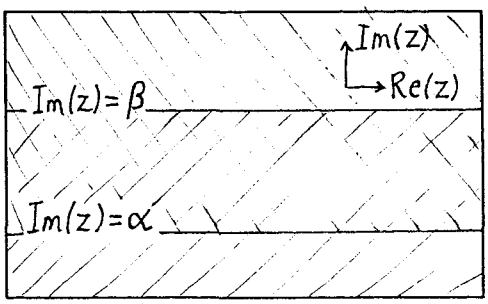

Figure D1

then by analytic continuation, f and g are analytic in all **C**. By Liouvilles theorem, the only function analytic in all **C** is a constant, hence (D1) can be written as

$$f(z)=g(z)=0 \qquad \text{-(D2)}$$

The major difficulty occurs in arranging the problem into a suitable form to be able to apply the Wiener Hopf Technique as above. Sometimes, even if this formulation is found and the Wiener Hopf Technique is applied, the form of solution is extremely complicated and is little more enlightening than the original problem [35,36]! The Wiener Hopf Technique does nevertheless provide us with a solution, and often this solution can be simplified using local analysis, asymptotic analysis etc. in order to provide useful information.

There are many techniques used to arrange a problem into the form of equation (D1) but we shall only present those techniques that are needed for this example [16,28,35,36].

i) If **H**(ω) is analytic and contains no zeros in the strip α<**Im**(ω)<β then

$$H(\omega)=\frac{H_+(\omega)}{H_-(\omega)}$$

$$H_+(z)=\exp\left\{\frac{1}{2\pi i}\int_{-\infty+i\gamma}^{\infty+i\gamma}\frac{\log_e H(\omega)}{\omega-z}d\omega\right\} \quad \text{analytic for } \alpha<\gamma<Im(z) \qquad \text{-(D3)}$$

where $\mathbf{H_-(z)}$ is similarly defined for γ analytic on $\beta>\gamma>\mathbf{Im(z)}$, and

$$\lim_{|\omega|\to\infty}\{\log_e H(\omega)\}=0 \qquad \text{-(D4)}$$

It is relatively simple to impose the condition in equation (D4) as $\omega\to\infty$ by normalising **H**. We must be careful to check that as $\omega\to-\infty$, **H** does not perform any circuits around **H**=0, as this would lead to $\log_e\mathbf{H}$ not tending to zero but to $2\pi\mathbf{ni}$ where $\mathbf{n}\in\mathbf{I}$ [16].

Proof of equation (D3)

H(z) is non zero and analytic in $\alpha<Im(z)<\beta$ *implies that* $\log_e H(z)$ *is analytic in* $\alpha<Im(z)<\beta$. *Hence* $\log_e H$ *can be written*

$$\log_e H(z)=\frac{1}{2\pi i}\int_C\frac{\log_e H(\omega)}{\omega-z}d\omega \qquad \text{-(D5)}$$

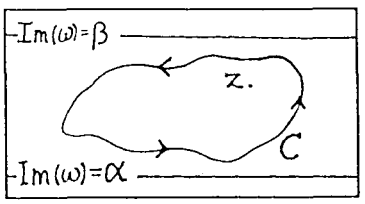

Figure D2

C is any closed curve within $\alpha<Im(z)<\beta$. *If we now let* **C** *be the curve* $C_1+C_2+C_3+C_4$

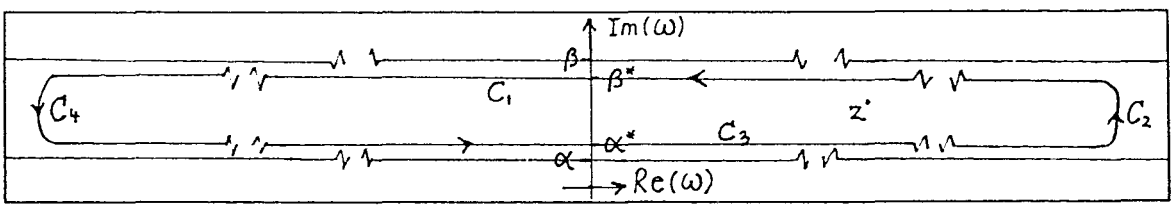

Figure D3

then by equations (D4,D5) we have

$$\log_e H(z)=\frac{1}{2\pi i}\left\{\int_{-\infty+i\alpha^*}^{\infty+i\alpha^*}-\int_{-\infty+i\beta^*}^{\infty+i\beta^*}\right\}\frac{\log_e H(\omega)}{\omega-z}d\omega=\log_e H_+(z)-\log_e H_-(z) \qquad \text{-(D6)}$$

We can show that the first integral is analytic for $Im(z)>\alpha^*$ *from Morea's Theorem, by showing that on integrating it around any closed contour in* $Im(z)>\alpha^*$*, the result is zero*

$$\frac{1}{2\pi i}\int_{-\infty+i\alpha^*}^{\infty+i\alpha^*}\log_e H(\omega)\int_{C_5}\frac{dz}{\omega-z}d\omega=0 \qquad \text{-(D7)}$$

$$\text{if}\quad \int_{C_5}\frac{dz}{\omega-z}=0$$

As all the points ω *must lie on* $Im(z)=\alpha^*$ *they will all be outside* C_5 *if* C_5 *lies in* $Im(z)>\alpha^*$*. If* $\log_e H_+$ *is analytic in* $Im(z)>\alpha$ *then* H_+ *is analytic and non-zero in* $Im(z)>\alpha$ *. A similar method shows the result for* $\log_e H_-(\omega)$*. From equation (D6) we have the final result* $\log_e H=\log_e H_+-\log_e H_-$*.*

ii) If $P(\omega)$ is analytic in the strip $\alpha<\text{Im}(\omega)<\beta$, then a similar analysis as in (i) will show

$$\begin{matrix}P_+(\omega)\\P_-(\omega)\end{matrix}=\pm\frac{1}{2\pi i}\int_{-\infty+\gamma i}^{\infty+\gamma i}\frac{P(\zeta)}{\zeta-\omega}d\zeta \quad \text{are analytic for} \quad \begin{matrix}\alpha<\gamma<Im(\omega)\\ \beta>\gamma>Im(\omega)\end{matrix} \qquad \text{-(D8)}$$

$$\text{where}\quad P(\omega)=P_+(\omega)+P_-(\omega)$$

Now if $P(\omega)$ is the Fourier Transform of $p(x)$ where $x\in\mathbf{R}$

$$P(\omega)=\frac{1}{\sqrt{2\pi}}\int_{-\infty}^{\infty}p(x)\exp i\omega x\,dx \qquad \alpha<Im(\omega)<\beta$$

$$p(x)=\frac{1}{\sqrt{2\pi}}\int_{-\infty+\bar{\gamma}i}^{\infty+\bar{\gamma}i}P(\omega)\exp -i\omega x\,d\omega \qquad \alpha<\bar{\gamma}<\beta \qquad \text{-(D9)}$$

then

$$P_+(\omega)=\frac{1}{\sqrt{2\pi}}\int_{0}^{\infty}p(x)\exp i\omega x\,dx$$

$$P_-(\omega)=\frac{1}{\sqrt{2\pi}}\int_{-\infty}^{0}p(x)\exp i\omega x\,dx \qquad \text{-(D10)}$$

Proof

Using equation (D8,D9) we can show

$$P_+(\omega)=\frac{1}{2\pi i\sqrt{2\pi}}\int_{-\infty}^{\infty}p(x)\left\{\int_{-\infty+\gamma i}^{\infty+\gamma i}\frac{\exp i\zeta x}{\zeta-\omega}d\zeta\right\}dx \qquad \begin{matrix}\alpha<\gamma<Im(\omega)\\ \alpha<Im(\zeta)<\beta\end{matrix} \qquad \text{-(D11)}$$

The required result is obtained by noting that by standard residue analysis

$$\int_{-\infty+\gamma i}^{\infty+\gamma i}\frac{\exp i\zeta x}{\zeta-\omega}d\zeta=\begin{matrix}2\pi i\ \exp i\omega x & x>0 \quad (\text{as } Im(\zeta)=\gamma)\\ 0 & x<0 \quad (\text{as } \alpha<\gamma<\beta)\end{matrix}$$

iii) If g(z)=f(z), and g(z),f(z) are analytic for Im(z)<β and Im(z)>α except that f(z) contains a pole of order n at $z=z_0$ where $z_0\in$ {Im(z)>α}, the equation can be written in the form required for (D1) if we subtract the pole from both sides ie.

$$g(z)-\sum^{k}\frac{A_k}{(z-z_0)^k}=f(z)-\sum^{k}\frac{A_k}{(z-z_0)^k} \qquad \text{-(D12)}$$

$$\Rightarrow \quad G(z)=F(z)$$

where **F** and **G** now obey the conditions in (D1)

<u>The formulation for the crack problem</u>

We need to solve

$$\nabla^4\chi\equiv\left(\frac{\partial^2}{\partial x^2}+\frac{\partial^2}{\partial y^2}\right)^2\chi=0$$

$$\tau_{xx}=\frac{\partial^2\chi}{\partial y^2}\quad \tau_{xy}=-\frac{\partial^2\chi}{\partial x\partial y}\quad \tau_{yy}=\frac{\partial^2\chi}{\partial x^2} \qquad \text{-(D13)}$$

$$\frac{\partial u_x}{\partial x}=\frac{1}{E}(\tau_{xx}-\nu\tau_{yy})\quad \frac{\partial u_y}{\partial y}=\frac{1}{E}(\tau_{yy}-\nu\tau_{xx})$$

subject to

$$\tau_{xy}|_{y=\pm a}=0$$

$$u_y|_{y=\pm a}=0 \quad x<0 \qquad \text{-(D14)}$$

$$\tau_{yy}|_{y=\pm a}=-p \quad x>0$$

If the complex fourier transform of χ ($\bar{\chi}$) exists, then it and its inverse can be expressed as

$$\bar{\chi}(\lambda,y)=\frac{1}{\sqrt{2\pi}}\int_{-\infty}^{\infty}\chi(x,y)\exp i\lambda x\ dx$$

$$\chi(x,y)=\frac{1}{\sqrt{2\pi}}\int_{-\infty+\gamma i}^{\infty+\gamma i}\bar{\chi}(\lambda,y)\exp -i\lambda x\ d\lambda \qquad \text{-(D15)}$$

$$\text{where } \bar{\chi} \text{ analytic in } 0<Im(\lambda)<\beta$$

For $\bar{\chi}$ to exist we must have that $\mathrm{Im}(\lambda)>0$ because $\chi\rightarrow -px^2/2$ as $x\rightarrow\infty$. Also in order that the transform exists, the strip over which it is defined must be non zero which implies that $\beta>0$. The transformed biharmonic equation (D13i), including condition (D14i) is now

$$\bar{\chi}(\lambda,y)=C(\lambda)(\cosh\lambda y(\sinh\lambda a+\lambda a\cosh\lambda a)-\lambda y\sinh\lambda y\sinh\lambda a) \qquad \text{-(D16)}$$

and the stress-strain equations from (D13) become

$$EV(\lambda)=-2\lambda C(\lambda)\sinh^2\lambda a$$

$$P(\lambda)=-\lambda^2 C(\lambda)(\cosh\lambda a(\sinh\lambda a+\lambda a\cosh\lambda a)-\lambda a\sinh^2\lambda a) \qquad \text{-(D17)}$$

$$\Rightarrow V(\lambda)=\frac{2P(\lambda)}{E}\frac{\cosh 2\lambda a-1}{\lambda(\sinh 2\lambda a+2\lambda a)}$$

Using the result (D10) and the conditions in (D14) we have

$$V(\lambda)=\frac{1}{\sqrt{2\pi}}\int_{o}^{\infty}u_y(x,a)\exp i\lambda x\ dx=V_+(\lambda) \qquad \text{-(D18)}$$

$$P(\lambda)=-\frac{ip}{\lambda\sqrt{2\pi}}+\frac{1}{\sqrt{2\pi}}\int_{-\infty}^{0}\tau_{yy}(x,a)\exp i\lambda x\ dx=-\frac{ip}{\lambda\sqrt{2\pi}}+P_-(\lambda)$$

where $P_-(\lambda), V_+(\lambda)$ are analytic in $\mathbf{Im}(\lambda)<\beta, \mathbf{Im}(\lambda)>0$.

We now let $\mathbf{H}(\omega)$ be defined as

$$H(\omega)=(\omega^2+4)^{\frac{1}{2}}\frac{\cosh 2\omega-1}{\omega(\sinh 2\omega+2\omega)} \qquad \text{-(D19)}$$

We observe that $\mathbf{H}(\omega)$ is analytic in a finite strip about the real axis, is normalised and performs no loops around $\mathbf{H}=0$ as ω goes from plus to minus infinity. All the conditions for the use of (D6) are obeyed therefore, and using (D6) on (D19) and condition (iii) to remove the pole at $\lambda=0$ (which is in the plane $\mathbf{Im}(\lambda)<\beta$), we have the **Wiener Hopf equation.**

$$\frac{EV_+(\lambda)(\lambda a+2i)^{\frac{1}{2}}H_+(\lambda a)}{2a}+\frac{ip}{\sqrt{2\pi}\ \lambda(-2i)^{\frac{1}{2}}} \qquad \text{-(D20)}$$

$$=\left(P_-(\lambda)-\frac{ip}{\lambda\sqrt{2\pi}}\right)\frac{H_-(\lambda a)}{(\lambda a-2i)^{\frac{1}{2}}}+\frac{ip}{\sqrt{2\pi}\lambda(-2i)^{\frac{1}{2}}}$$

The left hand side is analytic for $\mathbf{Im}(\lambda)>0$ and the right hand side for $\mathbf{Im}(\lambda)<\beta$. Both sides tend to zero as ω tends to infinity which implies that from (D2) both sides of (D20) equal zero.

Further analysis to calculate $\mathbf{p}$ and $\mathbf{u}_y$ would be very difficult. We shall consider a local analysis of the stress τ_{yy} in order to find the Stress Intensity Factor $\mathbf{K}$.

The stress τ_{yy} near the crack tip

The stress τ_{yy} is simply the inverse fourier transform of $\mathbf{P}(\lambda)$. Using (D20), (D15) and (D18) we obtain

$$\tau_{yy}(x,a)=\frac{1}{\sqrt{2\pi}}\int_{-\infty}^{\infty}\frac{ip}{\lambda\sqrt{2\pi}}\left[1-\frac{(\lambda a-2i)^{\frac{1}{2}}}{H_-(\lambda a)(-2i)^{\frac{1}{2}}}\right]\exp -i\lambda x\ d\lambda \quad x<0 \qquad \text{-(D21)}$$

We can easily show that this integral is singular as $\mathbf{x}\rightarrow\mathbf{0}$.

proof *Setting $x=0$ and performing the integral around a semi-circular contour in the lower half plane of λ gives zero because P_- is analytic. Extending this contour to infinity*

shows that our integral is equal to the integral along the 'semi circular' path from -∞ to ∞ in the lower half plane. The integrand as $\lambda\to\infty$ *is* $-ipa^{0.5}/(-4\pi i)^{0.5}\lambda^{0.5}$ *which shows that the integral must be infinite as* $\int d\lambda/\lambda^{0.5}\to\infty$ *as* $\lambda\to\infty$.

We only wish to find the singular behaviour of τ_{yy} near **x=0** so any finite contributions can be eliminated from (D21). If we define

$$P_{-}(\lambda)=-\frac{ip(\lambda a-2i)^{\frac{1}{2}}}{\lambda\sqrt{2\pi}(-2i)^{\frac{1}{2}}}+\frac{ip}{\lambda\sqrt{2\pi}}\left[1-\frac{(\lambda a-2i)^{\frac{1}{2}}}{(-2i)^{\frac{1}{2}}}\left\{\frac{1}{H_{-}(\lambda a)}-1\right\}\right] \qquad \text{-(D22)}$$

the integral of the second term on the right hand side is finite, and can be neglected. *Proof, Similar to previous proof except that* $(1/H_{-}-1)\to O(1/\lambda^2)$ *makes the integrand* $\sim O(\lambda^{-1.5})$ *so that the final integral of the second part is finite.*

We now have that

$$\lim_{x\to 0}\tau_{yy}(x,a)=-\frac{ip}{2\pi(-2i)^{\frac{1}{2}}}\lim_{x\to 0}\left\{\int_{-\infty}^{\infty}\frac{(\lambda a-2i)^{\frac{1}{2}}}{\lambda}\exp -i\lambda x\ d\lambda\right\} \qquad \text{-(D23)}$$

The integral given in equation (D23) can be evaluated as a contour integral in the upper half plane of λ.

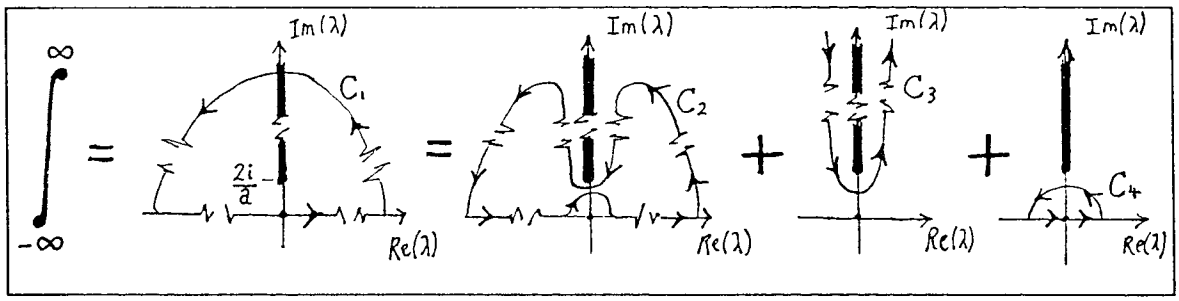

Figure D4

The integral from -∞ to ∞ can be considered as the sum of integrals along the contours $\mathbf{C_2}$, $\mathbf{C_3}$ and $\mathbf{C_4}$. The integral along $\mathbf{C_2}$ is zero by Cauchy's theorem and the integral along $\mathbf{C_4}$ is $\pi i(-2i)^{0.5}$ which is finite so can be neglected. We can therefore see that the singular part of the integral in (D23) is equivalent to the integral around $\mathbf{C_3}$. Now contracting the path of integration $\mathbf{C_3}$ close to the branch cut at $\lambda=2i/a$ to $i\infty$, gives

$$\int_{C_3}\frac{(\lambda a-2i)^{\frac{1}{2}}}{\lambda}\exp -i\lambda x\ d\lambda=\int_{i\infty}^{\frac{2i}{a}}\frac{(\lambda a-2i)_-^{\frac{1}{2}}}{\lambda}\exp -i\lambda x\ d\lambda+\int_{\frac{2i}{a}}^{i\infty}\frac{(\lambda a-2i)_+^{\frac{1}{2}}}{\lambda}\exp -i\lambda x\ d\lambda$$

$$=2\int_{\frac{2i}{a}}^{i\infty}\frac{(\lambda a-2i)_p^{\frac{1}{2}}}{\lambda}\exp -i\lambda x\ d\lambda$$

where the suffix p represents the principal value of the branch. If we now make the substitution $u=-i\lambda$ then the integral becomes

$$-2(i)_p^{\frac{1}{2}}\int_{\frac{2}{a}}^{\infty}\frac{(ua-2)_p^{\frac{1}{2}}}{u}\exp ux\ du$$

Note that the leading minus sign in the above expression arises because the above substitution gives the non principal value of the square root, which equals the negative of the principal value. The integral can now be evaluated as follows

$$z=ua-2$$

$$\Rightarrow \text{Int}=-2(i)^{\frac{1}{2}}\exp\left(\frac{2x}{a}\right)\int_0^{\infty}\frac{z^{\frac{1}{2}}}{z+2}\exp\frac{zx}{a}\ dz$$

$$=-2(i)^{\frac{1}{2}}\exp\left(\frac{2x}{a}\right)\int_0^{\infty}\frac{2y^2}{y^2+2}\exp-\left(-\frac{x}{a}\right)y^2\ dy$$

$$=-2(i)^{\frac{1}{2}}\exp\left(\frac{2x}{a}\right)\left[\sqrt{\frac{a\pi}{-x}}-4\int_0^{\infty}\frac{1}{y^2+2}\exp-\left(-\frac{x}{a}\right)y^2\ dy\right]$$

$$\sim -2(i)^{\frac{1}{2}}\exp\left(\frac{2x}{a}\right)\sqrt{\frac{a\pi}{-x}}$$

$$\text{as}\quad \lim_{u\to 0}\int_0^{\infty}\frac{1}{y^2+2}\exp -uy^2\ dy=\frac{\pi}{2\sqrt{2}}$$

The singular term of the integral has now been evaluated. From (D23), the stress intensity factor can finally be written

$$\lim_{x\to 0}\tau_{yy}(x,a)=p\sqrt{\frac{a}{\pi}}\left(\frac{1}{-2x}\right)^{\frac{1}{2}} \qquad \text{-(D24)}$$

$$\Rightarrow K=(\text{Stress Intensity Factor})=p\sqrt{\frac{a}{\pi}}$$

Appendix E

The very small time problem

The problems given in (5.1.1;3) can be written down in terms of a similarity transformation. The resulting equations cannot be solved analytically so we shall seek asymptotic and numerical solutions. We shall now consider separately the solutions for the EV and ML models.

i) EV model

$$-z\frac{dF}{dz}=\gamma F\frac{d^2F}{dz^2}+\left(\frac{dF}{dz}\right)^2$$

$$F(0)=1,\ F(C_0)=0,\ -\left.\frac{dF}{dz}\right|_{z=C_0}=C_0 \qquad \text{-(E1)}$$

The asymptotic solutions

We shall look for approximate solutions to (E1) for both large and small γ. These solutions will be useful in validating the numerical solution even though the case when $\gamma<1$ cannot be achieved in reality.

Large gamma

If we assume the asymptotic expansions

$$F(z)=F_0(z)+\frac{1}{\gamma}F_1(z)+\ldots$$

$$C_0=C_0^0+\frac{1}{\gamma}C_0^1+\ldots \qquad \text{-(E2)}$$

then standard asymptotic analysis of (E1) will show that

$$F(z)=(1-z)+\frac{1}{\gamma}\left(\frac{3z}{4}-\frac{z^2}{2}\right)\ldots$$

$$C_0=1+\frac{1}{4\gamma}+\ldots \qquad \text{-(E3)}$$

Small gamma

If we assume the expansions

$$F(z)=F_0(z)+\gamma\log_e\gamma\ F_1(z)+\gamma\ F_2(z)+...$$
$$C_0=C_0^0+\gamma\log_e\gamma\ C_0^1+\gamma\ C_0^2+... \qquad \text{-(E4)}$$

standard asymptotic analysis for the first order solution gives

$$F(z)=\left(1-\frac{z^2}{2}\right)+... \qquad \text{-(E5)}$$
$$C_0=\sqrt{2}+...$$

The second order analysis reveals that $F_1(z)$ must be constant. It would then seem reasonable to choose this constant to be zero so that the condition at z=0 is satisfied. However the analysis in calculating $F_2(z)$ will give inconsistent asymptotic expansions, so the choice of the constant to be zero must be wrong. Hence to satisfy the condition $F(0)=1$ it is necessary to introduce boundary layer near z=0 of the form

$$z=\gamma^{\frac{1}{2}}\xi \qquad \text{-(E6)}$$

Standard asymptotic analysis of the outer region shows that $F^o_2(z)$ must be of the form

$$F^o_2(z)=\frac{z^2}{4}-\log_e z+\text{const} \qquad \text{-(E7)}$$

Expansion of the boundary layer equations gives

$$F^i(\xi)=1+\gamma\ F^i_2(\xi)+...$$
$$\text{where}\quad -\xi F^{i\prime}_2=F^{i\prime\prime}_2+(F^{i\prime}_2)^2 \qquad \text{-(E8)}$$

we can now solve the equation for F^i_2 by substituting $g=F^i_2{}'$ and making the equation exact with the integrating factor $\exp(-\xi^2/2)/g^2$, to give

$$F^{i}_{2}(z)=\log_e\left[\frac{\int_{\xi_0}^{\xi}\exp\left(-\frac{y^2}{2}\right)dy}{\int_{\xi_0}^{0}\exp\left(-\frac{y^2}{2}\right)dy}\right] \qquad \text{-(E9)}$$

satisfying $F^{i}_{2}(0)=0$

Asymptotic matching of the inner and outer solutions shows that the expansions are consistent if $\xi_0\to\infty$.

On using (E6), the first order inner-second order outer expansion of F is

$$\{I_1O_2\}F=1+\gamma\log_e\gamma\left(A-\frac{1}{2}\right) \qquad \text{-(E10)}$$

which by the matching principle must equal the second order outer-first order inner expansion [34]

$$\{O_2I_1\}F=\{O_2\}\left[1+\gamma\log_e\left(\frac{1}{\sqrt{2\pi}}\int_{\gamma^{\frac{1}{2}}}^{\infty}\exp\left(-\frac{y^2}{2}\right)dy\right)\right]$$

$$=1-\frac{z^2}{2}+\frac{1}{2}\gamma\log_e\gamma+\gamma(-\log_e\sqrt{2\pi}z) \qquad \text{-(E11)}$$

$$\text{using}\quad \int_{x}^{\infty}\exp\left(-\frac{t^2}{2}\right)dt=\frac{1}{x}\exp\left(-\frac{x^2}{2}\right)\left(1-\frac{1}{x^2}+\frac{3}{x^4}+\ldots\right)$$

These equations can only match if A=1/2. Equation (E10) must then be written

$$\{I_1O_2\}F=1+\gamma\left(-\frac{\xi^2}{2}-\log_e\xi+const\right) \qquad \text{-(E12)}$$

We now match (E11) and (E12) to obtain the small γ asymptotic solution as

$$F^{o}(z)=\left(1-\frac{z^2}{2}\right)+\frac{1}{2}\gamma\log_e\gamma+\left(\frac{z^2}{4}+\log_e\left(\frac{\sqrt{2\pi}}{z}\right)\right)\gamma+\ldots$$

$$F^{1}(z)=1+\log\left[1-erf\left(\frac{\xi}{\sqrt{2}}\right)\right]\gamma+\ldots \quad z=\gamma^{\frac{1}{2}}\xi \qquad \text{-(E13)}$$

$$C_0=\sqrt{2}+\frac{1}{2\sqrt{2}}\gamma\log_e\gamma+\frac{1}{\sqrt{2}}\left(\frac{1}{2}+\log_e\sqrt{\pi}\right)\gamma+\ldots$$

Numerical solutions

Equation (E1) possesses a scaling symmetry so can be written

$$-yq'=\gamma qq''+(q')^2$$

$$q(0)=\frac{1}{C_0^2} \quad q(1)=0,\ q'(1)=-1 \qquad \text{-(E14)}$$

$$\text{where} \quad z=C_0y,\ F=C_0^2q$$

The numerical scheme will be a backward stepping finite difference method starting at y=1 and ending at y=0. The problem is then rescaled back into F and z variables. To obtain starting values for q near y=1 a power series solution can be found, the first few terms of which are

$$q(y)=(1-y)-\frac{(1-y)^2}{2(1+\gamma)}+\frac{\gamma(1-y)^3}{6(1+\gamma)^2(1+2\gamma)}+\ldots \qquad \text{-(E15)}$$

The numerical solutions are given in figures (E1) and (E2), showing the values of C_0 in terms of γ, and the dimensionless pressure profile in terms of the similarity variable z respectively.

ii) ML model

$$z\frac{d}{dz}(F^{\frac{1}{\gamma}})=\frac{d}{dz}\left(-F^{\frac{1}{\gamma}}\frac{dF}{dz}\right)^{\frac{1}{2}}$$

$$F(0)=1,\ F(C_0)=0,\ C_0=\lim_{z\to C_0}\left(\frac{-\frac{dF}{dz}}{F^{\frac{1}{\gamma}}}\right)^{\frac{1}{2}} \qquad \text{-(E16)}$$

It is difficult to proceed numerically with the ML model as it stands because both F and F′ →0 as we approach the fluid front at z=C_0. The function $F'/F^{1/\gamma}$ does appear to be well behaved, however so (E16) will be better posed if we define

$$G=F^{1-\frac{1}{\gamma}}$$
$$\Rightarrow G'=\left(1-\frac{1}{\gamma}\right)\frac{F'}{F^{\frac{1}{\gamma}}} \qquad \text{-(E17)}$$

Using the scaling symmetry of (E16) the problem may now be posed as

$$(-g')^{\frac{3}{2}}x=(\gamma(\gamma-1))^{\frac{1}{2}}\frac{g\,g''}{2}+\left(\frac{\gamma}{\gamma-1}\right)^{\frac{1}{2}}(g')^2$$
$$g(0)=\frac{1}{C_0^3},\ g(1)=0,\ -1=\left(\frac{\gamma}{\gamma-1}\right)g'(1) \qquad \text{-(E18)}$$
$$\text{where}\quad z=C_0x,\ G=C_0^3g$$

The analysis now proceeds much the same as before, so just the results will be presented.

The large gamma asymptotic solution is found to be

$$G(z)=(1-z)+\frac{z}{\gamma}\left(\frac{5}{3}-z\right)-\frac{z}{9\gamma^2}(6z^2-21z+10)+\ldots$$
$$C_0=1+\frac{2}{3\gamma}+\frac{1}{3\gamma^2}+\ldots \qquad \text{-(E19)}$$

The power series solution near x=1 is

$$g(x)=\frac{\gamma-1}{\gamma}(1-x)+\frac{1-\gamma}{\gamma^2}(1-x)^2+\ldots \qquad \text{-(E20)}$$

The numerical solutions are given in figures (E3) and (E4), showing the values of C_0 in terms of γ, and the dimensionless pressure profile in terms of the similarity variable z respectively.

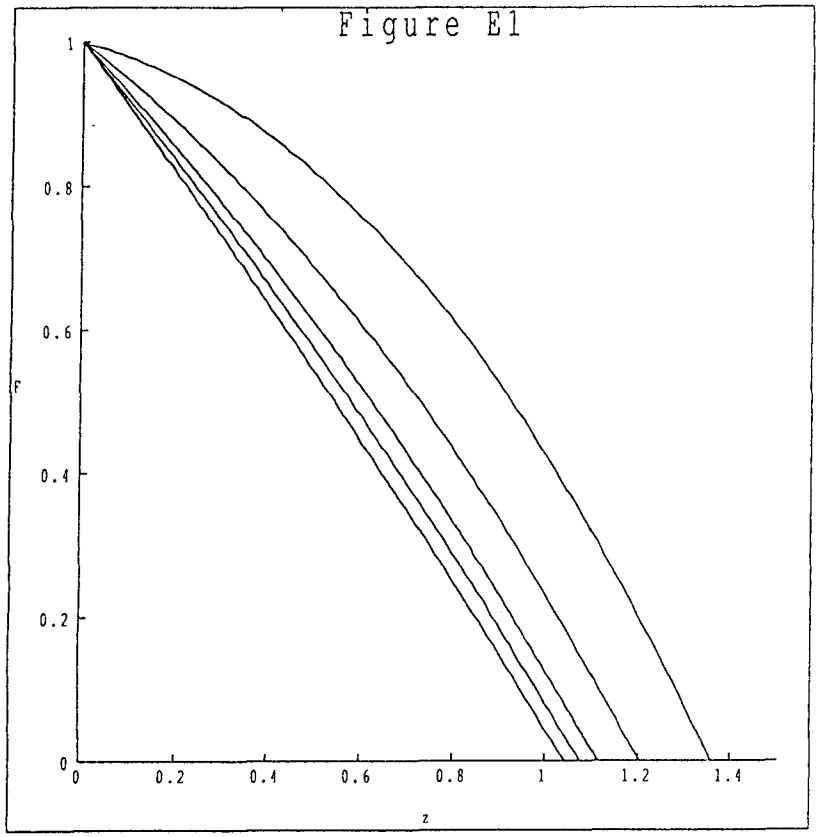

The dimensionless pressure of the small time, large borehole pressure, EV model solution in terms of similarity variable z for γ=5.0, 2.5, 1.4, 0.5, 0.05.

$$z=\frac{\zeta-1}{\sqrt{2f_1^3(\log_e f_1)^2\tau}} \qquad f=f_1F$$

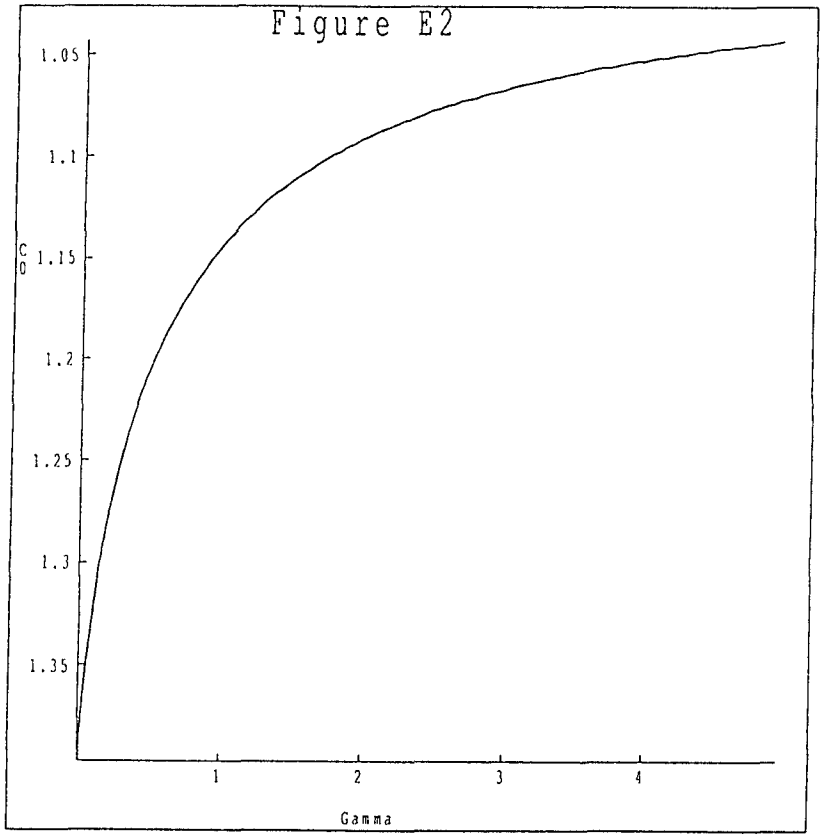

The gas front position (where F=0) for a continuous range of γ.

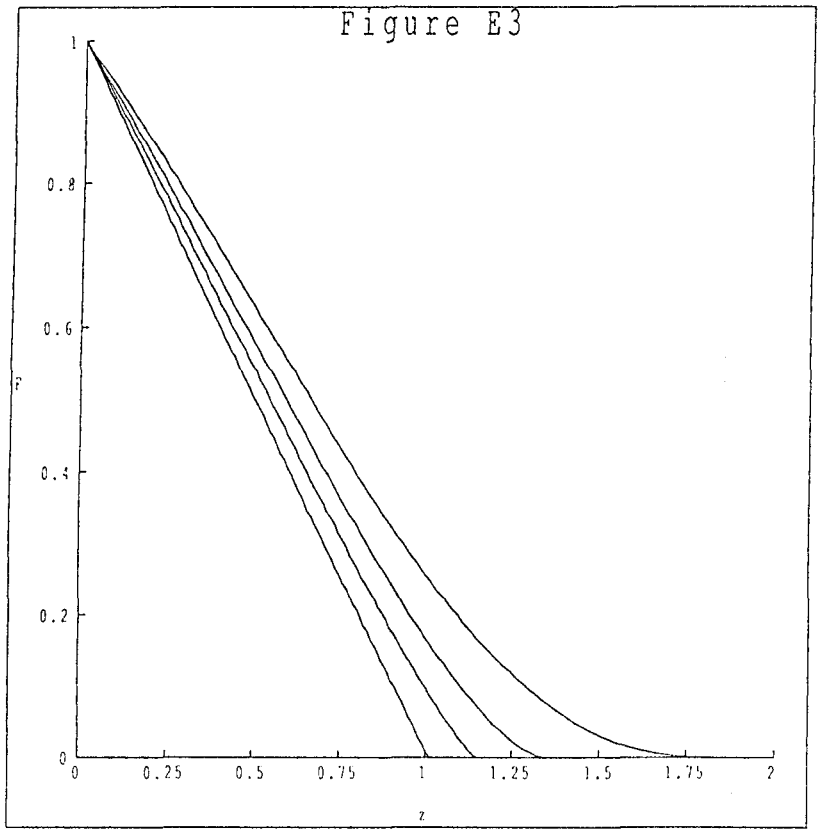

The dimensionless pressure of the small time, large borehole pressure, ML model solution in terms of similarity variable **z** for γ=50.0, 5.0, 2.5, 1.4.

$$z=\frac{\zeta-1}{\left(\frac{3}{2}f_1^{\frac{1}{2}\left(1-\frac{1}{\gamma}\right)}(f_1\log f_1)^{\frac{1}{2}}\tau\right)^{\frac{2}{3}}} \qquad f=f_1F$$

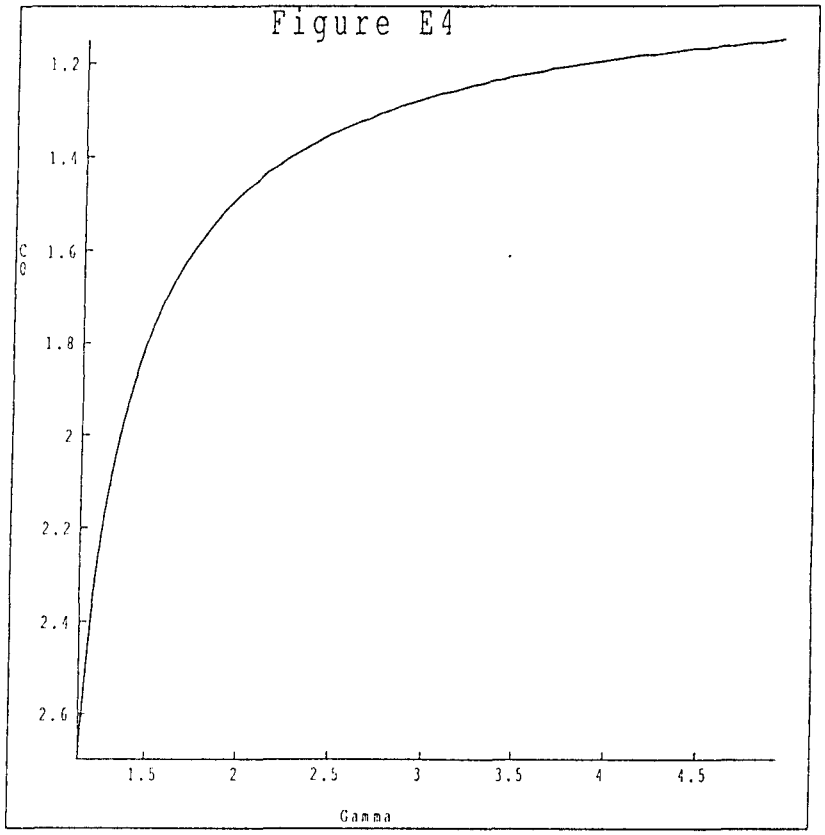

The gas front position (when **F**=0) for a continuous range of γ.

Appendix F

Calculations for the Intermediate time EV Model

i) To analyse equation (5.1.2;6).

$$\frac{dF}{dC}=\frac{-3CF^2+F(12+16C)-12-16C}{C^2(F-2)} \qquad \text{-(F1)}$$

Perfom a standard phase plane analysis as follows;

i) Draw isoclines of the zero gradient of F. This occurs when the numerator of (F1) is zero, ie. whenever

$$F=\frac{12+16C\pm\sqrt{(12+16C)^2-12C(12+16C)}}{6C} \qquad \text{-(F2)}$$

case i) No roots of (F2)

$$\left.\begin{array}{l}12+4C>0\\12+16C<0\end{array}\right\} \Rightarrow -3<C<-\frac{3}{4}$$

case ii)

$$\left.\begin{array}{l}12+16C<0\\12+4C<0\end{array}\right\} \Rightarrow C<-3$$

As $C\rightarrow-\infty$ $F=4$ or $4/3$

case iii)

$$\left.\begin{array}{l}12+16C>0\\12+4C>0\end{array}\right\} \Rightarrow C>-\frac{3}{4}$$

One root exists at $F(-3/4)=0$ and then double roots about the line $(12+16C)/6C$. As $C\rightarrow0$ then $F\rightarrow1$ or $4/C$. Double roots exist for $C>0$. As $C\rightarrow\infty$ $F=4$ or $4/3$

ii) Draw isoclines of infinite gradient of F. This occurs when the denominator of (F1) is zero

$$C=0$$

$$F=2$$

iii) Singular points (where the gradient is indeterminate) exist where the lines in (i) and (ii) cross. These exist at $F(0)=1$ and $F(-3)=2$.

The phase plane can now be drawn (See figure(F1)). We only really want to know about the physical region C>0 so we shall only study this region in any detail.

The starting point for F and C is at F(0)=1 (Appendix E). We can study the singular point at F(0)=1 by looking at the local behaviour of equation (F1)

$$\frac{dF}{dC} \sim \frac{3C-12(F-1)}{C^2} \qquad \text{-(F3)}$$

From (F3) we can show that the local solution for F is

$$F-1 \sim \frac{C}{4} - \frac{3A}{\exp -\frac{12}{C}}$$

where A is an arbitrary constant. There is only one solution then that comes from the singular point, and that is when A=0.

Small time asymptotics

We can find from (F1) an asymptotic solution for F in terms of small C

$$F=1+\frac{C}{4}-\frac{11C^2}{48}+\frac{C^3}{4}+\ldots \qquad \text{-(F4)}$$

If this equation is substituted into (5.1.2;5i) we obtain

$$\frac{C^2}{2}-\frac{C^3}{4}+\frac{5C^4}{48}+\ldots=t \qquad \text{-(F5)}$$

(F5) can be inverted to solve for C in terms of t, and then substituted into (F4) to obtain F in terms of t (see(5.1.2;7)).

Large time asymptotics

We know from the phase plane (Figure F1) that our solution for F must have a limiting value of 4/3 at infinity. We can now find an asymptotic solution for F in terms of small 1/C

$$F=\frac{4}{3}-\frac{6}{11C}+\frac{648}{605C^2}+\ldots$$

A similar procedure as used with the small time problem will give us the large time solutions in (5.1.2;8).

Numerical procedure

A backward difference method was used to calculate **F** in terms of **C** and then a central difference method to calculate **t** as a function of **C** from (5.1.2;5). The graphical output shows **F** in terms of **C** (figures F2) and **C** in terms of **t** (figures(5.1.2;1,2&3)).

FIGURE F1

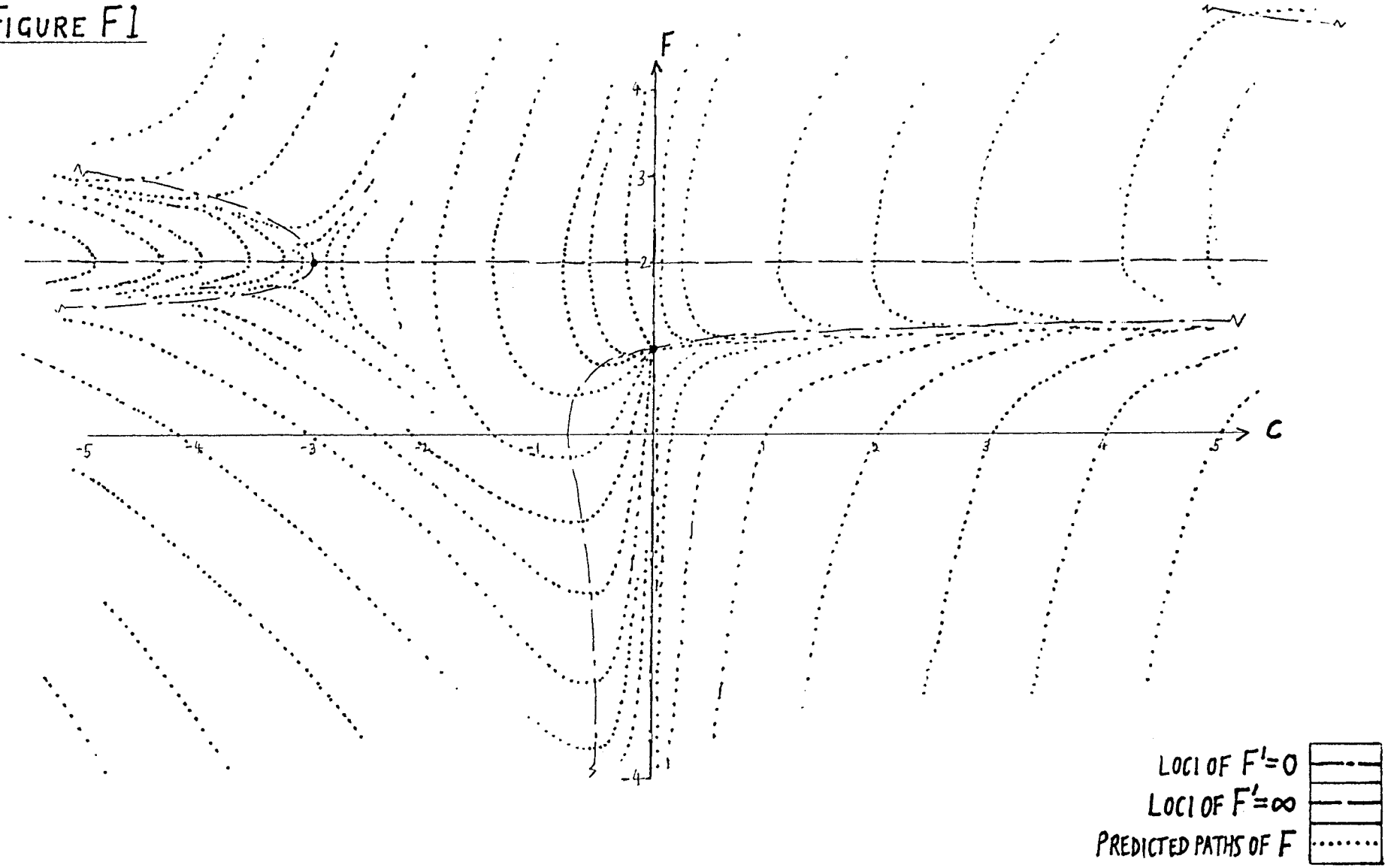

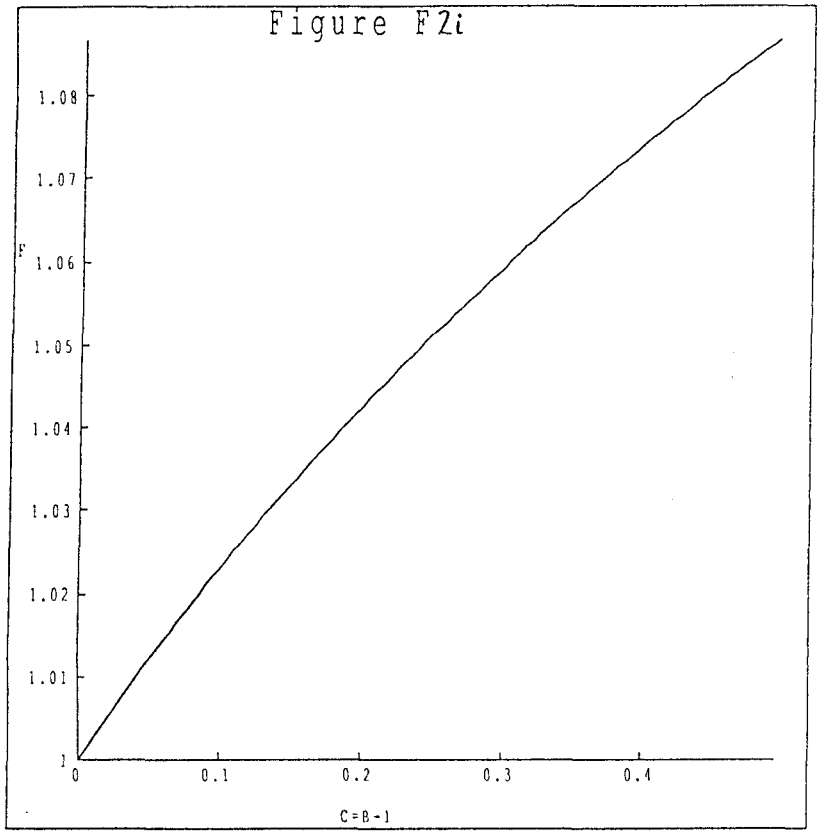

The numerical solution for the shape variable **F** in terms of the gas front position **C=B-1** for the intermediate time EV model with large constant borehole pressure and $\gamma=\infty$.

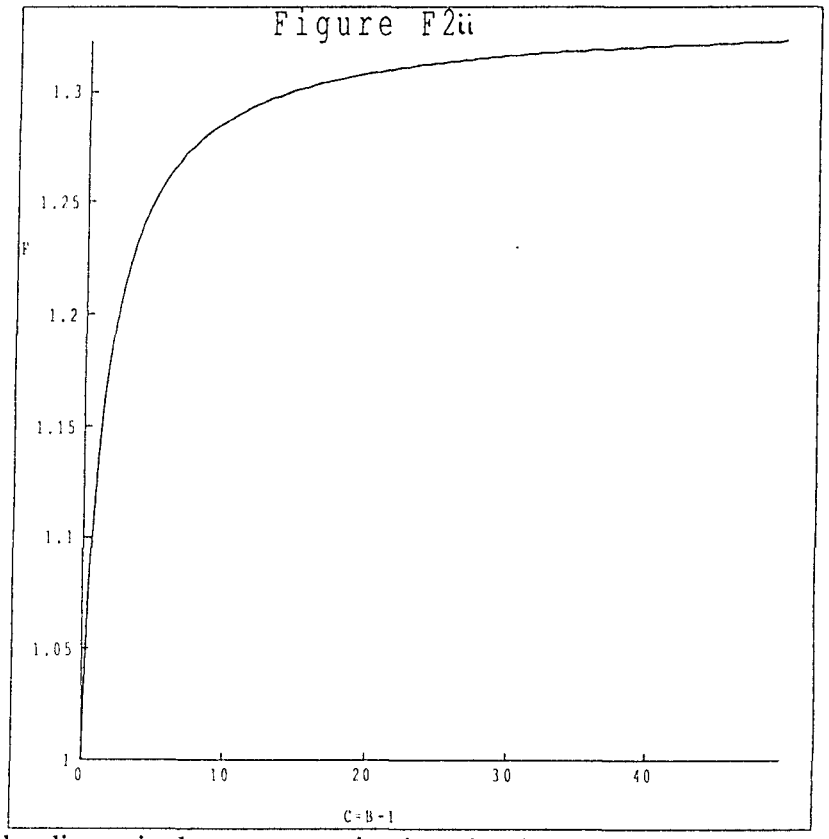

the dimensionless pressure is given by the equation

$$f=f_1\left[(F-1)\left(\frac{\zeta-1}{C}\right)^2-F\left(\frac{\zeta-1}{C}\right)+1\right]$$

Appendix G

The very long time problem for a small $K_{phys.}$

The very long time problem as defined in (5.2.3ii) with K=0 is

$$\frac{\partial}{\partial\tau}(f^{\frac{1}{\gamma}}H)=-\frac{\partial}{\partial\zeta}\left(-f^{\frac{1}{\gamma}}H^3\frac{\partial f}{\partial\zeta}\right)^q$$

$$\dot{A}=\left(-f^{\frac{1}{\gamma}}H^3\frac{\partial f}{\partial\zeta}\right)^q\frac{1}{Hf^{\frac{1}{\gamma}}}\Bigg|_{\zeta=A}$$

$$A\sim\frac{\int_0^A f\,dy}{1-f(A)} \qquad \text{-(G1)}$$

$$H=\zeta f+\int_\zeta^A\frac{1}{y}\int_0^y f\,dxdy-Af(A)$$

$$\int_0^A H\,dx=\frac{4\sigma 2^{\frac{1}{\gamma}}M}{E}-\frac{E}{4\sigma}$$

This problem does not have a similarity solution but we can examine the very long term behaviour as the gas pressure approaches the in-situ stress. From (4;5) we should note that at this stage of the blast the gas must have reached the crack front.

If we define the new variable

$$\xi=\frac{\zeta}{A(\tau)}$$

$$\Rightarrow\frac{\partial}{\partial\tau}\to\frac{\partial}{\partial\tau}-\xi\frac{\dot{A}}{A}\frac{\partial}{\partial\xi} \qquad \text{-(G2)}$$

$$\frac{\partial}{\partial\zeta}\to\frac{1}{A(\tau)}\frac{\partial}{\partial\xi}$$

and the expansions

$$f(\zeta,\tau)=\frac{1}{2}+\delta_1\left(\frac{1}{\tau}\right)F_1(\xi)+\ldots$$

$$A(\tau)=\delta_{-n}\left(\frac{1}{\tau}\right)A_{-n}+\delta_{-n+1}\left(\frac{1}{\tau}\right)A_{-n+1}+\ldots \qquad \text{-(G3)}$$

then the first order system of equations for (G1) are

i) The EV model

$$-\frac{1}{6}\left[1+\xi\frac{d}{d\xi}\right]h_0=\frac{d}{d\xi}\left(h_0^3\frac{dF_1}{d\xi}\right)$$

$$H=A\left[\frac{1}{\tau^{\frac{1}{3}}}\left\{\xi F_1-F_1(1)+\int_\xi^1\frac{1}{\omega}\int_0^\omega F_1\,dzd\omega\right\}+\ldots\right]=A\left[\frac{1}{\tau^{\frac{1}{3}}}h_0+\ldots\right]$$

$$\lim_{\xi\to 1}h_0^2\frac{dF_1}{d\xi}=-\frac{1}{6} \qquad \text{-(G4)}$$

$$\int_0^1 F_1\,dz+F_1(1)=0$$

$$\int_0^1 h_0\,dx=\frac{1}{A_{-n}^2}\left(\frac{4\sigma 2^{\frac{1}{\gamma}}M}{E}-\frac{E}{4\sigma}\right)$$

where the expansions can be written

$$f(\zeta,\tau)=\frac{1}{2}+\frac{F_1(\xi)}{\tau^{\frac{1}{3}}}+\ldots \qquad \text{-(G5)}$$

$$A(\tau)=A_{-n}\tau^{\frac{1}{6}}+A_{-n+1}\tau^{-\frac{1}{6}}+\ldots$$

ii) The ML model

$$-\frac{A_{-n}}{3}\left[1+\xi\frac{d}{d\xi}\right]h_0=-\left(\frac{1}{2}\right)^{-\frac{1}{2\gamma}}\frac{d}{d\xi}\left(-h_0^3\frac{dF_1}{d\xi}\right)^{\frac{1}{2}}$$

$$H=A\left[\frac{1}{\tau^{\frac{2}{3}}}\left\{\xi F_1-F_1(1)+\int_\xi^1\frac{1}{\omega}\int_0^\omega F_1\ dzd\omega\right\}+\ldots\right]=A\left[\frac{1}{\tau^{\frac{2}{3}}}h_0+\ldots\right]$$

$$\lim_{\xi\to 1}h_0\frac{dF_1}{d\xi}=-\frac{A_{-n}^2\left(\frac{1}{2}\right)^{\frac{1}{\gamma}}}{9} \qquad \text{-(G6)}$$

$$\int_0^1 F_1\ dz+F_1(1)=0$$

$$\int_0^1 h_0\ dx=\frac{1}{A_{-n}^2}\left(\frac{4\sigma 2^{\frac{1}{\gamma}}M}{E}-\frac{E}{4\sigma}\right)$$

where the expansions can now be written

$$f(\zeta,\tau)=\frac{1}{2}+\frac{F_1(\xi)}{\tau^{\frac{2}{3}}}+\ldots \qquad \text{-(G7)}$$

$$A(\tau)=A_{-n}\tau^{\frac{1}{3}}+A_{-n+1}\tau^{-\frac{1}{3}}+\ldots$$

Both of these problems can be integrated once to give third order non-linear intego-differential equations.

i) EV model

$$\frac{dF_1}{d\xi}=\frac{-\xi}{6\left[\xi F_1(\xi)-F_1(1)+\int_\xi^1\frac{1}{\omega}\int_0^\omega F_1\ dzd\omega\right]^2} \qquad \text{-(G8)}$$

$$\text{subject to} \quad \int_0^1 F_1 \, dz + F_1(1) = 0$$

ii) ML model

$$\frac{dF_1}{d\xi} = \frac{-\left(\frac{1}{2}\right)^{\frac{1}{\gamma}} A_{-n}^2 \xi^2}{9\left[\xi F_1(\xi) - F_1(1) + \int_\xi^1 \frac{1}{\omega} \int_0^\omega F_1 \, dz d\omega\right]} \qquad \text{-(G9)}$$

$$\text{subject to} \quad \int_0^1 F_1 \, dz + F_1(1) = 0$$

These problems can be dramatically simplified if we note that the solutions to (G8i,G9i) are invariant to the addition of a constant, so if we find any solution, an appropriate constant can be added to it so that the conditions (G8ii,G9ii) are satisfied. An appropriate substitution that satisfies this symmetry for F is

$$D(\xi) = \xi F_1(\xi) - F_1(1) + \int_\xi^1 \frac{1}{\omega} \int_0^\xi F_1 \, dz d\omega \quad \Rightarrow D(1) = 0$$

$$\Rightarrow D'(\xi) = \xi F_1' + F_1(\xi) - \frac{1}{\xi} \int_0^\xi F_1 \, dz \quad \Rightarrow D'(0) = 0 \qquad \text{-(G10)}$$

Equations (G8) and (G9) can now be written in terms of D. It will prove convenient in later numerical calculations however to write down the resulting equations in terms of variables that position the boundary condition at $\xi=1$ to x=a. This is possible because both the resulting equations possess an appropriate scaling symmetry

i) EV model

$$\omega y'' + y'\left(1 - \frac{\omega^3}{3y^3}\right) + \frac{2\omega^2}{3y^2} = 0$$

$$y(a) = 0, \; y'(0) = 0 \qquad \text{-(G11)}$$

$$\text{where} \quad \xi = \frac{\omega}{a}, \; D(\xi) = \frac{y(\omega)}{a}$$

where

$$A_{-n}=\left(\frac{\frac{4\sigma 2^{\frac{1}{\gamma}}M}{E}-\frac{E}{4\sigma}}{\int_0^a y\,d\omega}\right)^{\frac{1}{2}} a \qquad \text{-(G12)}$$

$$F_1(\xi)=-\frac{1}{6}\int_0^{\omega}\frac{x}{y^2}\,dx+\text{CONST}\ (=E+\text{CONST})$$

$$\text{CONST}=-\frac{1}{2}\left[\int_0^1 E\,dz+E(1)\right]=-\frac{1}{2}\left[\frac{1}{a}\int_0^a E\,dz+E(a)\right]$$

ii) ML model

$$\omega y''+y'\left(1-\frac{\omega^4}{y^2}\right)+\frac{5\omega^3}{y}=0$$

$$y(a)=0,\ y'(0)=0 \qquad \text{-(G13)}$$

$$\text{where}\quad \xi=\frac{\omega}{a},\ D(\xi)=\frac{y(\omega)}{a^2}$$

where

$$A_{-n}=2^{\frac{1}{6\gamma}}\left(\frac{3\left(\frac{4\sigma 2^{\frac{1}{\gamma}}M}{E}-\frac{E}{4\sigma}\right)}{\int_0^a y\,d\omega}\right)^{\frac{1}{3}} a \qquad \text{-(G14)}$$

$$F_1(\xi)=\left(\frac{\left(\frac{1}{2}\right)^{\frac{1}{\gamma}}A_{-n}^2}{9}\right)^{\frac{1}{2}}\left[-\frac{1}{a}\int_0^{\omega}\frac{x^2}{y}\,dx+\text{CONST}\right](=(\sim)^{\frac{1}{2}}[E+\text{CONST}])$$

$$\text{CONST}=-\frac{1}{2}\left[\int_0^1 E\,dz+E(1)\right]=-\frac{1}{2}\left[\frac{1}{a}\int_0^a E\,dx+E(a)\right]$$

The expressions containing **E** are ambiguously given over the ranges for ξ and ω but this should not cause any confusion.

These problems can now be solved numerically using a shooting method. Only one iterate will be necessary if we start at $\omega=0$ with $y'=0$ for any initial value for **y** and then define the point when $y=0$ as $\omega=a$. The start up values for **y** can be calculated from the small ω solutions which are

EV model:

$$y(\omega)=y(0)-\frac{2\omega^3}{27y(0)^2}+O(\omega^4)$$

ML model:

$$y(\omega)=y(0)-\frac{5\omega^4}{16y(0)}+O(\omega^5)$$

REFERENCES

1. **Atkinson B.K.** Fracture Mechanics of Rock. *Academic Press Geology Series (1987)*

2. **Barenblatt G.I.** The Mathematical Theory of Equilibrium Cracks in Brittle Fracture. *Inst. of Geology and Development of Combustible Minerals of the USSR.(1962)*

3. **Bradshaw P.** An Introduction to Turbulence and its Measurement. *The Commonwealth and International Library (1971)*

4. **Bradshaw P.** Topics in Applied Physics, Turbulence. *Springer-Verlag (1978)*

5. **Bradshaw P. and Cebici T.** Momentum Transfer in Boundary Layers. *Mc Graw Hill (1977)*

6. **Brinkman J.R.** Separating Shock Wave and Gas Expansion Breakage Mechanisms. *Proc 2nd Intl.Symp.on Rock Fragmentation by Blasting, Keystone, Colorado.(1987)*

7. **Cundall P.A.** A Computer Model for Simulating Progressive Large Scale Movements in Blocky Rock Systems. *Proc.Symp.Rock Mech.(ISRM,1971)*

8. **Edl J.N.Jnr** Estimating Explosive Gas Pressure Distribution *Internal report, U.S.Dept.of Energy Tech.Centre,Wyoming.*

9. **England A.H.** Complex Variable Methods in Elasticity. *Wiley-Interscience (1971)*

10. **Erhie H.E.** Phd Thesis *Oxford Uni. (1988)*

11. **Gross W.A.** Fluid Film Lubrication. *Wiley-Interscience (1980)*

12. **Hanson M. et al** Explosive Enhancement of Permeability. *Lawrence Livermore Lab.,Uni.of California,USA.*

13. **Hirs G.G.** A Bulk Flow Theory for Turbulence in Lubrication Films *J.Lubric.Tech.95. (1973)*

14. **Heuze et al** Propagation of Fluid Driven Fractures in Jointed Rock. *Int.J.Rock Mech and Min.Sci. and Geomech.Abstr.22.no 1,pp.3-19 (1985)*

15. **Hinze J.O.** Turbulence *Mc Graw Hill (1975)*

16. **Hochstadt H.** Integral Equations. *Pure and Applied Maths.Wiley-Interscience (1973)*

17. **Jaeger J.C. and Cook N.G.W.** Fundementals of Rock Mechanics *Methuen and*

Co.,London (1969)

18. **King J.R.** Approximate Solutions to a Non-Linear Diffusion Equation. *Jnl.of Eng.Math.22.pp.53-72 (1988)*

19. **Kopp J.W.** Stemming Ejection and Burden Movements of Small Borehole Blasts. *Internal report from Int.Bu.of Mines,Minneapolis*

20. **Lowdnes C.M.et al** Primary Fracture from an Array of Shotholes. *Jnl.Sth.African.Inst.of Mining and Metallurgy.(1976)*

21. **Nilson R.H.** Modelling of Gas Driven Fractures Induced by Propellant Combustion witin a Borehole. *Int.J.Rock Mech.Min.Sci.and Geomech.Abstr.* **22.** *no 1,pp.3-19 (1985)*

22. **Nilson R.H.** Similarity Analysis of Energy Transport in Gas Driven Fractures *Int.J.of Frac.30.pp.115-134 (1986)*

23. **Nilson R.H.** Similarity Solutions for Wedge Shaped hydraulic Fractures Driven into a Permeable Medium by a Constant Inlet Pressure. *Int.J.for Num.and Analytical Meth.in Geomech.12. (1988)*

24. **Ouchterlony F.** Fracture Mechanics Applied to Rock Blasting. *Swedish Detonic Research Foundation,Stockholm,Sweden.*

25. **Pine R.J. and Batchelor A.S.** Downward Migration of Shearing in Jointed Rock during Hydraulic Injection. *Int.J.Rock Mech.Min.Sci.and Geomech. Abstr.22, no5, pp.249-263 (1984)*

26. **Scheidegger** The Physics of Flow through Porous Media. *Oxford Uni.Press (1963)*

27. **Schlichting H.** Boundary Layer Theory. *Mc Graw Hill (1968)*

28. **Sih G.C.** Methods of Analysis and Solutions of Crack Problems. *Mech.of Fracture 1, Noordhoff (1973)*

29. **Sneddon I.N.** The Use of Integral Transforms. *Mc Graw Hill (1972)*

30. **Spence D.A. and Turcotte D.L.** Magma Driven Propagation of Cracks. *J.of Geophys.Res.90.B1,pp.575-580 (1985)*

31. **Stagg M.S. and Nutting M.J.** Influence of Blast Delay Time on Rock Fragmentation. *Internal report from Twin Cities Res.Ctr.,Bu.of Mines, Minneapolis*

32. **Street R.L.** Analysis and Solutions of P.D.E.s *Brooks/Cole Publishing Company,Monterey,California (1973)*

33. **Tada H.,Paris P.and Irwin G.** The Stress Analysis of Cracks Handbook *Del Research Corporation (1973)*

34. **Van Dyke M.** Perturbation Methods in Fluid Mechanics. *Parabolic Press (1975)*

35. **Westmann R.A.** Pressurised Star Crack. *J.Math.Physics.43.pp.191-196 (1964)*

36. **Williams W.E.** A Star Crack Deformed by an Arbitary Internal Pressure. *Int.J.Engng.Sci.9.pp.705-712 (1971)*